ABSTRACT

Title of Document: EVALUATION OF CRITICAL NUCLEAR POWER PLANT ELECTRICAL CABLE RESPONSE TO SEVERE THERMAL FIRE CONDITIONS

Gabriel James Taylor, M.S., 2012

Directed by: Professor James A. Milke
Department of Fire Protection Engineering

The failure of electrical cables exposed to severe thermal fire conditions are a safety concern for operating commercial nuclear power plants (NPPs). The Nuclear Regulatory Commission (NRC) has promoted the use of risk-informed and performance-based methods for fire protection which resulted in a need to develop realistic methods to quantify the risk of fire to NPP safety. Recent electrical cable testing has been conducted to provide empirical data on the failure modes and likelihood of fire-induced damage. This thesis evaluated numerous aspects of the data. Circuit characteristics affecting fire-induced electrical cable failure modes have been evaluated. In addition, thermal failure temperatures corresponding to cable functional failures have been evaluated to develop realistic single point thermal failure thresholds and probability distributions for specific cable insulation types. Finally, the data was used to evaluate the prediction capabilities of a one-dimension conductive heat transfer model used to predict cable failure.

EVALUATION OF CRITICAL NUCLEAR POWER PLANT ELECTRICAL CABLE RESPONSE TO SEVERE THERMAL FIRE CONDITIONS

by

Gabriel James Taylor

Thesis submitted to the Faculty of the Graduate School of the
University of Maryland, College Park, in partial fulfillment
of the requirements of the degree of
Master of Science
2012

Advisory Committee:

Professor James A. Milke, Chair
Professor Marino diMarzo
Dr. Francisco Joglar

Acknowledgements

I would like to thank my advisor Dr. James A. Milke for his guidance throughout my years at the University of Maryland Department of Fire Protection Engineering.

I would also like express my gratitude to the other committee members, Professor diMarzo, and Dr. Joglar for their involvement and time. Having a committee knowledgeable about fire-induced cable damage and fire probabilistic risk assessment has made me confident in the findings of this thesis. Many thanks must also go out to Associate Professor Emeritus Mowrer who gave me guidance early on in my pursuit of a masters degree.

From the Nuclear Regulatory Commission (NRC), I would like to first thank Mr. Pat Madden and Mark Henry Salley who both guided me into a career of fire protection engineering and provided valuable insights, knowledge and motivation to complete this thesis and earning an advanced degree in fire protection engineering. I would also like to thank Dr. Raymond Gallucci and Mr. Martin Stutzke who provided guidance in the world of statistics and reliability engineering. I would also like to thank Jennifer Uhle, Christiana Lui, and Richard Correia for supporting my education and a flexible work schedule which has allowed me to attend classes at the University of Maryland – College Park Campus.

I must thank Steve Nowlen and the other researchers at Sandia National Laboratories who performed the testing and thoroughly documented the results and experimental setup, along with providing the electronic data files. Without taking these detailed and numerous measurements, this thesis would not be possible. The work of Dr. Kevin McGrattan of the National Institute of Standards and Technology must also be

recognized for his development of the one-dimensional heat transfer model used to predict cable damage. In addition, Dave Stroup of the NRC was also instrumental in coding the THIEF model into a Microsoft Excel spreadsheet to supplement the Fire Dynamic Tools fire modeling inspector toolbox.

Lastly, I would like to thank my family for supporting my education and my parents for encouraging me to do whatever makes me happy and to pursue advanced degrees.

Thanks – Mom , Dad, Kate, Sara, Oscar and Karen.

Table of Contents

List of Tables

List of Tables (Continued)

List of Figures

List of Figures (Continued)

List of Abbreviations

ac	alternation current
ASTM	American Society for Testing and Materials
AWG	American Wire Gauge
BIW	Baltimore Insulated Wire
CAROLFIRE	Cable Response to Live Fire
CP	neoprene
CPE	chlorinated polyethylene
CPT	control power transformer
CSPE	chlorosulphonated polyethylene (also Hypalon)
DAQ	data acquisition system
dc	direct current
DESIREE-Fire	Direct Current Electrical Shorting in Response to Exposure Fire
EPR	ethylene propylene rubber
EPRI	Electric Power Research Institute
ETFE	ethylene tetrafluoroethylene
FAQ	frequently asked question
FDT^s	Fire Dynamic Tools
FM	Factory Mutual
HRR	heat release rate
IEEE	Institute of Electrical and Electronics Engineers
IR	insulation resistance
IRMS	insulation resistance measurement system
K-S	Kolmogorov-Smirnov
LOCA	loss of coolant accident
MC	Monte Carlo
MOV	motor operated valve
MQH	McCaffrey, Quintiere, Harkleroad
NEI	Nuclear Energy Institute
NFPA	National Fire Protection Association
NIST	National Institute of Standards and Technology
NPP	nuclear power plant
NRC	Nuclear Regulatory Commission

PE	polyethylene
PRA	probabilistic risk assessment
PVC	polyvinyl chloride
RES	Office of Nuclear Regulatory Research
SCDU	surrogate circuit diagnostic unit
SNL	Sandia National Laboratories
SOV	solenoid operated valve
SR	silicon rubber
SSC	structures, systems and components
THIEF	Thermally-Induced Electrical Failure Model
TP	thermoplastic
TS	thermoset
XLP, XLPE	cross-linked Polyethylene
XLPO	cross-linked Polyolefin
V&V	verification and validation

1 Introduction and Background

A fire at the Browns Ferry nuclear power plant (NPP) Unit 1 on March 22, 1975, forever changed the way fire protection was implemented at NPPs [Salley 2004]. The fire damaged multiple safety systems, and required operator manual actions to achieve a safe shutdown condition. Prior to this near miss accident fire was not viewed as a significant threat to reactor safety and as such fire protection was not regulated by the Nuclear Regulatory Commission (NRC), but by the local and state fire codes, along with any insurance underwriter requirements [NRC 2009]. NRC investigations of the 1975 Browns Ferry fire identified significant fire protection and design deficiencies and led to the development of a new set of fire protection requirements and guidelines, including a concept referred to as defense-in-depth [NRC 2002].

Defense-in-depth as applied to fire protection refers to a layered approach to design that includes the following echelons of safety,

- Prevent fire from starting
- Detect rapidly, control, and extinguish promptly those fires that do occur
- Protect structures, systems, and components (SSCs) important to safety, so that a fire that is not promptly extinguished by the fire suppression activities will not prevent the safe shutdown of the plant [NRC 2009]

The first two echelons of safety are typically covered in a NPP fire protection program by the use of administrative controls and properly designed conventional fire protection systems. The third echelon, however, has required significant resource and effort by the nuclear utilities' and the NRC to address, and 37 years following the worst fire to occur at a NPP, fire protection safety issues continue to be researched and addressed. This last echelon of defense-in-depth requires protecting one train of safe-

shutdown systems from fire damage. Safe shutdown systems are systems and equipment that perform functions needed to achieve and maintain a safe shutdown condition. Plant safe shutdown conditions are specified in technical specifications as standby, hot shutdown or cold shutdown reactor conditions [NRC 2009].

Virtually every NPP system relies on power, control, and instrumentation electrical cables to safely operate and shutdown the plant. Many of the most significant fire risk scenarios identified in past probabilistic risk assessments (PRAs) involve the postulated loss of safe-shutdown systems through the fire-induced failure of electric power, instrumentation, and control cables [Lambright, Nowlen, Nicolette, and Bohn 1989]. Detailed understanding of fire damage and environmental effects on electrical cable has been the subject of research even prior to the 1975 Browns Ferry Fire. However, only recently has research been focused on the evaluation of the failure modes associated with fire-induced cable damage. In the analysis of fire risk, postulated cable damage scenarios often represent dominant contributors to fire-induced core damage frequency estimates, and often overall plant core damage frequency [Nowlen 1991]. Advanced tools for performing fire PRA circuit analysis explicitly treating different cable failure modes and the resulting circuit and system impact are required to provide the most realistic representation of a NPPs overall fire risk [LaChance, Nowlen, Wyant, and Dandini 2003].

One of the objectives of the NRC's fire protection requirements and guidance are to provide reasonable assurance that fire-induced failure of circuits that could prevent the operation or cause maloperation, of equipment necessary to achieve and maintain post-fire safe-shutdown will not occur. In the late 1990's, following an increased number of

licensee event reports identifying problems associated with post-fire safe-shutdown circuit analysis, the NRC issued Enforcement Guidance Memorandum 98-02 and Information Notice 99-17, which identified the problem and allowed for some enforcement discretion while NPP licensees corrected any identified problems [NRC 1999, NRC 2000]. The root cause of the problems was often identified as differing interpretations of the regulations pertaining to fire-induced cable failure modes and a general lack of experimental data.

To provide a technical basis for understanding fire-induced circuit failure modes several sets of experiments were conducted by the Electric Power Research Institute (EPRI) and Sandia National Laboratories (SNL) [NRC 2004, Nowlen 2008, Nowlen, Brown, Olivier, Wyant 2012]. For the most part, the NPP industry testing illustrated that cable failure modes of concern[1] (hot shorts, spurious operations) were a greater risk than had previously been thought. The specifics of these tests are described in section 4.2.2.8 and the most recent tests are the focus of the evaluation conducted in this thesis.

In addition to the fire protection testing and research, NRC rule making has allowed for the voluntary use of performance-based, risk-informed fire protection programs via the National Fire Protection Association (NFPA) 805 standard, "Performance-Based Standard for Fire Protection for Light Water Reactor Electric Generating Plants, 2001 Edition [NRC 1976, NFPA 2001]." This NFPA standard along with the NRC/EPRI fire PRA methodology outlined in NUREG/CR-6850 (EPRI TR1011989) "EPRI/NRC-RES Fire PRA Methodology for Nuclear Power Facilities," has provided a state-of-the-art methodology, allowing those utilities' pursuing the

[1] failure modes of concern are defined in section 3.2

performance-based approach to quantify plant risk from fires and make risk-reducing modifications to the plant.

With the desire to use the most realistic information available in fire PRAs there remain numerous areas that could benefit from advancement. The application of recent fire testing data to improve the accuracy of the methods could provide such advancements. For example, the current NRC guidance provides a single point conservative thermal failure threshold to indicate cable electrical damage for the two broad categories of electrical cable insulation. In reality, cables do not fail at a set temperature, but fail in a range of temperatures. With a better understanding of electrical cable thermal fragility, quantification of cable failure probabilities using fire modeling and cable failure distributions can be developed. Testing has also shown that circuit configuration which can influence the failure mode and duration of particular failure modes. In order to advance the state-of-the-art methods, these new insights need to be implemented into the overall methodology. This thesis presents several uses of the test data in an attempt to advance these methods.

2 Objective

The objective of this study is to provide a comprehensive evaluation of the most recent fire-induced circuit failure experimentation conducted by SNL. The focus of this thesis is to evaluate the SNL data to suggest cable insulation material specific thermal failure thresholds, develop electrical cable thermal fragility distributions, evaluate parameters that influence fire-induced circuit failure modes and present an analytical approach used to identify a unique failure mode for ungrounded common power supply circuits. This thesis also evaluates the prediction capabilities of the Thermally-Induced Electrical Failure (THIEF) one-dimensional heat conduction model. Finally, this thesis uses the THIEF model and the electrical cable thermal fragility distributions to develop lookup tables of cable damage probabilities. This thesis builds upon previous work completed by the National Institute of Standard and Technology (NIST) which developed the THIEF model and previous testing and research conducted by EPRI that developed a basic understanding of parameters that affect fire-induced circuit failure modes.

3 Fundamentals of Electrical Cable Design and the Associated Fire Safety Concern

3.1 Insulated electrical cable fundamentals

A NPP can require up to 1,609 km of electrical cables to allow operators to control numerous plant processes from a central location [Subudhi 1996]. Virtually every system in a NPP depends on the continuous operation of electrical cables to provide a low resistance (highly conductive) transmission pathway for electrical energy to be conducted between two points while at the same time maintaining electrical isolation from other conductive pathways. Cable functionality implies maintaining the electrical integrity and electrical continuity of the associated circuit sufficient to ensure proper operation of a circuit or system [Subudhi 1996]. The nuclear regulating body (NRC) requires maintaining equipment necessary to shutdown the plant "free of fire damage." Therefore, electrical cables must be able to perform their intended function before, during, and after fire exposure as needed to achieve and maintain safe shutdown of the plant [Nowlen 2000]. A failure to do so would be considered an electrical cable functional failure.

Modern electrical cables use stranded metallic conductors, typically made from tinned copper or aluminum and surrounded by a high dielectric insulation material made of polymers, silicone-based or rubber-based materials [Anixter 1996]. Single or multiple stranded conductors surrounded by insulation grouped together within a single protective jacket, typically made of a polymeric material, to create a multi-conductor cable. The jacket serves a utilitarian purpose of providing physical protection of the insulated

conductors, environmental protection from water and ultraviolet radiation, and in some instances increased flame retardancy [Anixter 1996].

Advances in the manufacturing of electrical cables have allowed for a plethora of cable designs, including variations in the conductor size (expressed in American Wire Gage [AWG]), number of conductors, insulation and jacket materials, operating voltage, and inclusion of drain wires, shields, or metal armor to suit various applications. For operating NPP applications, cable functions can be binned into three generic categories, namely power, control, and instrumentation [Iqbal and Salley 2004].

Cables found in NPPs have different functions dependent on their application, thus the failure modes of cables cannot be generically evaluated, nor can the cable functional failure point be quantified without knowledge of the intend design function of the circuit that the cables are connected. The circuit specific failure characteristics are one factor that complicates the understanding of cable functional failure and the quantification of risks associated with fire-induced cable failure. The specific functions and functional failure mode characteristics of each cable type used in NPPs are discussed next.

Instrumentation cables are typically constructed of #14 AWG or smaller conductors with metallic shield, twisted conductor pairs or coaxial construction to eliminate induced or spurious signals from radio frequency or electromagnetic interferences. Instrumentation cables carry low level current (mA or μA), low voltage (50 volts or less) analog and digital signals to provide plant parameter indication and system status. These signals can be generated by sensors such as; temperature detectors, pressure transmitters, vibration detectors, thermocouples and fluid analyzers [Subudhi

1996]. Their delicate construction and low-level energy transmission causes instrumentation cables to be easily damaged from thermal conditions. Thermal damage can cause small leakage currents between conductive media which can result in abnormal circuit response (off-scale high/low, erroneous indication, erroneous permissive signals, etc). As a result, instrumentation cables damaged by fire may cause operator actions that are inappropriate for the actual state of the operating reactor.

Control cables are typically larger than instrument cables, ranging from #10-14 AWG in conductor size and constructed as a multi-conductor cable (i.e., more than one insulated conductor within a single cable). Control cables carry voltages in the range of 120-240 Vac or 125 Vdc and currents on the order of a few amperes. These cables are interconnected between components of a system, such as a motor starter, solenoid operated valve, medium voltage switchgear control circuit, relays, control switches/pushbuttons, and limit and torque switches. Control cables transmit signals to start, stop or change a systems operating state, along with providing component status indication such as plant annunciation, valve position, and motor operating status [Subudhi 1996]. Fire-induced damage to control cables can cause erroneous indication, loss of system control, maloperation or spurious operation of plant equipment. For these reasons, fire-induced damage to control cables poses a significant risk to NPP operations and the ability to achieve a reactor safe-shutdown condition.

Power cables are typically larger than #10AWG and can be single conductor or triplex cables (i.e., three conductor cable). Power cables supply the electrical energy to energize motors, load centers, motor control centers, heaters, batteries, and numerous other electrical loads. Operating voltage levels of power cables range from 120 Vac or

250 Vdc on up to the high voltage electrical transmission lines and can carry currents on the order of tens to thousands of amperes dependant on cable ampacity limits. Thus fire-induced damage to power cables will have minimal effects on the circuits powered from such cables up until a current limiting device is activated (fuse or circuit breaker) to clear the fault and de-energize plant equipment.

Figure 1 provides illustrations of common cable configurations for instrumentation, control and power multi-conductor cables. The black circles represent the electrical conductors, typically made of stranded aluminum or more commonly, tinned copper. The gray layer immediately surrounding the conductor is an extruded layer of insulation material. This insulation provides the electrical integrity cables rely on to provide their design function. There are many types of insulation materials, but most all can be categorized as either thermoset or thermoplastic materials. An explanation of these will be provided later. The last layer that is typically common to most electrical cables is the dark gray material that surrounds all of the insulated conductors in Figure 1. This is the jacket, also made of polymeric materials and provides a utilitarian protective function and is not relied on for electrical insulation [Anixter 1996].

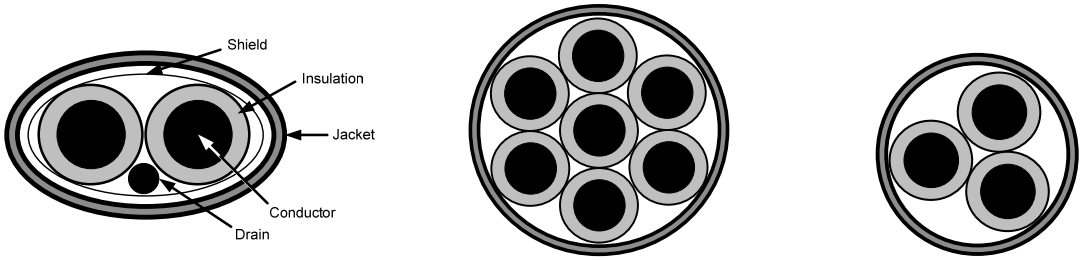

Figure 1. Illustration of multi-conductor instrumentation, control and power cables, respectively (not to scale)

Between the insulated conductors and the exterior jacket there can be various other materials including fillers to provide cable roundness, drain conductors and shield wraps to provide electromagnetic noise reduction for instrumentation and control cables, armoring to provide added physical protection, among other materials depending on the intended application and function of the cable [Anixter 1996].

Natural and synthetic polymers are typically used as insulation and jacket materials for insulated electrical cables. Polymers are composed of repetitive, simple units (monomers) that form longer molecules. The molecular properties such as the length, branching, and degree of crystallization will affect the characteristics of the polymers solubility, glass transition temperature, melting temperature, density, strength and other physical properties. In addition, additives and plasticizers can be used to increase the polymer performance regarding flame retardancy and the cable resistance to ultraviolet, water, oil, and biodegradation [Nowlen and Wyant 2008]. The type and amount of these additives can have an effect on the performance of electrical cable during severe fire conditions. Cable manufacturers use their own unique proprietary blends to achieve the desired cable specifications. This variation in additives and plasticizers cause the performance of cables using the same base polymer materials to behave slightly different under fire conditions. Therefore, not all PVC insulated cable fail at the same time from a constant exposing temperature or heat flux. Babrauskas also identifies lack of repeatability among cable fire short circuit testing due to short-circuiting involving mechanical contact between the conductors, but this was determined both by the stress in the conductors and by the exact details of the melting of the polymers [Babrauskas 2003].

The polymeric materials used in insulated electrical cables can be classified into two groups, thermoplastic (TP) and thermoset (TS). Thermoplastics such as polyvinyl chloride (PVC), polyethylene (PE), and ethylene tetrafluoroethylene (ETFE) are materials which soften and deform when heated without irreversible changes to the material and can re-solidify if cooled. Thermoplastic degradation occurs at a higher temperature than that of liquefaction. Thermoset materials such as chlorinated polyethylene (CPE), neoprene (CP), cross-linked polyethylene (XLP or XLPE), ethylene propylene rubber (EPR), and chlorsulphonated polyethylene (CSPE or Hypalon), are infusible, insoluble, and do not melt or flow after polymerization [Hirschler and Morgan 2008]. Thermoset materials cannot be liquefied by heat and cooled to solid form, but undergo chemical degradation. Materials classified in each group have a wide thermal degradation range, but in general TS polymers can withstand higher temperatures during longer periods of time than TP polymers [Nowlen and Wyant 2008]. Table 1 presents a listing of common electrical cable polymer insulation materials separated by class.

Table 1. List of common thermoset and thermoplastic electrical cable insulation materials [Anixter 1996]

Thermoplastic		Thermoset	
CPE	chlorinated polyethylene	CPE	cross-linked chlorinated polyethylene
PVC	polyvinyl Chloride	CP	neoprene
ETFE	tefzel	XLP, XLPE	cross-linked polyethylene
PTFE, FEP, PFA	teflon	EP, EPR, EPDM	ethylene propylene rubber
PE	polyethylene	CSP, CSPE	cross-linked chlorosulfonated polyethylene (trade name: Hypalon)
PP	polypropylene	SR	silicone rubber
TPE	thermoplastic elastomer	k-fiber	blend of polyaramid, phenolic-based and fiberglass fibers
PUR	polyurethane		

During heatup, polymer molecules increase vibration and intermolecular interactions have less effect as the molecules separates and the polymer expands. At the decomposition stage, covalent bonds begin to break causing the long polymer chains to

break into smaller segments. At this point, the damage to the polymer structure is irreversible. For thermoplastic materials, the decomposition point is above its melting temperature causing material to flow prior to any physical/chemical changes. For thermoset materials, their decomposition temperature is below it melting temperature. These characteristics explain why thermoplastic cables melt and thermoset cables tend to char and flake away during fire conditions. When a cable is heated sufficiently, the mechanical properties of the insulation will degrade, causing the electrical insulation resistance (IR) between conductive paths to decrease. If the IR decreases low enough for a current to flow across a voltage potential, an electrical fault may result [Nowlen and Wyant 2008].

Kazarians and Apostolakis describe the thermal threshold as a point where cable damage starts. At this temperature a cable will experience drastic physical changes, however, circuit failure would be delayed depending on the shape and characteristics of the cables. They go on to state that the exact modeling of these processes involved very complex formulations and its solution could be extremely time consuming, if not impossible [Kazarians and Apostolakis 1981]. From this it is understood that the threshold as a point where cable materials (jacket/insulation) begin to degrade, but doesn't refer to the point of cable electrical functional failure (i.e., cable is no longer able to perform its intended design function.)

Cable manufactures have recently developed "fire proof" cables designed to address redundant safety circuit requirements within NPPs. These cables are constructed of flexible stranded, high temperature conductors surrounded by composite inorganic layers, by electrical grade ceramified silicone rubber, or by mineral insulation

[Rockbestos-Surprenant 2003, Draka 2012]. These cables are not specifically evaluated in this thesis.

This section has provided a fundamental understanding of the design function and construction of electrical cables used in NPPs. For a more in-depth understanding of electrical cable design characteristics and cable construction, a cable handbook such as "The Wire and Cable Technical Information Handbook," available online from Anixter should be referenced.

3.2 Fire-induced cable and circuit failure modes

As discussed in the previous section, fire can damage electrical cables which may result in adverse effects to plant operations. In the commercial nuclear industry, the process of identifying fire-induced circuit failure modes is generally referred to as "circuit analysis." With an understanding of possible cable failure modes from fire effects, the resulting effect on circuit response and ultimately system response can be determined.

Circuit analysis can be broken down into three distinct tasks, namely, cable failure analysis, circuit failure analysis and functional impact assessment and quantification [LaChance, Nowlen, Wyant and Dandini 2003]. This concept is shown illustratively in Figure 2. What follows is a detailed description of the cable failure modes, circuit failure effects and functional impact assessment.

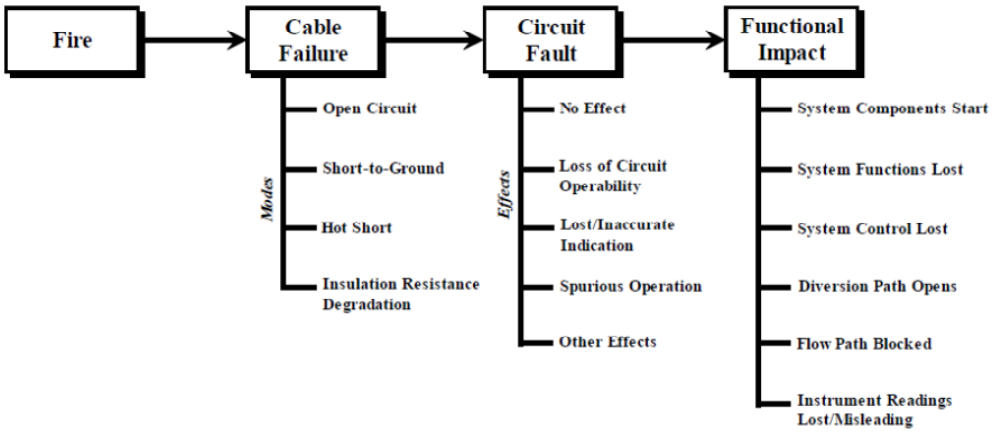

Figure 2. Circuit analysis process structure and associated terminology. [LaChance, Nowlen, Wyant, and Dandini 2003]

As discussed in this thesis, electrical cable functional failure refers to failure of an electrical cable to achieve its design function as a result of an exposure fire. Cable damage caused by other mechanisms (physical damage, water intrusion, aging, etc.) are not discussed here nor will cable damage caused by self-ignited cable fires. Although self-ignited cable fire are possible, NPPs' design compliance with standards on cable ampacity limits has greatly reduced the likelihood of these events.

There are three basic cable failure modes, which are:

- open circuit

  This failure mode results in the loss of conductor integrity (i.e, breaking of conductor). Figure 3 provides an illustration of a cable conductor open circuit. Note that opening of a circuit protective device (fuse, circuit breaker) can result in the same effect to a circuit as a cable conductor open circuit [LaChance, Nowlen, Wyant and Dandini 2003].

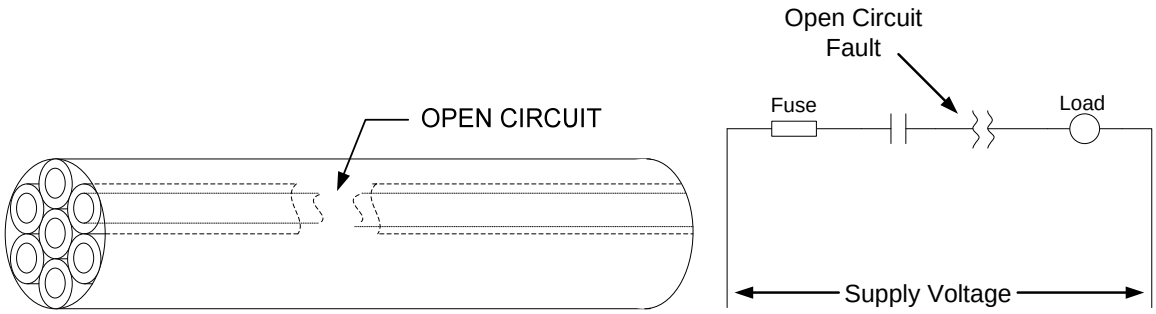

Figure 3. Illustration of electrical conductor open circuit (cable illustration on left, circuit illustration on right)

- conductor to external ground short circuit

  This failure mode involved formation of a short between one (or more) conductors and an external ground plane. The external ground plane can include (but is not limited to) grounded cable raceway, grounded cable shield wrap, grounded cable drain wire, or grounded cable armor. Figure 4 presents an illustration of a conductor short to external ground shown in blue on the left, and the corresponding circuit response on the right. Note that this failure mode doesn't include conductor-to-grounded conductor shorts, as this would be classified as conductor-to-conductor short [LaChance, Nowlen, Wyant and Dandini 2003].

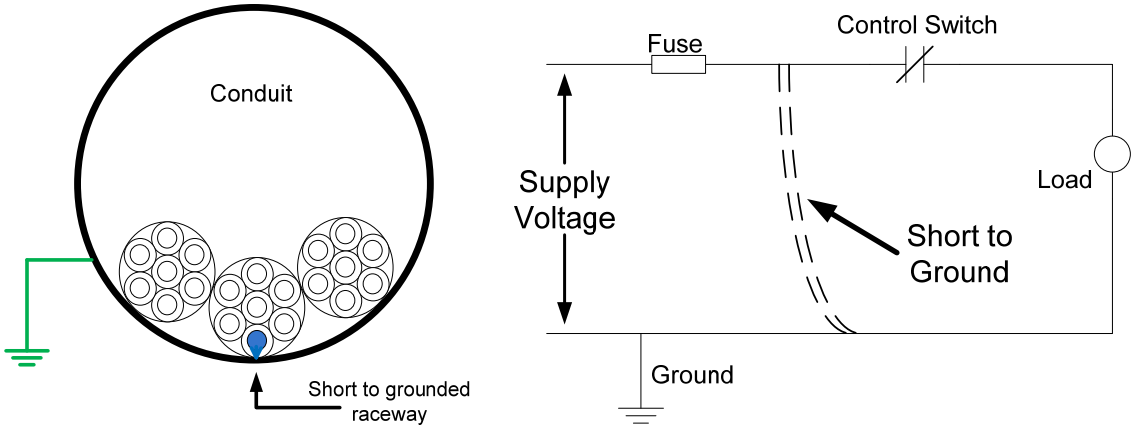

Figure 4. Illustration of conductor-to-external ground short circuit

- conductor-to-conductor short circuit:

  This failure mode involves formation of a short circuit between two (or more) conductors independent of any external ground. The conductor-to-conductor shorts may all be within the same cable (intra-cable shorting) or between conductors of different cables (inter-cable shorting) [LaChance, Nowlen, Wyant and Dandini 2003]. Figure 5 provides illustrative examples of an intra-cable and inter-cable conductor-to-conductor short circuit failures.

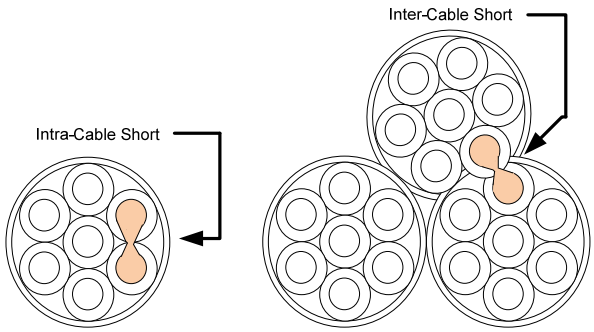

Figure 5. Intra-cable (left) and Inter-cable (right) conductor-to-conductor short circuit illustration

- Hot short

  A unique conductor-to-conductor short circuit where one (or more) energized conductors come in contact with one (or more) normally

non-energized or non-grounded conductors [LaChance, Nowlen, Wyant and Dandini 2003]. Figure 6 presents an circuit illustration of a hot short. Hot shorts are a circuit dependent failure mode.

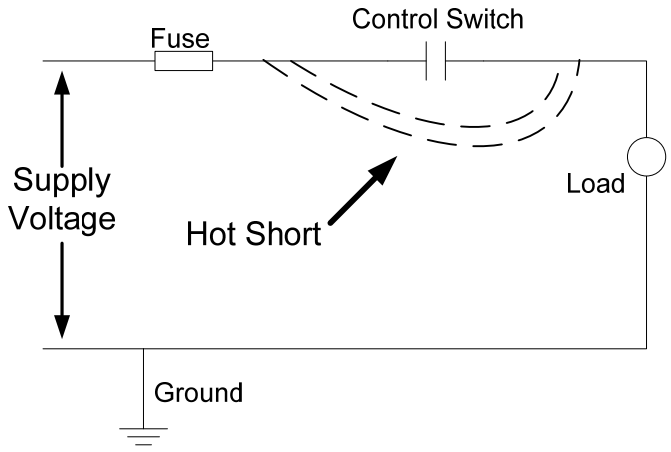

Figure 6. Illustration of Hot Short

In addition, some circuits are sensitive to leakage of current caused by changes in cable insulation resistance at elevated temperatures. This failure mode refers to either a "conductor-to-external ground" or a "conductor-to-conductor" short where a breakdown in the electrical quality of the insulation of one or more conductors occurs such that a high impedance short circuit is formed, and electrical isolation is degraded. The level of electrical insulation resistance reduction that constitutes a cable failure can only be defined in terms of the circuit of interest. (i.e., some circuits may function properly with only 1,000 Ω insulation resistance, while another circuit may be more sensitive and fail at higher insulation resistances, such as 10,000 Ω). These particular failures are of importance when analyzing instrumentation circuits, annunciation circuits and indication portions of control circuits.

Conductor-to-conductor hot shorts are of interest in risk quantification studies because they can lead to what are known as spurious operations, which is a circuit fault

effect. A spurious operation results in a component changing position as in the case of a valve or a component starting/stopping as in the case of a motor, pump, or compressor. Spurious operations are of concern because they can result in a valve re-position to an undesired state and possibly diverting reactor core coolant flow or blocking a flow path, thus challenging the operators' ability to achieve and maintain the reactor in a safe shutdown condition.

As shown in Figure 2, circuit fault effects are dependent on the circuit to cable conductor configuration along with the circuit function and design. The following provides a brief list of circuit fault effects, but is by no means exhaustive [LaChance, Nowlen, Wyant and Dandini 2003].

- No effect:

  the cable failure has no effect on circuit operation and continues to operate as if no cable failure was present

- Loss of power:

  the cable failure causes the circuit to become de-energized or trip upstream overcurrent protective devices (fuses, circuit breakers, etc.) due to cable failure modes that result in overcurrent conditions

- Loss of control:

  control of the circuit becomes unavaliable, any action to operate the circuit will be ineffective

- Lost/inaccurate indication:

  several cable failure modes can cause the loss of instrument indication or component position, or it could cause the instrumentation reading and

component position indication to be inaccurate. The ladder effect is of potential concern as a false indication that are neither off-scale low or off-scale high may result in operator actions that are inappropriate for the actual plant conditions.

- Spurious operation:

  an inadvertent energization of a device due to a hot short cable failure. It should be clarified that not all hot shorts lead to spurious operations. Only hot shorts to conductors that cause a circuit fault effect that energizes an end device are considered spurious operations. Spurious operations are synonymous to spurious actuations and refer to a device (solenoid, motor starter contactor, breaker trip/close coil) becoming energized and thus causing a component to change position or start/stop inadvertently. Circuits where equipment fails in the desired safe position as a result of circuit design (fail safe) when circuit power is lost, are not considered a hot short induced spurious operation.

- Other effects:

  depending on PRA analysts' objectives, there may be other circuit failure effects that are important to identify for risk quantification.

3.3 Risk contributions from insulated electrical cable

The traditional definition of risk is the probability of an event occurring times the consequences of that event. A simplified view of risk can be sought by asking three questions, referred to as the risk triplet; "What can go wrong?" "How likely is it?" and "What are the consequences?" [Callan 1998]. Fire PRA methods follow this general

structure, by estimating the fire-induced core damage frequency using a three-term model. These terms are (1) the frequency of the postulated fire or class of fire (f_i), (2) the conditional probability that the postulated fire will cause damage to some set of plant equipment ($P_{ed,j|i}$), and (3) the conditional probability that given the postulated equipment damage, the operators will fail to recover the plant and core damage would result ($P_{CD:k|i,j}$), expressed mathematically as [LaChance, Nowlen, Wyant and Dandini 2003]

$$CDF = \sum f_i \left(\sum P_{ed,j|i} \left(\sum P_{CD:k|i,j} \right) \right) \qquad \text{Equation 1}$$

Identifying components important to safely shutting down the plant, identifying areas where a fire could adversely affect these components, identifying fire ignition frequencies, mitigating features, and fire scenario consequences provides an overall quantitative assessment of the plant risk due to fire. A result of a high volume of electrical cables used in NPPs, the consequences that result from unique cable failure modes and the likelihood of having a fire affect electrical cables required to shutdown the plant results in certain cables being classified as high-risk contributors.

A cable doesn't have to ignite and burn to pose a risk to the operation of a NPP. For example an exposure fire may elevate the temperature of a cable to a point where an electrical cable functional failure occurs due to thermal breakdown of the conductor insulation, but below the cable jacket's ignition point. Loss of a cable's electrical functionality can cause various plant responses depending on the cable failure mode and the associated circuit(s).

Depending on the circuit and specific conductor failure mode, the circuit and thus plant response may vary widely. For instance, a conductor-to-conductor hot short may energize a specific indication lamp on a control panel in a main control room, while a

conductor-to-external ground short on the same conductor would result in the indication lamp becoming unavailable. Given the wide variety of circuit designs, numerous cable designs and plant cable routing configurations, along with varying plant fire hazard scenarios, efforts to develop a deterministic model to predict cable failure modes has become difficult to achieve. Because of this, most deterministic fire analysis methods assume all cables within a fire area under analysis fail in their worst case position to evaluate their affect on shutdown of the reactor.

The fire PRA methods used today attempt to quantify electrical cable failure by assuming cable damage occurs at a specific temperature and then assigning a probability likelihood estimate of that circuit experiencing a failure mode of concern. These likelihood estimates are based on a limited set empirical data to quantify the probability of a fire damage cable/circuit combination experiencing a spurious operation. Thus, using current methods, the fire PRA analyst calculates the thermal exposure to a cable via fire modeling and then assumes cable damage when the cable temperature exceeds generic single point threshold values. If the cable exceeds the generic threshold temperature, the analyst then assigns a likelihood estimate for the cable to experience a spurious operation. Although the previous section discussed the numerous functional failure modes of the cables and failure modes of the circuit, current fire PRA methods are not and may possible never be capable of predicting specific failure modes without large uncertainties.

In summary, probabilistic risk methods attempt to quantify the risk associated with fire scenarios capable of damaging electrical cables, identify the worst-case failure mode of an associated cable of a particular system in the fire area under consideration

and then assign failure mode likelihood estimates to quantify the risk to that specific cable failure. The failure mode likelihood estimates used today are based on expert judgment and a limited number of empirical evidence provided by EPRI.

4 Literature Survey

4.1 Standard test methods and the term qualified cable

Several standards exist related to the fire performance of electric cable. Most of these standards evaluate electrical cable ignition or flame spread characteristics and qualification of cables for use in a NPP environment. However, there is one standard that evaluates the electrical functionality and provides a rating of 1 or 3 hours for special fire resistant electrical cables. This section presents a summary of fire standards relating to electrical cable.

4.1.1 Standard Cable Flame Tests

NRC accepted flame propagation standards include IEEE 383, "IEEE Standard for Qualifying Class 1E Electric Cables and Field Splices for Nuclear Power Generating Stations," and IEEE 1202, "IEEE Standard for Flame-Propagation Testing of Wire and Cable" [NRC 2009, NRC 1978, NRC 1976]. IEEE 383 test standard qualifies an electrical cable to design basis events that are postulated to occur during the life of the plant. The standard addresses cable degradation with time (aging), followed by exposure to the environmental extremes of temperature, pressure, humidity, radiation, mechanical stress, or chemical spray or a combination of these events [IEEE 2004]. The flame propagation portion of this standard (current edition endorses IEEE 1202) provides a test procedure to determine flame propagation characteristics of cable in vertical cable trays due to ignition sources either outside of or within the cable system [IEEE 2006]. Thus if a cable is type tested to IEEE 383 and IEEE 1202 and passes, it is commonly referred to in the industry as a "qualified cable."

The term "qualified" indicates that a cable has passed the flame propagation portion of IEEE 1202, but doesn't directly indicate the cable's ability to maintain electrical functionality during fire conditions or provide any indication of cable robustness to fire from an electrical standpoint. Regardless, the terms "qualified" and "nonqualified" or "unqualified" cables have been used in the literature to classify cable electrical functional failure characteristics (critical heat flux, minimum thermal damage temperature threshold, etc.) Salley identified this flaw in the EPRI FIVE methodology which used insulation ignition temperatures based on data from qualified cables to indicate the temperature at which cable functionality is lost [Salley 2000]. Recent testing has shown that cable ignition is not synonymous with loss of electrical functionality, as cables have been shown to experience an electrical functional failure prior to ignition, concurrent with ignition, and after ignition. In several special cases, cables have ignited and not failed electrically [Nowlen and Wyant 2008, Gonzalez and Dreisbach 2008].

4.1.2 Fire Rated Cable Standard

Underwriters Laboratories (UL) has developed UL 2196, "Tests for Fire Resistive Cables" [Underwriters Laboratories 2001] and the Institute of Electrical and Electronic Engineers (IEEE) has developed IEEE 1717, "IEEE Standard for Testing Circuit Integrity Cables Using the Hydrocarbon Pool Fire Test Protocol," [IEEE 2011] that provide fire endurance ratings for electrical cables. These standards focus on circuit integrity cables, which are of a different design than those found in the current generation of operating NPPs. Circuit integrity cables are unique cables that are typically made of materials that undergo a chemical transformation into a ceramic material when heated or are constructed from special materials that prohibit the movement of cable conductors during

a thermal exposure, while maintaining a satisfactory high level of insulation resistance. In essence, these cables are constructed with a rated fire barrier already installed [Taylor 2010]. These standards expose cables to the standard time-temperature profile of ASTM E-119 or NFPA 251 for a 20 minute duration followed by a hose stream test. The circuit integrity is monitored by two incandescent lamps per circuit. The cable is deemed to fail if the lamp does not remain illuminated for the duration of the fire test.

The UL standard presents a very severe exposure and hose stream test, however the acceptance criteria is questionable. The use of an indicating lamp to signify cable functionality is an unrealistic comparison to actual plant equipment response. An incandescent lamp will remain illuminated with energized with only a fraction of its rated voltage. It is difficult to correspond cable functionality from an illuminated lamp to actual plant equipment where specific voltage and current requirements are needed to properly operate equipment such as motor starters and solenoid operated valves.

4.2 Cable fire testing

Numerous experimental and confirmatory fire test results can be found in the literature evaluating the performance of electrical cables to elevated thermal conditions. This section provides a summary of the fire testing conducted in the past related to nuclear safety.

4.2.1 Cable ignition and flame propagation testing

Prior to the 1975 Browns Ferry Fire, testing was conducted to evaluate the separation criteria specified in Regulatory Guide (RG) 1.75, "Physical Independence of Electrical Systems" which later endorsed IEEE 384 Standard Criteria for Independence of Class 1E Equipment and Circuits. The original intent of RG 1.75 was focused on

protecting redundant trains of equipment from a cable initiated fire in an opposite train. It was later shown through testing, that exposure fires presented greater risk to damaging redundant trains. After the Browns Ferry Fire the area of fire research expanded dramatically to evaluate the fire hazards associated with electrical cables. These testing programs focused on quantifying cable flame spread, ignition characteristics, and the performance of various systems or components such as cable tray covers, cable electric raceway fire barrier systems and cable coating. Although this testing provided valuable information on the fire hazards of electrical cable, there was typically no attempt to electrically monitor cable specimens to identify when an electrical cable functional failure occurred. Cable functionality was typically assumed to be lost when the cable ignited or in some cases when the cable jacket material showed signs of physical degradation. It wasn't until the early 1980's when the first tests instrumented electrical cables to determine when cable functionality was lost from fire exposure.

This type of testing included those done by Przybyla and Christian who performed vertical flame spread type testing to identify the sensitivity of altering various parameters of the IEEE 383 standard flame spread standard [Przybyla and Christian 1978]. Klamerus also preformed numerous testing to evaluate the physical separation guidance, and cable protective systems (coatings, covers, electric raceway fire barrier systems) [Klamerus 1977, 1978a, 1978b].

4.2.2 Cable fire testing using electrical functionality as failure criteria

The private and government bodies have conducted numerous cable fire testing projects to evaluate various aspects of the fire hazards cables pose to the safe operation of

a NPP. The following provides a brief summary of those testing projects relevant to this Thesis.

4.2.2.1 EPRI Electrical Cable Damageability Study

EPRI performed a study to evaluate the damageability characteristics of cables under varying thermal environment. The critical heat flux and critical energy (product of available heat flux and time to initiate damage) were two parameters used to quantitatively define the damage potential of electrical cables. The Factory Mutual (FM) combustibility apparatus consisting of four coaxially arranged radiant heaters was used to expose the cable sample to a maximum heat flux of 70 kW/m^2. A variety of qualified and unqualified cables were evaluated for insulation degradation, piloted ignition, and electrical functional failure [Lee 1981, LaChance, Nowlen, Wyant and Dandini 2003].

Electrical functionality was monitored by using a voltage drop principle that involved connecting all conductors within a test to each other via resistors, with a variable resistor connecting one end of the conductor network to ground and the other end connected to a power source. The variable resistor allowed for recording voltage drop which would change as conductors shorted together. A short to ground would also be identified when the voltage reading was zero volts. The results indicated that the critical heat flux ranged from 9-24 kW/m^2, with critical energies ranging from 5,560 to 23,700 kJ/m^2.

4.2.2.2 Cable Damageability Experiments

Lukens conducted one of the first experiments that evaluated the thermal damage threshold for functionality of electrical cables [Lukens 1982]. This testing was part of a larger program to determine the adequacy of the 6.1 m separation criteria required by

NRC regulations. The cable damageability program tested both IEEE-383 qualified and unqualified cables by exposing them to a variety of constant heat flux exposures in the first phase of testing and to a variety of constant temperature environments in the second phase. The results reproduced in Figure 7 indicated a critical heat flux of 18 kW/m^2 for qualified cables and 8 kW/m^2 for non-qualified cables would be sufficient to cause electrical failure. Under constant temperature environments (oven tests) electrical damage was observed at a temperature of 250 ˚C for qualified cable and 130 ˚C for non-qualified cable when exposed for 60 minutes at constant temperatures.

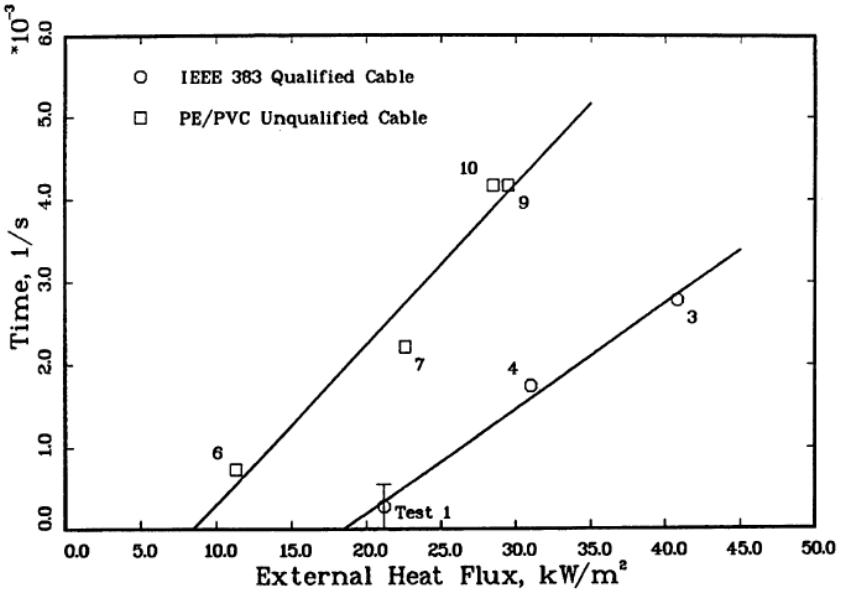

Figure 7. Reciprocal time to electrical failure as a function of external heat flux

Lukens' work provided early insights to the relative robustness of qualified versus non-qualified cables and provided indication that the IEEE-383 standard supports extending the time to electrical damage along with the standards intent of flame spread limitations. The methods used to determine electrical functional failures, were crude at best, and although the methods could distinguish gross cable failure, it is unable to identify the point of cable functional failure. The critical radiant heat flux results using a

linear least squares approach were in good agreement with the data, however, the application of a constant thermal environment is questionable and difficult to use in cable damageability evaluations. The lack of data reporting makes it difficult to relate the occurrence of electrical failure with a specific cable temperature, but summary tables are provided to allow for a crude approximations of cable temperature at electrical cable functional failure. Nowlen later took this data and developed time to damage plots (discussed in section 4.2.2.5).

4.2.2.3 Cable Damageability Test Results Phase 1

Wheelis performed 13 tests using qualified and unqualified cables to evaluate the electrical failure to non-steady state fire environments [Wheelis 1986]. The qualified cable was a three conductor, #12 AWG with XLPE insulation and jacket, rated for 600 volts (i.e., low voltage power cable). The unqualified cable was a three conductor, #12 AWG, with 20/10 PE/PVC insulation and PVC jacket. Electrical functionality was determined by connecting the conductors of the cables to three phase 120VAC power supply. Voltage measurements on each conductor could determine when conductor-to-conductor short or conductor-to-ground short occurred. Cable thermocouple measurements were made underneath the cable jacket.

This testing instrumented the same cable for electrical and thermal response, which may have resulted in self-induced cable failure from the interaction between the electrical circuit and the conductive thermocouple leads. It was also note that both qualified and unqualified cables "heal" themselves to some extent. During cool down it was observed that the insulation resistance increased between conductor-to-conductor shorts, in some cases the insulation resistance returned to pre-test measurements. This

phenomenon was attributed to the cable thermal expansion and contraction of the metallic conductors. The results indicated that the qualified cables failed between 4.16 and 10.25 minutes with an average failure temperature of 427 °C, while the unqualified cables failed between 4.5 and 9.25 minutes with an average failure temperature of 457 °C. These results contradict the basic assertion that qualified cables are more robust to thermal insult than unqualified cables. The author noted that these inconsistencies may have been due to the types of thermocouples used as both sleeved and unsleeved sub-jacket thermocouples were used and an approximate 50 °F difference in temperature measurements were noted.

4.2.2.4 High Temperature Steam Testing

Jacobus and Fuehrer performed high temperature steam and submergence testing on cables that had been aged by thermal and radiation energy to achieve a simulated "end of life" condition [Jacobus and Fuehrer 1990]. The testing included 12 cable types representative of typical cables used inside containment of light water reactors. For each cable type, a sample was aged for three, six, and nine months with one sample left unaged. The six month sample represented a 40-year life assuming activation energies of 1.15 eV, an ambient temperature of 55 °C, and a cumulative radiation dose of 400 kGy. The high temperature steam testing is not required for cable qualification per IEEE-383.

Following aging each set of cables was exposed to a loss-of-coolant accident (LOCA) simulation. The LOCA simulation included exposure to accident radiation for 210 hours and 193 hours for the six and three month samples, respectively. Following the accident radiation exposure, the cables were exposed to a high temperature and

pressure steam LOCA environment similar to that given in IEEE-323, "IEEE Standard for Qualifying Class 1E Equipment for Nuclear Power Generating Stations."

All of the six month aged cables that survived the LOCA testing were then subjected to a submergence test that lasted 1000 hours at 95 °C. The set of cables aged for three months were subjected to the high temperature steam testing consisting of a steam exposure at temperatures as high as 400 °C. Nowlen and Jacobus suggested that these steam test results can be applied to cable thermal damageability estimates based on the assumption that superheated steam and heated dry air produced consistent results (±10 °C) [Nowlen and Jacobus 1992]. However, the purpose of these tests were specifically for obtaining some quantitative information on the failure thresholds of cable exposed to high temperature steam conditions.

During testing, the intended temperature profile for the steam exposure was not followed due to complication with the steam system. The actual profiles are shown in Figure 8.

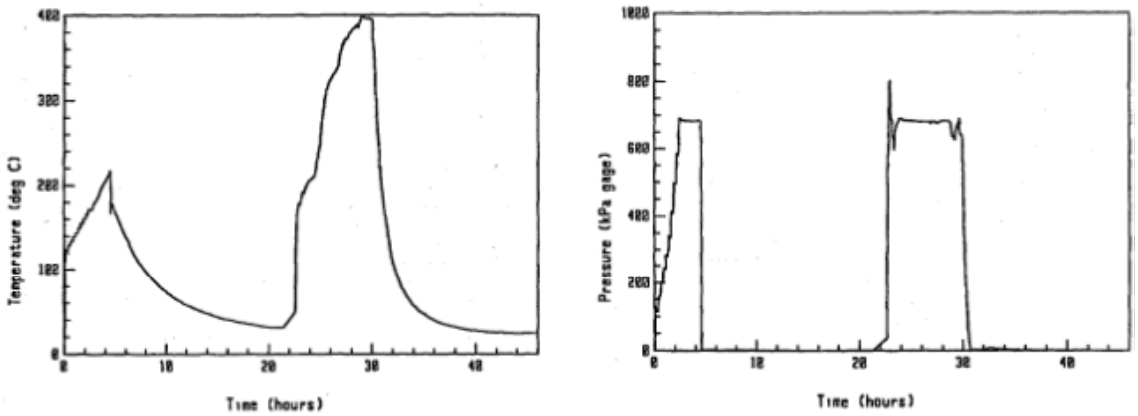

Figure 8. Pressure and Temperature profile for High Temperature Steam 3-month aged samples [Nowlen and Jacobus 1992]

The failure thresholds reported are presented in Table 2 for each insulation material for a 1,000 Ω/100 m and a relaxed 100 Ω /100 m insulation resistance failure

criteria. It is interesting to note that current NRC guidance uses the relaxed failure criteria in several of its guidance documents, except for the Kerite-FR material [EPRI/NRC-RES 2005, NRC 2005]. A basis for the use of the relaxed criteria could not be found.

Table 2. NUREG/CR-5655 cable insulation failure criteria from high temperature steam tests.

Insulation Material	Sample Size	Failure Temperature Range (°C)	
		IR Failure Criteria 1,000 Ω/100 m	IR Failure Criteria 100 Ω/100 m
XLPO	13	254-378	299-388
EPR	16	235-400	370-400
Silicone Rubber	2	396-400	396-400
Kerite FR	2	153-171	372-282
Polyimide	1	399	399

4.2.2.5 Fire Safety Research at Sandia National Laboratories

Nowlen identifies time to damage data for unprotected cables of the qualified and unqualified varieties. A 3/C #12AWG XLPE insulated/jacketed qualified cable failed in 9 minutes, while a 3/C #12AWG 20/10 PVC/PE insulation and PVC jacket unqualified cable failed in 6 minutes when exposed flame region of a 41 kW fire [Nowlen 1989].

Nowlen later evaluated the cable damageability tests done by Lukens and developed time to electrical failure plots, presented in Figures 9 and 10 for unqualified and qualified cables respectively. Iqbal and Salley later refined these estimates [Iqbal and Salley 2004]. Cables were energized with 320 Vdc and 5 A and monitored for when a conductor-to-ground short occurred, indicating failure. Sub-jacket and air thermocouples were used to measure temperature.

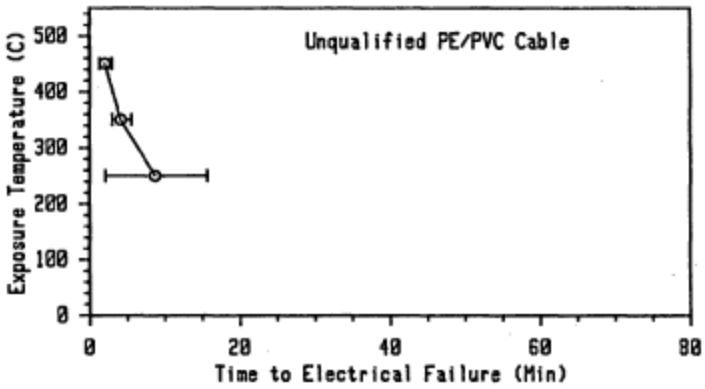

Figure 9. Cable steady-state thermal damageability results for a non-rated PE/PVC 3-conductor power cable [Nowlen 1989]

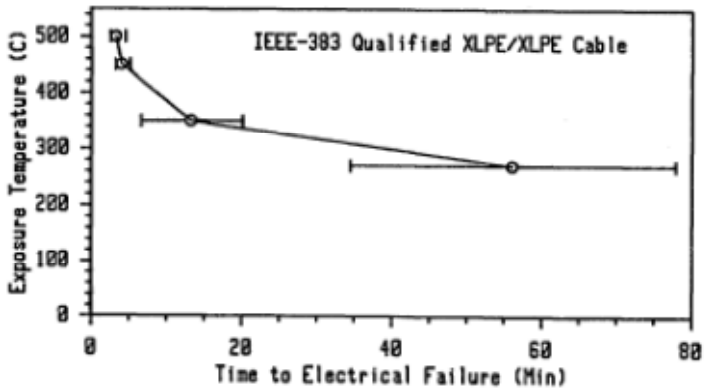

Figure 10. Cable steady-state thermal damageability results for a rated low flame XLPE 3-conductor power cable [Nowlen 1989]

4.2.2.6 Fire Dynamics Tools (FDT^s)

Iqbal and Salley present a compilation of cable failure threshold and time to damage information. Based on the information collected from NRC sponsored research [Nowlen 1989, Nowlen 1991, Jacobus and Fuehrer 1990], testing performed by the Tennessee Valley Authority [Salley 2000], and expert opinions from Mowrer, Funk and Salley [Budnitz 2002], Iqbal and Salley suggest a failure threshold of 330 °C for thermoset and 205 °C for thermoplastic insulated cables [Iqbal and Salley 2004].

In specifying the thermoset threshold, Salley and Iqbal discredit the test results from NUREG/CR-5384 due to the relatively long failure times and early vintage of cable tested. Also disregarded are the XLPO results from the high temperature steam tests as a

result of its lack of use in NPPs. Therefore, the specification of 330 °C is based on the performance of the XLPE insulated Rockbestos Firewall III material, a product the authors view as a poor performing thermoset material. The authors made a special exception to a cable product identified as Kerite-FR a thermoset material they suggest should use the lower thermoplastic failure criteria (205 °C) due to its poor performance.

The EPRI/NRC-RES fire PRA method uses generally agreed upon threshold values for each class of cable insulation (330 °C for thermoset insulated and 205 °C for thermoplastic insulated cables). The fire PRA method also presents the recommended thermoset material specific thresholds, as presented in Table 3 [EPRI/NRC-RES 2005].

Table 3. Current NRC Accepted Cable Insulation Specific Thermal Damage Criteria

Conductor Insulation Material	Sample Size	Reported Failure Temperature Range (°C)	Recommended Failure Threshold (°C)
Cross-linked PolyOlefin (XLPO)*	13	299-388	299
Cross-linked Polyethylene	12	320-388	320
Ethylene Propylene Rubber (EPR)	16	370-400	370
Silicone Rubber	2	396-400	396
Kerite FR	2	372-382	372
Polyimide or Kapton	1	399	399

*Includes the specific subclass Cross-linked Polyethylene

These values were obtained from equipment qualification testing performed to evaluate the performance of electrical cable under submerged and high temperature steam environments [Jacobus and Nowlen 1990]. Nowlen and Jacobus suggest that these steam test results can be applied to cable thermal damageability estimates based on the assumption that superheated steam and heated dry air produced consistent results (±10 °C) [Nowlen and Jacobus 1992]. The thermal failure temperatures obtained from

the superheated steam experiments corresponded to the electrical cable functionality being reduced to an insulation resistance of ≤100 Ω/100 m.

A more stringent electrical functionality threshold of ≤1,000 Ω / 100 m may be applicable to actual circuit configurations and an evaluation of the electrical failure point based on electrical insulation materials may be warranted. At a ≤1,000 Ω / 100 m insulation resistance threshold, the corresponding failure temperature would be lower than those specified in Table 3. This brings into question the NRC guidance specific to Kerite-FR cable which used the lower 100 Ω/100 m criteria. It is unclear as to why the more conservative criteria were not used for all cable insulation types from this testing.

The recommendations for the thermoplastic failure criteria are based on test results from PVC and PE insulated cables and expert judgment from Mowrer, Funk and Salley [Budnitz 2002]. Their recommendations are consistent among one another and tend to imply less uncertainty.

Iqbal and Salley also present a synopsis of cable thermal failure data related to the time to electrical failure based on constant temperature and constant heat flux experiments. Their results are presented in Equations 2 and 3 and Figure 11 for the time to damage estimation based on exposure temperature.

Thermoplastic cable time to damage (constant temperature)

1/(time to damage : seconds) = 3.488E-05 x (Temp: °C) - 7.467E-03 Equation 2

Thermoset cable time to damage (constant temperature)

1/(time to damage: seconds) = 3.343E-05 x (Temp: °C) - 1.044E-02 Equation 3

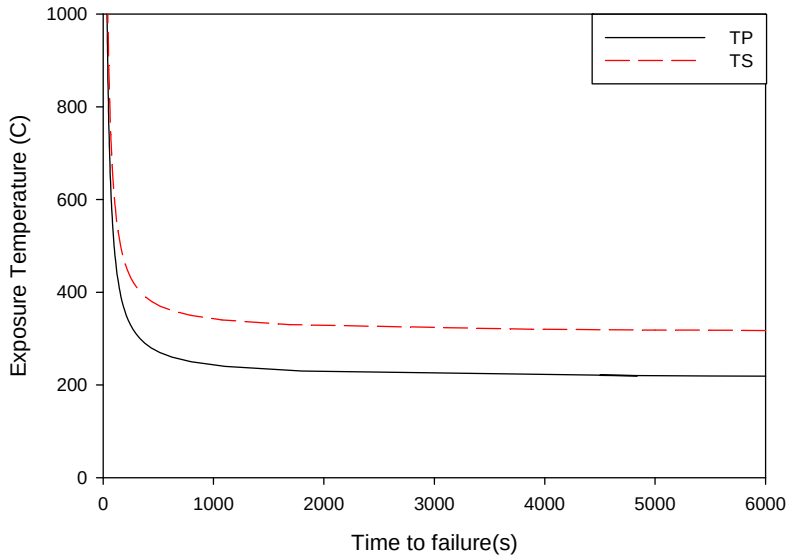

Figure 11. Plot of Cable Thermal Damage Curve Exposure Temperature vs. Time to Failures [Iqbal and Salley, 2004]

4.2.2.7 Thermal Aging Effect Testing

Nowlen stipulated electric cable damageability thermal threshold based on his accelerated aging tests on cables to evaluate thermal performance for aged cable samples [Nowlen 1991]. Salley later suggested that the aging procedure may have been severe enough to change the chemical properties of the cable thus invalidating the results [Salley 2000]. However, the testing does provide valuable information on unaged (control) cable samples of the XLPE and EPR variety. Nowlen documents the failure threshold of an unaged Rockbestos Firewall III, XLPE insulated, Neoprene jacketed, 3/C, #12 AWG, 600V light power/control cable to be 325-330 °C, and that of a BIW Bostrad 7E EPR insulated, CSPE jacketed 2/C, #16 AWG, 600 V instrumentation/signal cable to be 365-370 °C. The thermal environment was convective in nature and failures of the cables were indicated by clearing a 2 A fuse on a 208 V three phase system. Nowlen's conclusions indicated that the aging improved the performance of the Rockbestos cable (350-365 °C) and decreased the performance of the BIW cable (345-350 °C).

4.2.2.8 EPRI/NEI Spurious Actuation of Electrical Circuits Due to Cable Fires

The first testing project to specifically evaluate fire-induced functional failure modes of electrical cable for use in risk applications was jointly sponsored by the EPRI and the Nuclear Energy Institute (NEI). The testing program evaluated electrical cables performance under severe fire conditions to assess the various parameter effects on the likelihood of cable hot shorts and their potential to cause spurious actuations. A follow-on effort sponsored by EPRI documents an expert elicitation panel evaluation of the EPRI/NEI testing results, along with establishing conditional best estimate probabilities for spurious operations. This report provides some general insight on how the tests were performed as documented in EPRI Report 1006961, "Spurious Actuation of Electrical Circuits Due to Cable Fires: Results of an Expert Elicitation" [EPRI1006961].

The following is a brief description of the EPRI/NEI testing program,

> "Briefly, the test series, carried out in 2001, covered three different types of cables: a specific type of armored cable, several types of thermoplastic cable, and several types of thermoset control cable. Within these three broad types, different cables consisting of different numbers of conductors were tested, ranging from single-conductor to eight-conductor cables. With the exception of a few instrument cables tested by Sandia National Laboratories, all cables tested were control cables, not instrumentation or power cables. Eighteen different tests comprised the test matrix. The test fire, using a diffusion flame burner, was itself always external to the cables being tested, but sometimes the cables were in the direct fire plume and sometimes they were in the hot gas layer. The tests concentrated on cables in cable trays of differing loadings, but a few tests studied cables in conduit. Two tests used cables in a vertical configuration. The tests were all conducted in a steel room enclosure, 8 feet high by 10 feet square, with a simple opening for external ventilation in one wall, whose vertical location varied from test to test. During discussions among the expert panelists, it was observed that some of the tests appeared to be characterized by limited ventilation. However, it is not known whether this had an important influence on the results, expressed in terms of temperature measured at the cable or of "cable damage" (however defined)." [Budnitz 2002]

The results from the testing and expert elicitation were subsequently used to develop conditional probability of fire-induced spurious operations, given cable damage that are found in NUREG/CR-6850 (EPRI TR 1011989), which documents the current state-of-the-art methods for performing fire PRA at NPPs.

As mentioned previously, the NRC was invited to observe and participate in this testing. The NRC supported this participation by contracting with SNL to instrument cables in most of the tests, which provided additional data on fire-induced circuit failures and a better characterization of the testing environment. The information on this work is found in NUREG/CR-6776 "Cable Insulation Resistance Measurements Made During Cable Tests" [Wyant and Nowlen 2002]. Additionally, Appendix D in NUREG/CR-6834 "Circuit Analysis – Failure Mode and Likelihood Analysis," provides details on the results of the EPRI/NEI testing [LaChance, Nowlen, Wyant, and Dandini 2003].

Figure 12 provides a plan view of the EPRI/NEI experimental set up. The chamber door opening was 76 cm wide by 2.1 m high in the center of one wall. This was the only vent in the room. A diffusion sand burner was 30 cm by 30 cm providing a fire intensity controlled by a propane flow rate in the range of 70 to 350 kW. Most of the tests used ladder back cable tray formed with a 90 degree bend intended to provide a constant physical stress to the cable and conductors. The cable tray assembly was elevated 1.5, 1.8, or 2.1 m above the concrete floor. A manually activated water sprinkler head located in the top corner of the test enclosure was used as needed during the testing [Wyant and Nowlen 2002, LaChance, Nowlen, Wyant and Dandini 2003].

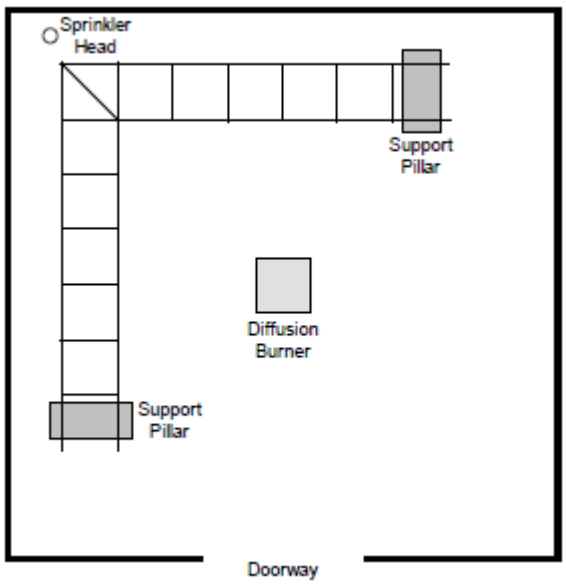

Figure 12. Plan view of EPRI/NEI test arrangement [Wyant and Nowlen 2002]

The EPRI/NEI testing used surrogate circuit to monitor the electrical response of the fire damaged cables. These circuits mimicked a motor operated valve circuit commonly found in NPPs. The circuit was connected to the cables exposed to the fire conditions such that there were several source and target conductors co-located within the same multi-conductor cable and also located among various cables in a cable bundle (see Figure 13). Source conductors are considered any conductor in a cable that is energized and can provide electrical power. Target conductors are any non-energized conductors that are connected to an end device or indication lamps. When a source conductor comes in electrical contact with a target conductor, a hot short occurs. A spurious operation occurs when the target conductor was connected to an end device that when energized changes state, or when a component such as a motor starts or stops without operation action. The physical circuits themselves were not exposed to any fire conditions. Each cable conductor was monitored for voltage and current response to allow for post test evaluation. Temperature measurements were also made at numerous locations within the

cable tray. Type K thermocouples were placed on the jacket surface and wrapped with one layer of fiberglass tape to ensure sufficient thermocouple bead contact with the cable jacket surface.

Figure 13. EPRI/NEI cable bundle [LaChance, Nowlen, Wyant, and Dandini 2003]

NRC/SNL fielded two types of circuit diagnostic systems during the EPRI/NEI testing. One system referred to as the insulation resistance measurement system (IRMS) measured the electrical resistance between conductors and between conductors and any common ground conductive path (cable tray, conduit, other cable conductors, etc.).

The second system used was a mock-up instrumentation circuit. The circuit simulated a 4-to-20 mA instrumentation loop commonly used in NPP and monitored the degradation of the transmitted signal. An electrical schematic of the instrumentation loop is shown in Figure 14. A constant current source located on the upper left corner of this figure provides a constant 15 mA current source and a voltage transducer located on the right of the illustration measure the voltage drop across a known resistance that represents an indication dial and allows for the calculation of current on this side of the circuit. Any current measurement less than 15 mA indicates that current was leaking from the conductor and the cable was experiencing some level of insulation degradation.

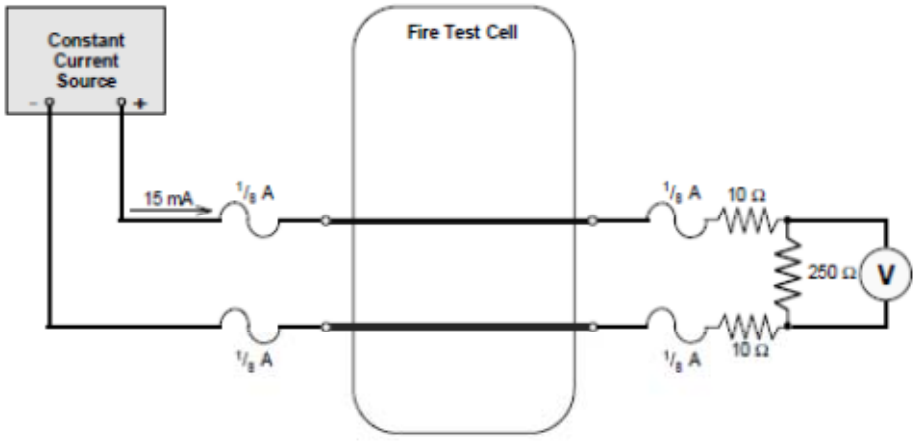

Figure 14. Illustration of instrumentation current loop. [Wyant 2002]

The NRC/SNL test circuit results identified two important facts about fire-induced cable failures. First it was noted that multi-conductor cables tend to display initial failure modes involving intra-cable hot shorts (i.e., shorts between conductors within a multi-conductor cable). Second the failure modes for thermoset and thermoplastic instrumentation cables tended to be different. The thermoplastic cables failed abruptly to an off scale low signal, while thermoset instrumentation cables showed a gradual loss of current over a finite period. In real life applications, these thermoset type cable failures would cause plant indication (tank level, system pressure, etc.) to show that the parameter of interest was decreasing and could result in the operator taking inappropriate actions. Similar failure modes were not observed in the control cable testing.

The NRC/SNL report identified several phenomena that the author felt required further investigation, including comparison between ac and dc failure modes, tray versus conduit likelihood of shorting to ground. Both of these suggestions were evaluated during subsequent testing described in section's 4.2.2.10 and 4.2.2.12. The author also noted that open circuit failure modes were not observed in any test and suggested that

these failure modes are not likely to occur at the systems operating voltages (120 Vac, 100 Vdc).

4.2.2.9 Determination of Failure Criteria for Electric Cables Exposed to Fire For Use in a Nuclear Power Plant Risk Analysis

Murphy performed radiant cable damage tests using the Sandia National Laboratories Penlight apparatus to evaluate failure criteria [Murphy 2004]. The experimental program focused on power and control cables including two thermoset insulated (EPR, XLPE) cable types. These cables were exposed to heat fluxes ranging from 14 kW/m^2 up to 97 kW/m^2. Cable functionality was evaluated using the SNL IRMS to measure insulation resistance drop between conductors during the thermal exposure. Murphy could not recommend a single cable failure temperature for all cable types, but suggested a temperature between 400 and 450 °C for EPR and XLPE insulated cables. It was also noted that regarding relative cable robustness to thermal insult, the EPR cable was more robust than the XLPE cable.

4.2.2.10 SNL Fire-Induced ac Circuit Response Testing (CAROLFIRE)

The testing programs described in this section and section 4.2.2.12 provide the data set that will be evaluated in this thesis. Current use of the data from these two experimental testing programs has been limited to risk-informing fire protection inspections and has not yet been used widely to advance the state of the art methods for quantifying the risk associated with fires in NPPs. The data from these two testing programs will be used to evaluate the THIEF one-dimension heat conduction model.

The NRC sponsored Cable Response to Live Fire (CAROLFIRE) testing project was conducted by SNL to address two areas of research; namely, provide experimental

data to support resolution of regulatory concerns identified as 'Bin 2' circuit failure items in NRC Regulatory Issue Summary 2004-03 Revision 1, "Risk-informed Approach to Post-fire Safe-Shutdown Circuit Inspections," and to improve fire modeling techniques to reduce uncertainty in predictions of cable response to fires. Small-scale radiant and intermediate-scale diffusion flame exposures were used on a variety of power, control, and instrumentation cables. The cables were monitored for thermal and electrical response. The small-scale testing monitored electrical cable functionality using the IRMS, while the intermediate-scale tests used the IRMS and a surrogate circuit designed to mimic an NPP alternating current (ac) motor operated valve (MOV) motor starter circuit [Nowlen and Wyant 2008].

A small-scale radiant exposure apparatus, known as the "Penlight," was used, as pictured in Figure 15, with an illustration shown in Figure 16. A horizontal hollow cylindrical inconel metal shroud acted as a gray body radiator that was heated by 0.61m long liquid cooled quarts lamps which surround the exterior of the shroud. The shroud had a 0.514 m inside diameter and was 0.813 m long. The test specimen (cables) were placed in the center of the shroud, along with any cable raceway supports, and exposed to the well control symmetrical radiant heat flux. The temperature and heat flux emitted from the shroud was nominally uniform over the central 0.61 m heated portion of the shroud surface. For the temperatures used in testing, the shroud emissivity was approximately 0.81-0.82 [Nowlen and Wyant 2008]. Insulation covers are placed on the ends of the shroud during testing to reduce convective heat loss.

Figure 15. Photograph of Penlight small-scale radiant heat apparatus shown during startup testing for the DESIREE-Fire project, without cables in apparatus [Nowlen and Wyant 2008]

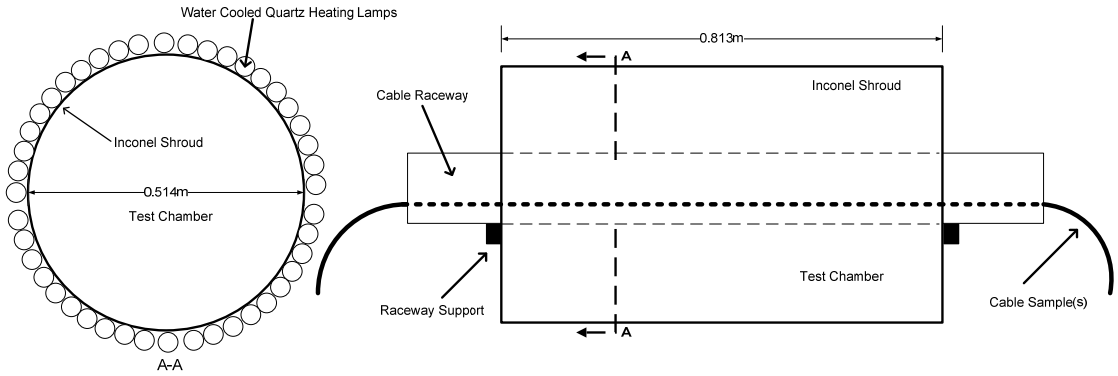

Figure 16. Small-scale radiant exposure apparatus

Nowlen provides temperature profiles of the inconel shroud in NUREG/CR-6931 Volume 2, showing that "the most intense exposure was at the center of the shroud's axial dimension (half way through the horizontal cylinder)" [Nowlen and Wyant 2008]. This indicates that the cables thermal exposure was greatest at the center for the shroud radial axis and was likely the location of cable failure. Factors that affect the uniformity of the cable exposure conditions included the shroud end conditions, raceway shadowing

effect, and cable location within chamber. The shroud ends were closed using 24 mm thick low-density solid refractory insulation board material. These end covers were used to reduce convective losses but did not provide a perfect seal around cables and cable raceways. The insulating ends were not heated during any of the tests. This causes the temperature profile to drop off near the end of the cylinder. Cable trays and rigid steel conduits were used during penlight tests. Both raceway types provided some level of shadowing the incident heat flux from the shroud. In the conduit case, the conduit acted as a secondary shroud that heated up from the penlight exposure and subsequently heated the cables within the conduit by radiation and conduction. The cable tray sides and rungs also shadowed the heat flux of the shroud but due to the open ladder back type cable trays used, the majority of the cables surface area was still in direct line of sight with the penlight shroud. The penlight exposure was controlled using a feedback loop that used a thermocouple shroud temperature measurement taken horizontal from the radial and axial center of the shroud. For the exposures used in CAROLFIRE, constant heat fluxes were used for all penlight tests. The penlight apparatus typically reached steady state conditions within 120 seconds.

An intermediate-scale testing apparatus was used to provide more realistic flame exposure conditions without the costs and time demands associated with full-scale testing. The intermediate-scale apparatus was based off of the ASTM E603 standard room fire facility with slight modifications. Figure 17 presents a diagram of the testing apparatus. The test apparatus was 0.6 m higher than the standard fire room size and had the bottom 1.8 m open to allow sufficient ventilation to eliminate the possibly of oxygen-limited combustion, a defect that apparently occurred during the NEI/EPRI testing

[Wyant and Nowlen 2002]. The top 1.2 m was enclosed, including the ceiling, with a gypsum type material to allow the development of a hot gas layer. As Figure 17 shows, there were numerous cable exposure locations in the apparatus labeled A-G to provide flame, plume, and hot gas layer exposure conditions within one test. The entire intermediate-scale assembly was located within a larger room to reduce environmental effects, however the room configuration did not allow for oxygen consumption calorimetry. A surrogate circuit simulating an ac motor starter contractor, commonly used in MOV circuits, was instrumented to monitor voltage and current on all cable conductors. The IRMS system was also used.

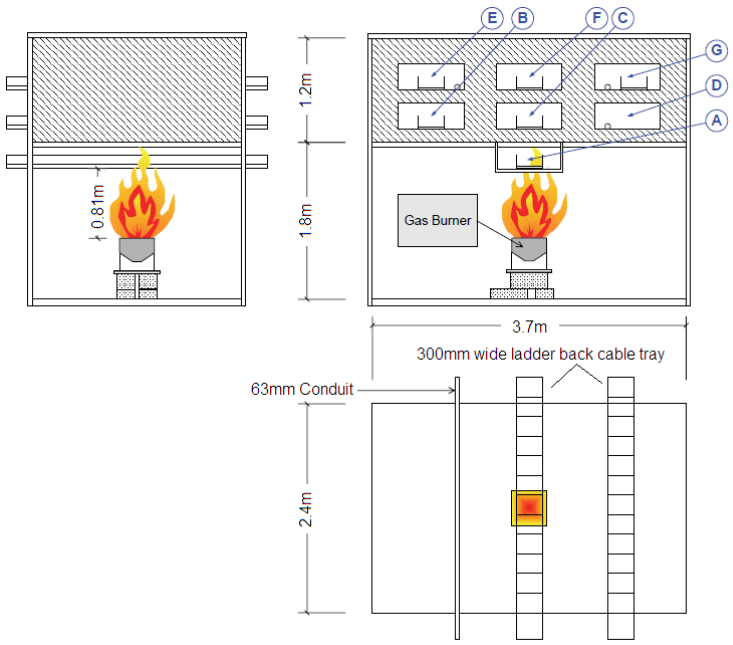

Figure 17. Intermediate-scale diffusion flame exposure apparatus [Nowlen and Wyant 2008]

Both scales of testing instrumented the cables similarly for thermal response. Type K (Chromel-Alumel) thermocouples were used in all tests, with bare-bead Teflon insulated TC's typically used to measure cable jacket surface and air temperatures and stainless steel sheathed ungrounded TC's used for measuring sub-jacket and cable core

temperatures. Nowlen notes the difficulty of measuring cable jacket surface temperatures due to the struggle to maintain the thermocouple bead in contact with the cables surface during testing as the cable tends to swell and blister when heated [Nowlen and Wyant 2008]. Cable surface thermocouples were attached to the jacket with one and a half wraps of 3M fiberglass tape, ensuring that only one layer of tape was between the thermocouple bead and air. This configuration is not ideal as the tape adds an additional barrier between the bead and exposure environment, but was done to try and achieve consistent temperature results. Sub-jacket thermocouples were used to measure the cable temperature just below the cable jacket material to characterize the temperature profile of the cable conductor insulation. To achieve a representative measurement, an incision was made 20-30 cm from where the thermocouple bead was desired to be located. Then the thermocouple was inserted into the incision and slide along the conductors just below the cable jacket. The distance a thermocouple could be slide under the jacket was depending on the cable construction. After the sub-jacket thermocouples were inserted, the incision was closed by wrapping with fiberglass tape. Figure 18 provides an illustration of sub-jacket thermocouple placement. Thermocouple measurements were taken at 100 hertz with a simple average of 100 samples recorded every second.

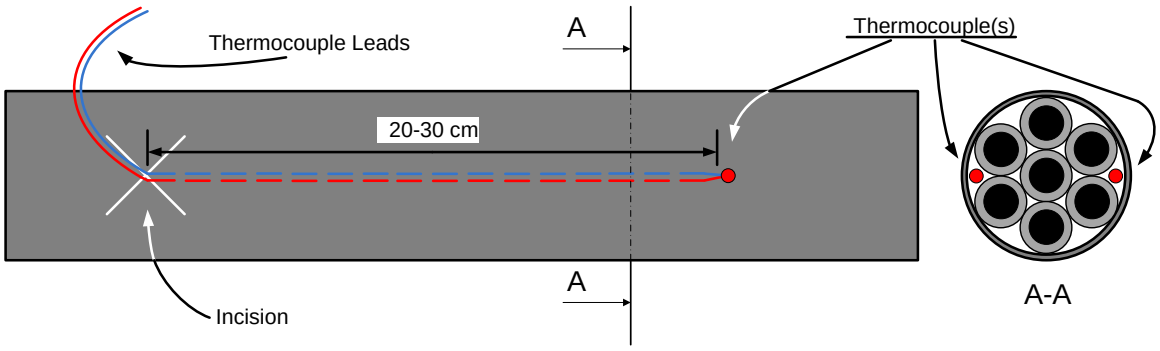

Figure 18. Illustration of sub-jacket thermocouple placement

Cable electrical response was monitored using an identical but separate cable from the thermocouple instrumented cable. This was done to eliminate the possibility of interference from the metallic thermocouple leads and the electrical conductors. The ends of the cables were connected to either the IRMS or surrogate circuits using wing nuts.

As previously mentioned, two electrical circuit systems were used to test for cable electrical functionality. The IRMS measures the electrical resistance between conductors and between conductors and any common ground conductive path (cable tray, conduit, other cable conductors, etc.). The surrogate circuit mimics an ac motor starter circuit, measuring conductor current and voltage throughout the test. These measurements were used to identify when hot shorts and shorts to ground occur.

The IRMS system is patented by SNL and an illustrative schematic of the IRMS is shown in Figure 19. The switch/controller systematically toggles through the conductive paths allowing a single conductive path to become energized, while another conductive path is connected to ground (common return of power supply). The voltage polarity is then switched between conductive paths and the two measured voltages across the ballast resistor are used to calculate the resistance using ohms law.

Ohms Law: Voltage [V] = Current [I] x Resistance [R] Equation 4

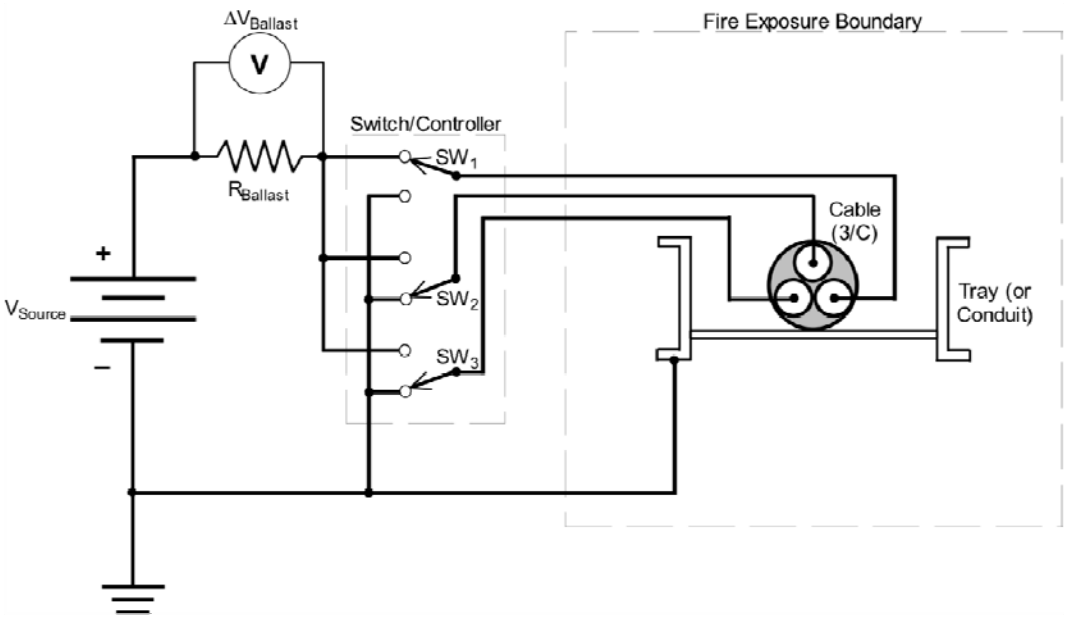

Figure 19. Simplified electrical schematic of IRMS for 3/C cable with ground monitoring [Wyant 2002]

One defect of the IRMS measuring process is that the cycle time increases exponentially as the number of monitored conductors' increases. A method to reduce this cycle time was to gang groups of alternating conductors together into one measurement channel. This method is illustrated in Figure 20. Although the detail of conductor failure was reduced, the overall evaluation of cable failure was preserved.

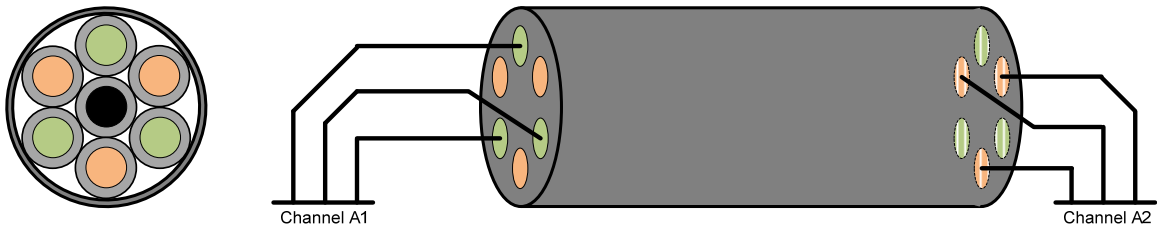

Figure 20. Illustration of ganging cable conductors into groups to monitor cable response

The second system used by SNL to monitor circuit electrical response to fire-induced cable failure was the surrogate circuit diagnostic units (SCDUs) which mimicked an ac MOV circuit. Figure 21shows a schematic of the SCDU. When the SCDU was connected to a control cable there are two source paths (labeled 1 and 2) that can provide

electrical potential, three target paths (labeled 4, 5, and 6) that can become energized if shorted to the source conductors, one spare conductor path (labeled 8), and one return conductor path (labeled 7) that was connected directly to the return side of the power supply. The power supply for the SCDUs were typically a control power transformers (CPTs) and could be grounded or ungrounded depending on the desired testing configuration. For the majority of the tests, the CPTs were grounded as this was typically practice for NPP ac MOV circuits. Each conductive path of the SCDU was monitored for current and voltage. These measurements were used for post test evaluation of the cable failure modes.

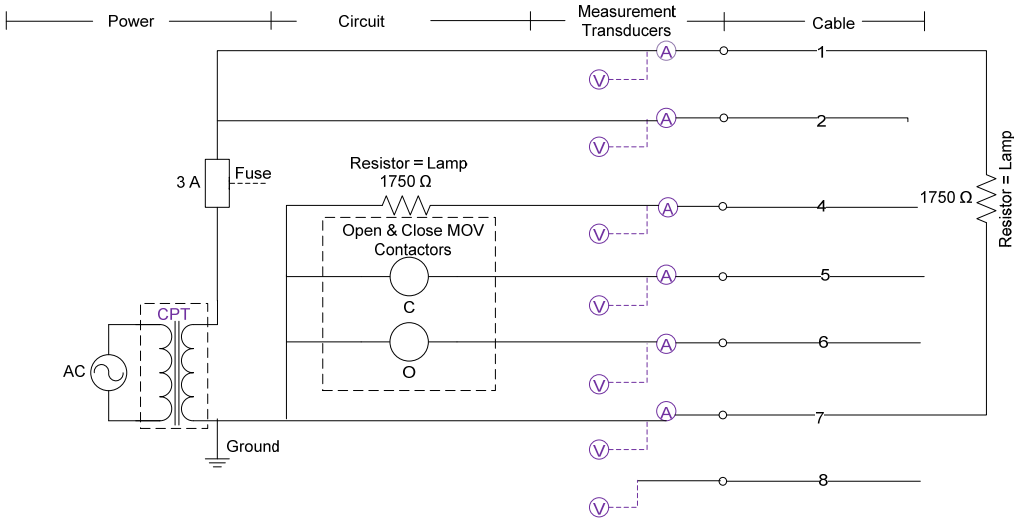

Figure 21. SCDU ac MOV circuit

In total, 96 tests were conducted in CAROLFIRE, including 78 tests using the small-scale radiant exposure apparatus and the IRMS collecting data to support fire model advancements. Eighteen intermediate-scale tests were conducted using the SCDU and IRMS to collect data on the cable failure modes in support of resolving the regulatory issue. Both testing scales provided severe thermal exposure conditions to ensure that the cables would experience failure, in order to provide information on the fire-induced

failure modes. Thus, these experiments were not intended to provide information on determining the probability of cable damage ($P_{ed,j|i}$).

A secondary objective of CAROLFIRE was to improve fire modeling of cable damage. Volume 3 of NUREG/CR-6931, "Thermally-Induced Electrical Failure (THIEF) model" documents this effort. The report concludes that the THIEF model "has been shown to work effectively in realistic fire environments" and while various refinements could be made, it is unlikely that any enhancements would dramatically improve its overall accuracy, in light of the uncertainties associated with fire modeling of the entire fire compartment [McGrattan 2008]. The THIEF model makes several assumptions that allow for a simple numerical solution of the one-dimensional heat conduction equation with a homogenous cylinder with fixed temperature-independent properties. The THIEF model assumptions, governing equations and numerical approach are discussed next.

4.2.2.11 The THIEF model for predicting cable damage

Petra Andersson and Patrick Van Hees of the Swedish National Testing and Research Institute initially presented a model to predict cable damage. It predicts cable damage via a simple one-dimensional heat transfer calculation, under the assumptions that the cable can be treated as a homogenous cylinder [Anderson and Van Hees 2005]. NRC sponsored research at NIST resulted in the refinement of the Swedish model into what has become known as the THIEF model. The specific assumptions that allow the THIEF model to work are as stated in NUREG/CR-6931, Volume 3:

Assumption 1. Heat penetration into a cable of circular cross section is largely in the radial direction.

- This assumption greatly simplifies the analysis, and is conservative because it is assumed that the cable is completely surrounded by the heat source.

Assumption 2. The cable is homogenous in composition.

- In reality, a cable is constructed of several different types of polymeric materials, cellulosic fillers, and a conducting metal, most often copper.

Assumption 3. The thermal properties – conductivity, specific heat, and density – of the assumed homogenous cable are independent of temperature.

- In reality, both the thermal conductivity and specific heat of polymers are temperature-dependent, but this information is very difficult to obtain from manufacturers.

Assumption 4. It is assumed that no decomposition reactions occur within the cable during its heating, and ignition and burning are not considered in the model.

- In fact, thermoplastic cables melt, thermoset form a char layer, and both off-gas volatiles up to and beyond the point of electrical failure.

Assumption 5. Electrical failure occurs when the temperature just inside the cable jacket reaches an experimentally determined value.

- Functional failure of electrical cable occurs when conductor insulation resistance degrades significantly to cause interaction between conductive media.

From these assumptions, the governing equation for multi-dimensional unsteady heat transfer for the cable temperature, T(r,t) are:

$$\rho c \frac{T_i^{n+1}-T_i^n}{\delta t} = \frac{2k}{(r_{i+1}+r_i)} \frac{1}{2\delta r}\left[r_i \frac{T_{i+1}^n - T_i^n}{\delta r} - r_{i-1}\frac{T_i^n - T_{i-1}^n}{\delta r} + r_i \frac{T_{i+1}^{n+1}-T_i^{n+1}}{\delta r} - r_{i-1}\frac{T_i^{n+1}-T_{i-1}^{n+1}}{\delta r}\right] \quad \text{Equation 5}$$

where ρ, c, and k are the effective density, specific heat, and conductivity of the solid, all assumed constant. The boundary condition at the exterior boundary, r=R are given by:

$$k \frac{T_{N+1}^n - T_N^n}{\delta r} = \dot{q}"(t^n) \quad \text{Equation 6}$$

where $\dot{q}"$ is the assumed axially-symmetric heat flux to the exterior surface of the cable. Fire modeling or fire analysis provides the heat flux information for the thermal environment of the fire compartment where the cable target is located.

As the THIEF model is only a one-dimensional heat transfer calculation, it can only predict the interior temperature and infer electrical failure when a user specified failure temperature is reached. A result of electrical cable construction and heat transfer to the cable from an exterior source, the centermost point of the cable is not necessarily the indicator of electrical failure. Instead, the conductors nearest to the exterior of the cable will have their insulation degrade first and it is this temperature, just beneath the cable overall protective jacket that is of importance when determining the cable temperature associated with cable electrical failure.

Using threshold failure temperatures of 400 °C for thermoset cables and 200 °C for thermoplastic cables, McGrattan used THIEF to predict time to damage values and compare these results to the experimentally measured time to damage failures. These threshold values differ from those proposed by Iqbal and Salley and were used because the CAROLFIRE experimental results indicated that thermoplastic cables failed

electrically when their sub-jacket temperature reached somewhere between 200 and 250 °C and for thermoset cables between 400 and 450 °C [McGrattan 2008]. The results indicated that the THIEF model under-predicted the time to damage by 3 % on average with a standard deviation of 20 % [McGrattan 2008]. These prediction models runs were conducted in Fire Dynamics Simulator. NRC has subsequently implemented the THIEF model into its FDT^s Microsoft Excel™ spreadsheets. The FDT^s THIEF model requires several input parameters, such as cable properties (cable diameter, cable mass per unit length, cable jacket thickness), cable failure threshold, cable raceway type, along with the exposing gas temperature profile. The temperature profile can be user defined or it can be calculated based on several of the other FDTs models (MQH, FPA, etc.). Cable specific parameters used in this thesis are presented in Section 5.3.

In fire PRA applications, it is important to know how long it will take a particular fire scenario to damage a target cable. The THIEF model can provide the time to damage based on the calculated thermal environment as an input. Any error or uncertainties associated with the thermal environment prediction will be carried through the THIEF model. As presented by McGrattan, the THIEF model predictions are only as accurate as the input thermal exposing conditions. Thus if the MQH hot gas layer calculation was used as the exposing temperature profile input to the THIEF model, any uncertainty (error) from the MQH calculation are carried through the THIEF calculation [McGrattan 2008].

4.2.2.12 SNL Fire-Induced dc Circuit Response Testing (DESIREE-FIRE)

The NRC and EPRI working under a memorandum of understanding sponsored a follow-on project to CAROLFIRE, namely, the Direct Current Electrical Shorting in

Response to Exposure Fire (DESIREE-Fire) testing project performed by SNL. This testing focused mostly on the failure modes of direct current (dc) powered control circuits. The same thermal testing apparatus were used as in CAROLFIRE, however only surrogate circuits were used to diagnose the fire-induced electrical cable failure modes (i.e., no IRMS). These surrogate circuits were based on NPP circuit designs for dc powered 1) motor operated valves, 2) small pilot solenoid operated valves, 3) small direct acting solenoid operated valve, 4) large direct acting solenoid operated coil assembly, and 5) medium voltage circuit breaker control circuits. The circuit simulators used for the dc circuits were similar to the ac SCDU MOV system with the exception of using different current and voltage transducers to measure dc signals and a different power source.

All dc test circuits were powered from the same nominal 125 Vdc power source. This source was from a Class 1E battery bank with approximately 13,000 A short circuit fault current capability. This source was sought to be realistic of actual NPP dc power sources. A photo of the battery bank is shown in Figure 22.

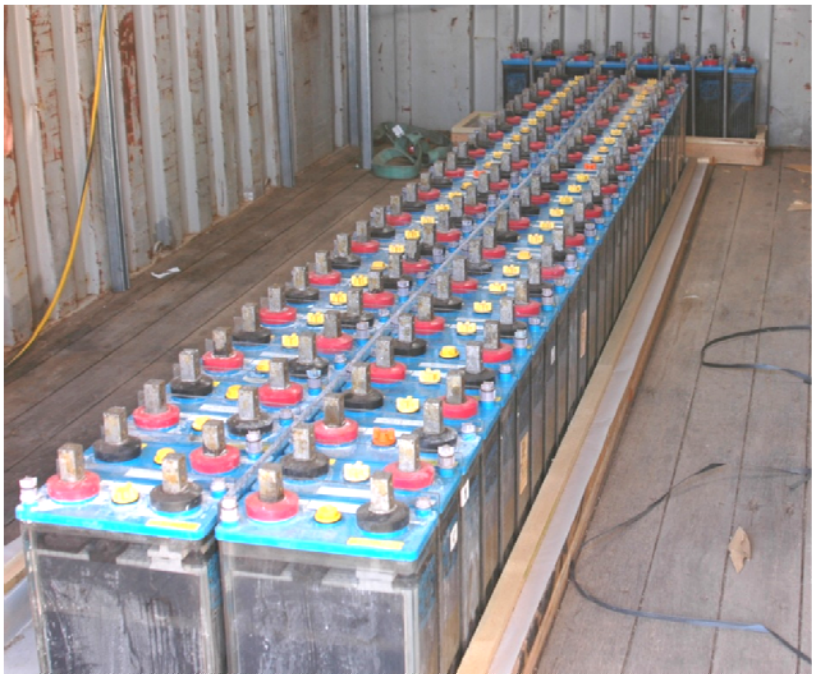

Figure 22. Photo of nominal 125Vdc battery bank used as power source in dc circuit testing. Photo is prior to terminal connection and located in climate controlled sea container.

A schematic diagram of the dc MOV circuit simulator is shown in Figure 23. All of the dc circuits differed from the ac circuits in that they were intentionally left ungrounded and two fuses were used in each circuit. Both of these characteristics are representative of typical dc circuits used in NPPs. The schematic diagrams for the other surrogate dc circuits are presented in Appendix A.

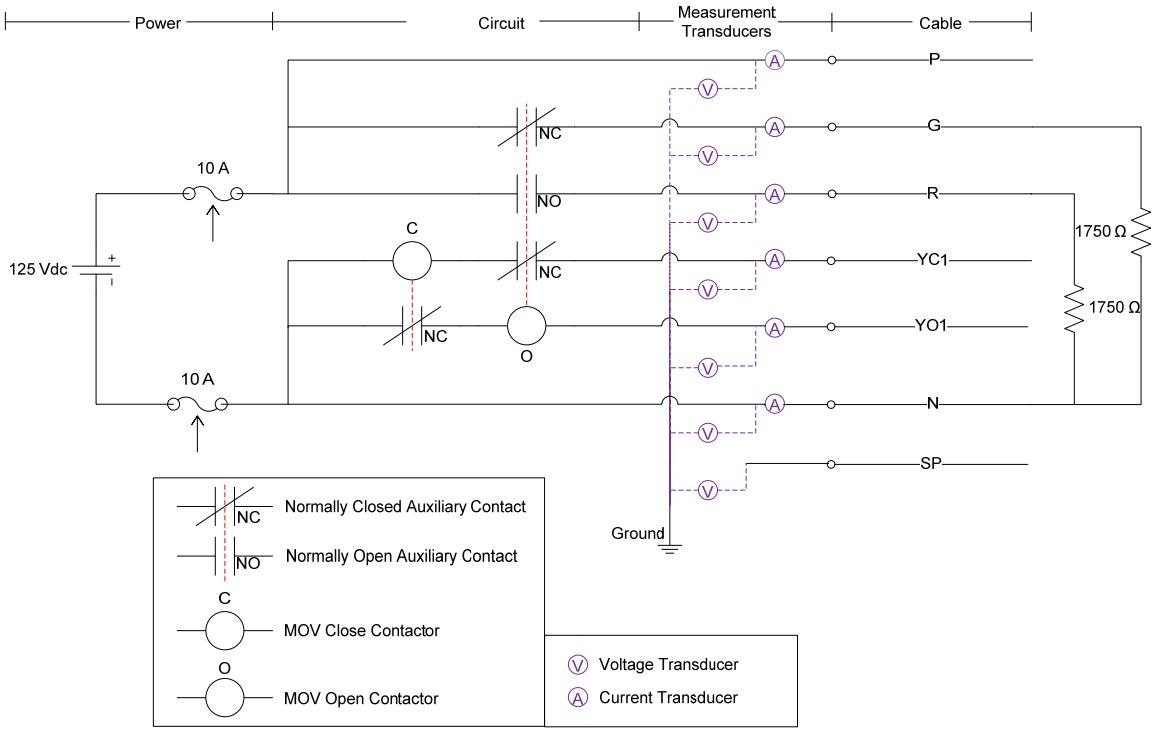

Figure 23. dc MOV circuit simulator schematic

One complicating factor associated with the circuit setup used was that the power source was left ungrounded, however the voltage transducers required a reference potential. Rather than referencing them to battery negative voltage potential, the transducers were connected to electrical ground. In addition, a ground monitoring circuit consisting of two 10 kΩ resistors in series connected across the battery potential with the center tap of the series resistors connected to ground provided two benefits. First, voltage transducers connected across each resistor of the ground monitoring circuit could be used to identify when either side of the battery shorted to ground via cable conductor short to ground. Second, the voltage transducer signal were used in the data processing phase to baseline the individual conductor voltage signals which cleaned up the voltage signal and allowed for easier interpretation of the voltage results without interference from conductor shorts to ground. Figure 24 provides an illustration of the voltage plot before

and after the baseline data processing. The ground monitoring circuit is illustrated in Figure 25.

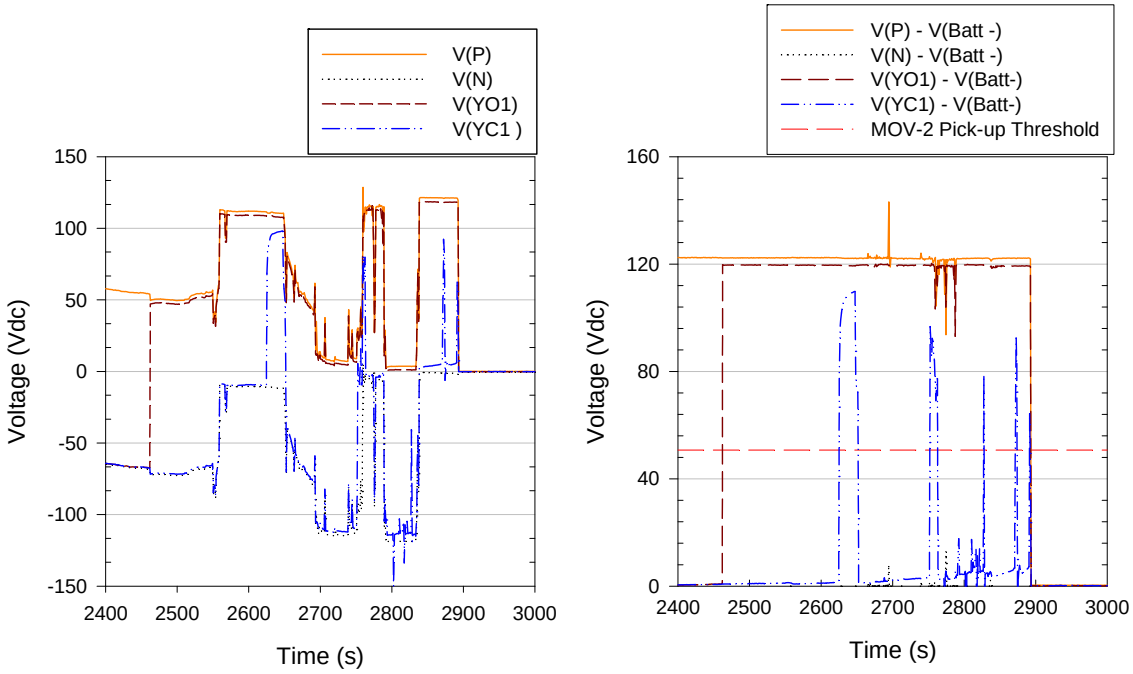

Figure 24. Illustration of benefit to base-lining the conductor voltage data.

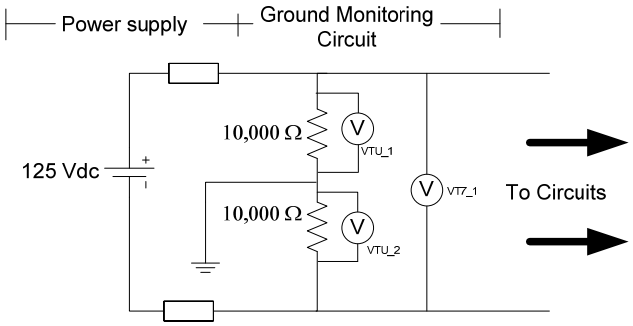

Figure 25. Ground fault monitoring circuit

In general, the DESIREE-Fire results indicated that failure modes for dc operated circuits, as compared to ac powered circuits, were more energetic, lasted longer in duration, and were the only cases where open circuiting as a primary failure mode was observed. The report presented the results in a very simplistic manner and did not provide any analysis on the results, other than the general observations previously stated [Nowlen, Brown, Olivier, Wyant 2012]. In particular, the SNL report was inconclusive

as to how fire PRA should address the duration of spurious operations. For instance, should the fire PRA assume a dc fire-induced circuit spurious operation last for a long time (i.e., not clear) or should some duration limit be used. The SNL work didn't include any evaluation of multiple cable shorts to ground that can result in hot short induced spurious operations when a common ungrounded power supply was used.

The NRC sponsored DESIREE-Fire tests used an ungrounded common power supply to energize all circuit tested. To evaluate the data for these failure mechanisms, the data for individual conductor voltage and current plots were used to understand which conductors are involved. Voltage alone does not provide sufficient information to identify which conductor is supplying the energy (source conductors) and which conductors are receiving the energy (target conductors).

Fuse operability status becomes beneficial in ruling out potential source circuits. When a circuit fuse clears, the portion of the circuit associated with the cleared fuse is no longer capable of performing its function and thus was no longer of concern for involvement with ground fault equivalent spurious operation. The dc test circuits had two fuses per circuit, one on the positive and one on the negative side of the circuit power leads and simultaneous clearing of both fuses did not always occur. In about one-half of the tests only one fuse of a particular circuit would clear. This single fuse clearing would cause one side of the circuit to remain functional and a potential target or source of multiple short to ground failure mode. When a circuit's positive battery side fuse cleared, its source conductors were no longer considered a source, likewise, when a circuit's negative fuse cleared the circuit's target conductors were no longer considered targets (i.e., a hot short to target conductors could no longer cause a circuit to respond). With

this particular configuration, it is important to acknowledge that if only one of the two circuits fuses clear then the circuit can still experience inter-cable shorting faults, that can cause spurious operations. Figure 26 presents a schematic diagram illustrating two circuits experiencing a multiple short to ground spurious operation. Here, Circuit A has experienced a fuse clear (represented by the X) on the positive battery voltage side of the circuit resulting in the de-energization of Circuit A source conductors "P" and "G." In short, Circuit A can no longer supply energy to cause a spurious operation. Circuit B has experienced a fuse clear on the negative battery voltage side of the circuit resulting in the target conductors "YC1", and "YO1"no longer being able to support a spurious operation. However, one portion of each circuit has a fuse that remains operable. As shown in Figure 26, if conductor(s) "P" or "G" of Circuit B shorts to ground and conductor(s) "YC1" or "YO1" of Circuit A short to ground, a multiple short to ground spurious operation will occur, provided that the shorts are of low impedance.

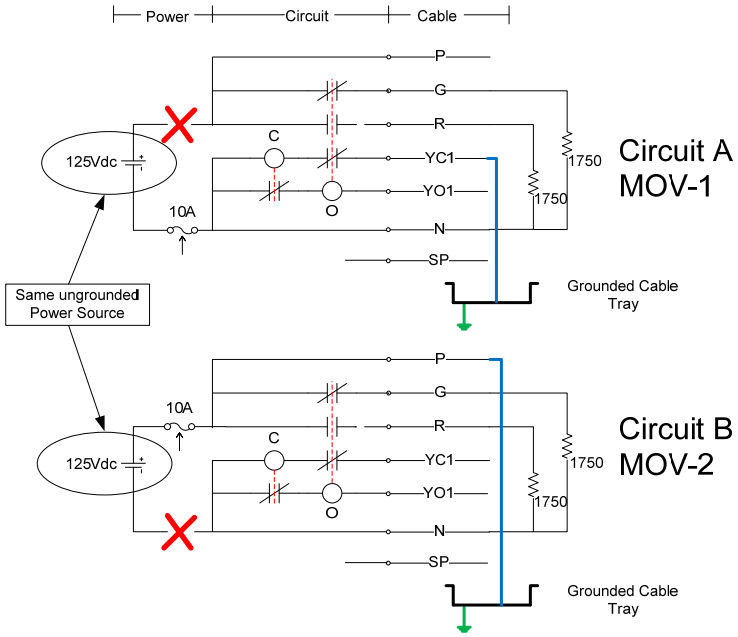

Figure 26. Illustration of possible combination for ground fault equivalent hot short induced spurious operation showing a target conductor (YC1) shorting to ground in Circuit A and source conductor in Circuit B shorting to ground. Loss of only one fuse on each circuit does not eliminate possibility of ground equivalent hot short.

The ungrounded battery supply also complicates the evaluation of the data for inter-cable shorting. By having the dc battery ungrounded (which is common practice in NPPs), a single short to ground from a conductor of positive or negative battery potential would not cause a fuse to clear. In order to cause a fuse clear, either direct plus to minus conductor shorts would be required or multiple shorts to a ground plane (plus and minus) of sufficiently low resistance to cause a fuse clear.

A review of the ac test data will not identify these multiple short to ground inter-cable spurious operations, because no more than one circuit was left ungrounded in any test. This eliminated the possibility of observing these events. In ac tests the control power transformer (CPT) secondary winding was typically grounded (as is done in a majority of NPPs) and any energized conductor experiencing a low resistance short to the reference ground (due to fire damage) would experience a high current rush resulting in clearing an upstream protective device (fuse or circuit breaker) and de-energizing the circuit.

4.4 Probability Estimation of Spurious Operation, and General Conclusions on Literature Survey

4.4.1 Risk Studies and Methods

4.4.1.1 Early Fire Risk Analysis of NPPs

Early fire risk analysis studies done by Kazarians and Apostolakis argue that there should be three frequencies: 1) the frequency of cable failure given that it is exposed to flames, 2) the fraction of these failures that lead to a certain failure mode, and 3) the duration of the failure mode [Kazarians and Appostolakis 1981]. In an attempt to address the second frequency, they note that data on "hot shorts" are very sketchy, but given the

spurious starts of the emergency core cooling system during the Browns Ferry Fire in the first half hour, the fraction of cable damage failures leading to a certain failure mode is a significant frequency on the order of 0.1 or larger for wire in a multi-conductor cable to touch one another before touching ground.

4.4.1.2 Conditional Probability of Spurious Operation Likelihood Estimate, Task 10, NUREG/CR-6850

The current state of the art method for performing a fire probabilistic risk assessment (PRA) is contained in a joint NRC/EPRI report, "EPRI/NRC-RES Fire PRA Methodology for Nuclear Power Facilities." The method consists of a multistep iterative process to calculate overall plant risk from fire. Task 10 of the EPRI/NRC-RES Fire PRA methodology provides instruction on estimating the probability of hot short failure modes of interest. Typically, spurious operations are the failure mode of interest because they can cause maloperation of plant equipment that can lead to core damage or complicate the ability of the plant operators to achieve and maintain the plant in a safe-shutdown condition. The EPRI/NRC-RES document presents two methods of evaluation. A table lookup methods presents likelihood estimates for simplistic circuit configurations, based on the results of the EPRI/NEI tests. The second method uses a formula based on the cable conductor-to-circuit configuration. The formula was developed from the results of the EPRI/NEI test data. The guidance document suggests using the table method for simple circuit configurations such as those tested and the formula method for complex configurations.

$$P_{FM} = CF \times P_{CC}$$

$$CF = \{C_T \times [C_S + m(0.5/C_{Tot})]\} / C_{Tot}$$

$$P_{CC} = (C_{Tot} - C_G) / [(C_{Tot} - C_G) + (2 \times C_G) + n]$$

Where:

P_{FM} = The probability that a specific hot short failure mode of interest will occur
P_{CC} = The probability that a conductor-to-conductor short will occur prior to a short-to-ground or short to a grounded conductor
CF = A configuration factor applied to P_{cc} to account for the relative number of source and target conductors.
C_{Tot} = total number of conductors in the cable of interest, including spares
C_G = number of grounded or power supply common conductors in the cable of interest
C_S = number of source conductors in the cable of interest
C_T = number of target conductors in the cable of interest
n = 1 for cable trays, 3 for conduits, and 0 for ungrounded systems
m = 1 for non-armored cables, 0 for armored cables

In the look-up table method, five tables are presented. Tables 10-1 and 10-2 present thermoset while Tables 10-3 and 10-4 present thermoplastic cable best estimate point probabilities for circuits with and without a CPT. A fifth table presents the best estimate point probabilities for cables with armor or shields. The tables show that the use of CPTs reduce the probability by a factor of two, while a cable in a tray is four time more likely to experience a hot short than when located in a conduit. A summary of pertinent information is presented in Table 4.

Table 4. Summary of multi-conductor information presented in NUREG/CR-6850 EPRI TR1011989

Cable Type	CPT	Raceway Type	Type of Hot Short	Best Estimate
TS	Yes	Tray	Intra-cable	0.30
			Inter-cable	0.01-0.05
		Conduit	Intra-cable	0.075
			Inter-cable	0.005-0.01
	No	Tray	Intra-cable	0.60
			Inter-cable	0.02-0.1
		Conduit	Intra-cable	0.15
			Inter-cable	0.01-0.02
TP	Yes	Tray	Intra-cable	0.30
			Inter-cable	0.01-0.05
		Conduit	Intra-cable	0.075
			Inter-cable	0.005-0.01
	No	Tray	Intra-cable	0.60
			Inter-cable	0.02-0.1
		Conduit	Intra-cable	0.15
			Inter-cable	0.01-0.02

4.4.2 General conclusions on the use of historical cable fire test data

Based on the information available and reviewed, the following conclusions can be made on historical cable fire testing:

- Cable failure times have ranged from 1.0 to 20 minutes; in some cases cables did not fail.
- Cable failure criteria are not consistent among tests (ignition, short to ground, conductor-to-conductor short, physical cable degradation, etc.)
- There is no standard method to determine the loss of electrical cable functionality due to severe thermal exposure.
- Limited variation of fire incident characteristics, will limit the applicability of statistical use of the results to represent a wide variety of plant fire scenarios.
- Different fire tests have resulted in contradictory conclusions

5 Data Analysis

This section documents the use of the recent NRC sponsored fire test data to;

- evaluate cable minimum thermal failure threshold (section 5.1)
- development cable thermal fragility distributions (section 5.2)
- evaluate the FDT^s THIEF model prediction capabilities (section 5.3)
- evaluate influence parameter effects on fire-induced circuit failure modes (section 5.4)
- evaluate the dc test data to identify spurious operations caused by multiple cable conductor shorts to ground (section 5.5).

Some of the highest quality data on fire-induced cable failure modes available in open literature were from the NRC sponsored fire testing (CAROLFIRE and DESIREE-Fire). These experimental programs were discussed in detail in section 4. However, the information collected through these two projects have only been used to address specific regulatory concerns. As such, the data has not been thoroughly reviewed to understand the thermal damageability limits of the electrical cables tested or specific circuit failure characteristics. Therefore, the data from these two test projects were the sole subject of the evaluation conducted in this thesis.

For each NRC sponsored test, a corresponding Microsoft® Excel data file(s) were available containing time stamped thermocouple, voltage and current transducer measurements. All measurements were made at sampling intervals on the order of less than one second. Using the information provided from the NRC sponsored testing, a Microsoft® Excel "database" was developed. The database was populated with test information from the NUREG/CR test reports and the electronic data files. The database allowed for the information to be sorted by parameter. For each test, the database was populated with the following information;

- time to damage
- failure mode type (hot short, spurious actuation, fuse clear, open circuit)

- duration of hot shorts and/or spurious operations
- temperature measurement(s) at time of first electrical failure
    - sub-jacket
    - air
    - penlight shroud (if applicable)
- cable configuration
    - cable conductor count
    - conductor size (in American Wire Gauge [AWG])
    - insulation/jacket material (chemical composition)
    - insulation/jacket type (thermoplastic, thermoset)
    - special cable features (shield, armor, drain wire)
- thermal exposure condition (flame, plume, hot gas layer, radiant)
- raceway routing configuration
    - raceway type (conduit, tray, air drop)
    - cable orientation (vertical, horizontal)
    - raceway fill
- circuit characteristics
    - circuit fusing size
    - power supply (ac, dc)
    - power supply type (control power transformer, line, battery)
    - circuit grounding configuration
    - number source conductors vs. target conductors

The time to damage was identified from the data as the first occurrence of any fire-induced circuit fault (fuse clear, hot short, or a short to ground) for the specific cable under evaluation. These failure modes were determined from conductor voltage thresholds identified in Table 5. These voltage thresholds correspond to the minimum voltage required to cause the associated device to operate as identified in the corresponding test reports. The time to damage information was entered into the database and then cross referenced with the test reports to ensure the database entries matched the report information and no transcriptions errors were made.

Table 5. ac and dc threshold values used for determining cable hot shorts and spurious operations

Test Circuit	Failure Modes			
	Spurious Operation	Non-Spurious Hot Short	Positive Fuse Clear	Negative Fuse Clear
ac MOV	> 72 V	> 80 V	<10 V	N/A
dc MOV	29-89 V*	20-89 V*	Positive Conductor <10 V	Negative conductor >100 V
dc SOV	>56 V	>60 V		
dc 1-inch valve	>48 V	>100 V		
dc large coil	>60 V	>60 V		
dc circuit breaker close	Conductor G status	>100 V		
dc circuit breaker trip	Conductor G Status	>100 V		

* spurious operation of dc MOV was determined by contactor dependent pickup voltage.

Next, the thermocouple measurements at the time of damage were entered into the database. These measurements included air temperatures near the electrically monitored cable, sub-jacket temperatures, and shroud temperature (if applicable).

To allow for an evaluation of the effect different thermal exposure conditions had on the cables failure mode, cable locations within the experimental configuration were grouped into different categories. All Penlight tests were assigned a “radiant” exposure condition due to the highly radiative heat transfer environment of this apparatus. For the intermediate-scale testing cables located in position A (refer to Figure 17) were assigned a “flame” exposure condition because the cables were immersed in the flame region for the duration of the test. Cables in locations C and F were assigned a “plume” exposure because they were immersed in the fire driven buoyant plume. The other cable locations B, D, E, and G were assigned a “hot gas layer” exposure due to the rapid development of a optically thick hot gas layer during testing. The remainder of the information populated into the database was taken directly from the test reports.

Not all data from the NRC sponsored tests were of value for the evaluation conducted here. For instance, cable that did not experience functional failures did not

provide any information regarding cable failure modes. This information was not included. Each section that follows, identifies the data used and provides explanations of any data that was removed from the evaluation.

5.1 Minimum Thermal Failure Threshold

This section evaluates the NRC fire-induced cable failure data specifically looking at the sub-jacket cable temperatures at the time electrical cables functional failure occurs. For this evaluation, the small-scale Penlight radiant tests provided the most conservative information pertaining to the failure temperature of electrical cables. Penlight's well controlled thermal environment produces consistent results, and uncertainty associated with larger intermediate-scale tests (i.e., cable ignition, combustion efficiency, active fuel load, etc.) is minimized. Thus the small-scale radiant test results are used to provide empirical evidence to define thermal failure damage thresholds based on the minimum failure temperature at electrical failure.

Data removed for this evaluation included any test where the cable experienced a functional failure after the cable had ignited and sustained burning. This was done to reduce uncertainty regarding the sub-jacket temperature measurement. When the cable ignited, the cable jacket materials were being consumed and depending on material type, the thermocouple was no longer reliably measuring the sub-jacket temperature. As the cable polymer material degrades, it become more likely that the thermocouple bead was measuring other effects than the sub-jacket materials temperature. The thermocouple bead measurement would likely be influenced by a combination of flame radiation, exposure radiation, hot gas convection, soot deposits, etc. Thus, to provide a reliable temperature measurement, all test data where cable ignition occurred prior to an electrical

functional failure were removed from further use in the evaluation of cable insulation specific cable failure thresholds.

Sub-jacket thermocouple measurements for ac and dc Penlight test results at the point of first electrical functional failure are shown in Figure 27. The figure separates the data by cable insulation type (TS, TP) and each insulation type was separated by circuit power classifications (ac, dc). The separation of ac data and dc data was done to determine if circuit power type has any effect on the thermal failure threshold of the cable. The majority of the test data was from 7-conductor control cables.

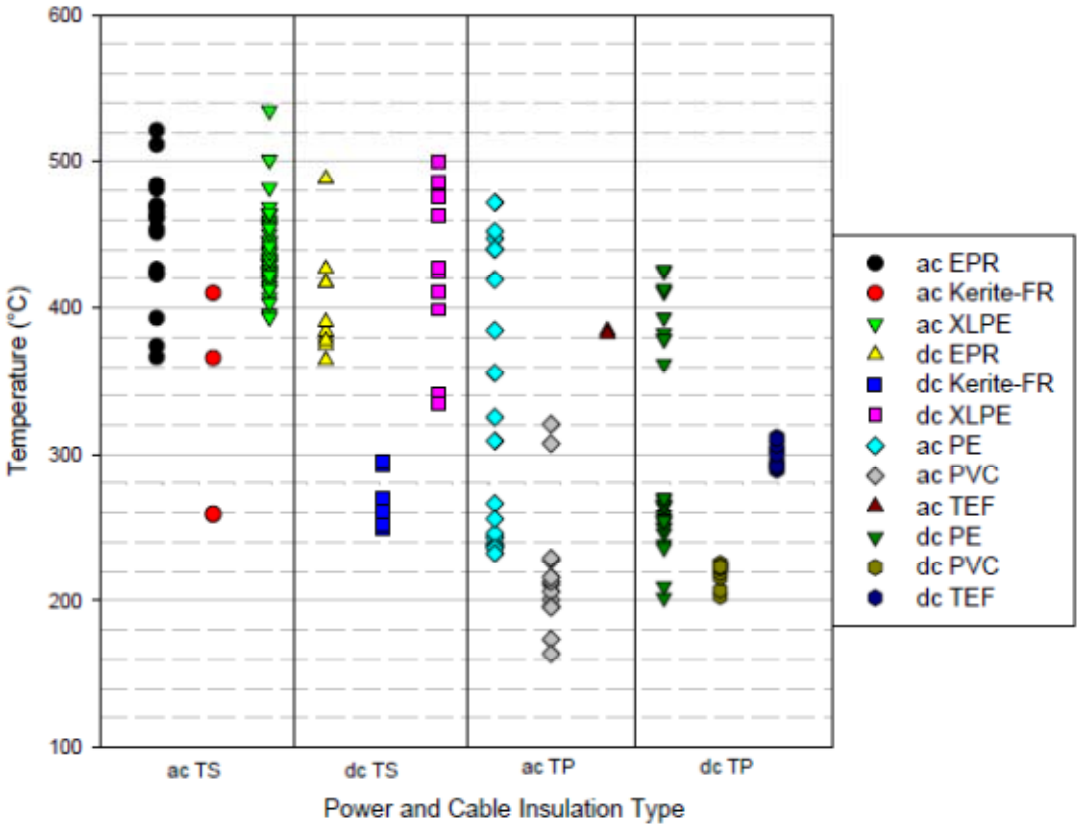

Figure 27. Cable Sub-Jacket Thermal Failure Observations Small-Scale (Radiant) Tests

Figure 27 clearly illustrates the poor performance of Kerite FR as a thermoset material. The poor performance is also consistent with recent NRC guidance on the treatment of Kerite-FR cable documented in NRC NFPA frequently asked question

(FAQ) 08-0053, "Close-out of National Fire Protection Association Standard 805 Frequently Asked Question 08-0053, 'Kerite-FR Cable Failure Thresholds' [Klein 2012]." The thermoset EPR and XLPE data have similar failure ranges. The data from the thermoplastic cable samples indicates that the PVC is the least robust and PE is the most robust, with Tefzel failures more representative of the PE insulated cable.

One reason the DESIREE-Fire tests were conducted was to determine if the duration of fire-induced hot shorts of dc powered control circuits differed from control circuits powered from an ac source. The ac waveform crosses the zero voltage/current axis twice per cycle (120 times per minute for 60 Hz power systems). The dc waveform was a constant voltage/current and does not cross the zero axis. Thus, it was thought that the lack of the zero axis crossing would reduce the likelihood of a short circuit extinguishing itself. The results indicated that this lack of zero axis crossing along with the larger fuse sizes used in dc control circuits resulted in spurious operation durations that were longer than durations observed in ac control circuits. However, the DESIREE-Fire test report did not evaluate the effect, if any, that the power source has on influencing the cable failure temperature.

To determine if the circuit power source type (ac or dc) had any effect on the thermal failure threshold, a two sample Kolmogorov-Smirnov (K-S) statistical test was conducted for each insulation type (XLPE, EPR, PVC, PE) using Matlab R2011b. The Matlab K-S test compares the distributions of the values in the two data vector (ac, dc). The null hypothesis is that both data vectors are from the same continuous distribution, as indicated by an 'h' value of 0 and a 'p' value greater than the significance level of 5 % [MathWorks 2012]. The K-S tests confirmed that the ac and dc data for each cable

insulation material (XLPE, EPR, PVC and PE) can be combined. Therefore, the power source type (ac or dc) had no effect on the thermal failure thresholds of the cable insulation materials from these two test programs.

Next two sample K-S tests was conducted to determine if the thermoset cable types (XLPE, EPR, Kerite-FR) could be combined into one data set (thermoset), as well as the thermoplastic cable types (PE, PVC, TEF) combined into another data set (thermoplastic). The TP materials did not pass the K-S test due to the bulk of the PVC cables failing at lower temperatures than the PE insulated cables. The K-S test results indicated that the data from the TEF cable type could not be combined into either PE or PVC data sets. Thus, this evaluation indicated that the thermoplastic cable types should be evaluated independently. For the TS material, EPR and XLPE could be pooled, but Kerite-FR could not. Therefore, when developing cable thermal fragility distributions in section 5.2, a distribution for TS insulation materials (XLPE, EPR) and two distributions for TP insulation materials (PVC and PE) were developed.

Based on the sub-jacket thermal failure data obtained from the NRC sponsored testing, Table 6 was populated. This table identifies the range, minimum, mean, and standard deviation of failure temperatures for each cable insulation material tested as well as for the combined TS class of cables. Because of the Kerite-FR low thermal failure threshold observed in the NRC sponsored testing and the current EPRI/NRC-RES fire PRA guidance to use the thermoplastic threshold for Kerite-FR, it was not included in the generic TS grouping and is reported here separately.

Table 6. DESIREE-FIRE & CAROLFIRE Empirical Fire-Induced Damage Cable Failure Thresholds

	Insulation Material	Failure Temperature (°C)			
		Range	Minimum	Mean	StDev
TS	XLPE	335-535	335	435	33.5
	EPR	364-521	364	431	46.5
	TS*	335-535	335	434	38.0
TP	PE	202-471	202	311	81.9
	PVC	163-320	163	220	32.7
	Tefzel	289-384	289	311	31.5
Other	Kerite-FR	249-410	249	284	51.6

* Does not include Kerite-FR

5.1.1 Evaluation of Minimum Failure Threshold Results

Current NRC guidance uses minimum empirical cable failure temperatures to represent a single point failure criteria to use in risk-informed performance-based methods. Section 5.1 identifies the NRC sponsored test cables sub-jacket temperatures at the time of electrical functional failure. Using these minimum failure temperatures, a comparison is made to current guidance and historical test data.

The NRC sponsored data set included three thermoset materials; XLPE, EPR, and Kerite-FR. The minimum failure temperature observed for the XLPE insulated cable was 335 °C. This result compared well to the current NRC insulation specific guidance of 320 °C and Nowlen's finding of 325 °C for XLPE. These findings suggested that the NRC use of XLPE failure data to bound cables with thermoset insulation material from a fire exposure damage standpoint seems to be valid given that the generic thermoset threshold was 330 °C and the other thermoset material (EPR) failed at temperatures above 370 °C.

The minimum failure temperature for an EPR insulated cable was identified as 370 °C from the NRC sponsored testing. This result corresponded well to Nowlen's baseline aging tests of an EPR insulated cable which failed as low as 365 °C. NRC guidance documents suggest a thermal threshold value of 370 °C for EPR. One outlier from this EPR failure threshold was identified from the high temperature steam testing conducted by Jacobus and Fuehrer. Their testing indicated that when a more robust acceptance criteria of 1,000 Ω insulation resistance was used, the EPR insulated cable failed at temperatures as low as 235 °C. However, this data point should be used with caution. As identified in their report, Jacobus and Fuehrer observed some cables were damage due to accelerated aging prior to the high temperature steam test. Because their test procedure exposed cables to severe accelerated aging conditions that may not have adequately simulate the aging mechanism to represent actual plant conditions, it was unclear the actual state of the cables prior to high temperature steam testing. Thus, damage from the accelerated aging may have caused the cables to perform worse than cables aged under normal plant conditions. Therefore, the results from the NRC sponsored testing indicate that the current guidance for an EPR insulated cable were appropriate.

The Kerite-FR cables tested for the NRC sponsored testing were manufactured in the 1970's and stored at a utilities warehouse until donated for the test program. The Kerite-FR cable samples used in the high temperature steam tests conducted by Jacobus and Fuehrer were also 1970's vintage cable. The NRC sponsored testing of Kerite-FR results identified the lowest Kerite-FR failure temperature at 249 °C, approximately 81 °C below the current NRC generic thermoset threshold of 330 °C. A closer evaluation

of the individual Kerite-FR trials indicated that of the eight trials, Kerite-FR cable product failed prior to the generic threshold seven times (approximately 87.5 %). However, this minimum failure temperature was approximately 96 °C above the results obtained by Jacobus and Fuehrer (153 °C) when the 1,000 Ω insulation resistance failure criteria was used. Even with the concerns identified previously regarding the use of the accelerated aging test results, the NRC sponsored testing indicates that Kerite-FR insulated cables failed at temperatures below those typically identified with a thermoset material. Although Kerite-FR cables were chemically a thermoset insulation material, the data obtained from the NRC sponsored testing did not support using the thermoset failure threshold of 330 °C for this cable insulation material. The evidence presented here suggests that Kerite-FR should be treated as a thermoplastic, as suggested by the current NRC guidance.

NRC guidance did not provide insulation specific thermal failure thresholds for thermoplastic materials. Following the NRC selection guidance, the NRC test data suggested the minimum failure temperatures presented in Table 6. These results correlated well to the NRC generic thermoplastic threshold with the exception of PVC. The PVC cable samples experienced electrical functional failures prior to the generic thermoplastic 205 °C failure threshold. The minimum temperature at failure for a PVC cable sample was 164 °C. This indicated that the current NRC guidance for thermoplastic insulated cables may not bound all thermoplastic cable insulation formulations.

The NRC sponsored testing results have shown that with a few exceptions, the current NRC guidance on fire-induced electrical cable failure thresholds were

appropriate. Care should be used for specific insulations such as Kerite-FR and PVC when applying these generic threshold values. When the generic failure thresholds for these two insulation materials were used, the estimated time to damage results were longer than the associated cables actual ability. This would result in the analyst using a non-conservative non-suppression probability in the fire PRA. Therefore, to be consistent with current NRC guidance, suggested minimum failure temperatures identified here be used in determining the time to cable damage. In addition, the testing only evaluated a small variety of typical control cable insulation types and physical constructions found in NPPs. Due to the proprietary nature of the polymer formulations used among cable manufacturers, the results presented here may not be bound all cable types. Thus, the results presented here should only be used for control cables manufactured with the same insulation and jacket material type. In addition, these results do not bound special cable designs, such as cables with armor or cables constructed with other unique components.

5.2 Development of Cable Thermal Fragility Distributions

As an alternative approach to the minimum cable thermal failure thresholds for performance-based approaches, the NRC sponsored data were used to develop thermal fragility probability distributions. These distributions could be used in Fire PRA to complement fire model cable damage predictions by assigning the probability of cable damage at specified thermal conditions. For instance, the fire modeling efforts may develop a probability distribution for the temperature of a specific target cable. This temperature profile could be combined with the cable thermal failure threshold

probability to result in a joint probability of cable damage ($P_{cd,i|j}$). This approach is found in section 5.3.2.

To develop thermal threshold probability distributions, a select set of data from the NRC tests was used. First, any test where the cable ignited before electrical failure occurred was removed. This was done so that uncertainties associated with temperature measurements were eliminated. Under cable combustion conditions, the electrical cable's jacket and insulation materials were being consumed. During this process it was unknown if the thermocouple was measuring the actual sub-jacket temperature or some combination of air temperature and flame radiation due to the cable material degradation. The NRC intermediate-scale data was not used for similar reasons, specifically, there were no indications when the cables ignited and burned. Therefore these distributions were developed using only the highly controlled, small-scale radiant "Penlight" tests where electrical failure occurred prior to cable ignition.

The first task in developing these distributions was to plot the data for each cable insulation material using histograms. The shape of these histograms indicated that the thermoplastic data may fit a log-normal distribution, while the thermoset data may fit to a normal or log-normal distribution. The distribution parameters were estimated from the data and confirmed using Matlab R2011b. The resulting distributions were plotted against the original data set represented by histograms to visually inspect the goodness of fit. To quantitatively address the goodness of fit, K-S statistical tests were conducted using Matlab R2011b. The K-S results indicated that the log-normal distribution fit the data better and the log-normal distribution was then used exclusively to define the distributions for all cable categories (TS, PVC, PE). Figure 28 and 29 show the

developed distributions. Distributions for Kerite-FR and TEF were not developed due to the limited amount of failure data. Additionally, Kerite-FR data was not poolable with the TS data distribution and TEF data could not be pooled with either the PE or PVC data sets. The bin size used to develop these histograms was 20 °C.

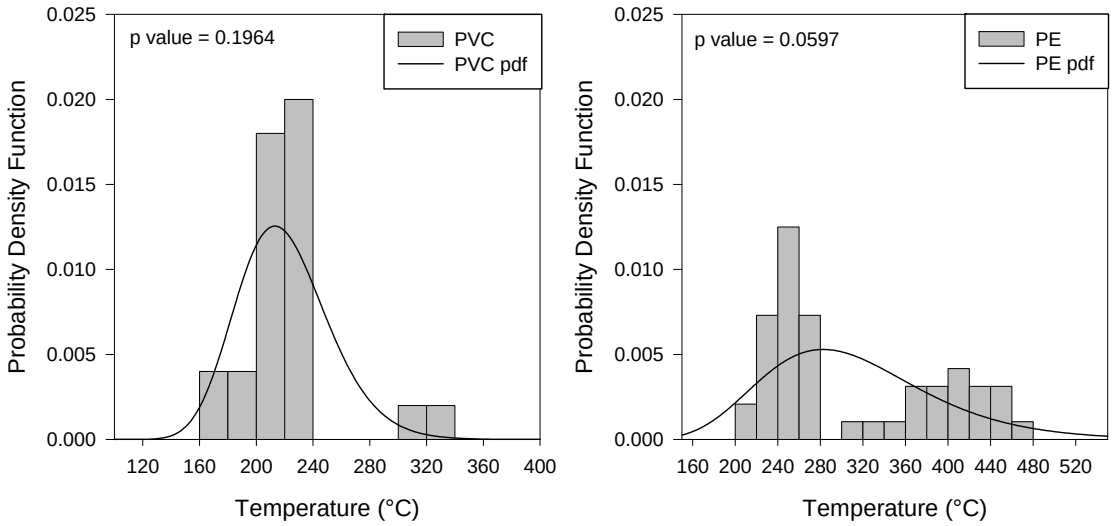

Figure 28. Overlay of PVC and PE log-normal distribution on SNL PVC and PE data histograms (original data)

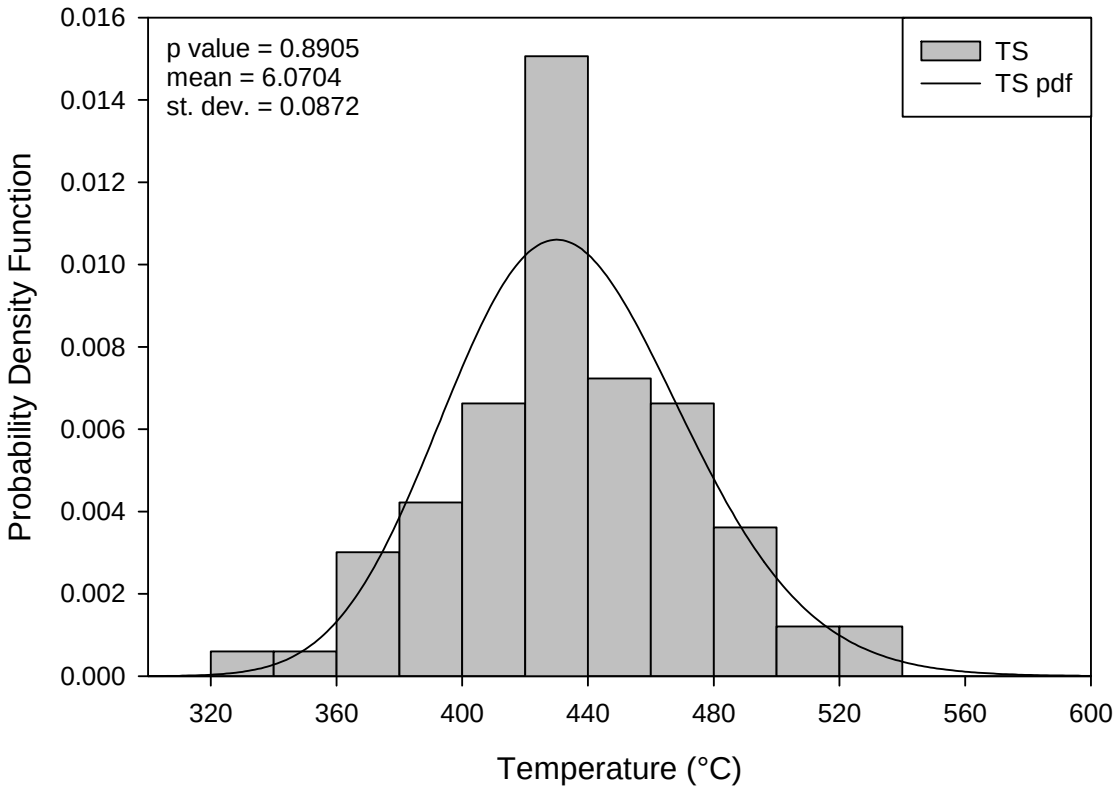

Figure 29. Overlay of thermoset log-normal distribution on SNL thermoset data histogram

The thermoplastic distributions showed a possible bi-modal failure mechanism, especially for the PE data set. The NRC sponsored data contained a group of PE insulated cable failure temperatures in the range of 200 – 270 °C and then another group of failure temperature between 310 – 475 °C. A review of the parameters associated with each group was not able identify the cause of this phenomena. One possibility of this result may have been a phenomena identified in the recent SNL testing to quantify the failure threshold of Kerite-FR cable. During this testing, it was observed that there were two failure ranges. At the lower failure range the cables would either fail or experience a small insulation resistance decreased followed by a recovery to pre-test IR values. For those cables that didn't fail at the lower temperatures, cable failure occurred at temperatures approximately 100 °C higher. During these tests, it was observed that a

conductive fluid developed during heatup of the cable and in combination with localized insulation defects lower temperature failure was observed [Nowlen and Brown 2011]. This could be one possible cause of the two failure ranges observed in the PE. This phenomena may likely be attributed to the cable manufacturers proprietary blend of materials to manufacture cable insulation polymers. As discussed in section 3.1, the amount of additives and plasticizers can have an effect on the performance of electrical cable during severe fire conditions. Since the data set for the two thermoplastic insulated cable materials are a composite of cables manufactured from different cable manufacturers, the differences in insulation blends may be influencing the failure point and causing the bi-modal results. To refine the understanding of the specific failure temperature, a utility or cable manufacturer could pursue testing specific cables to refine the thermal failure point and develop thermal fragility distributions based on their results. As a result of the thermoplastic data sets poor distribution fit, the desire to develop a bounding cable thermal fragility curve for PE and PVC, and the lack of understanding related to cause of the bi-modal phenomena, it was determined that removal of the group of data that failed at the higher temperature range would enhance the representation of the thermoplastic electrical failure temperatures. Thus, the reduced thermoplastic data set was plotted in a histogram shown in Figure 30 with the associated distribution curve plotted on top of the histogram. The various cable insulation specific thermal failure threshold probability distribution numerical results suggested for use in fire PRA applications are presented in Table 7. A generic TP distribution was not developed due to the failure of PVC and PE to be combined.

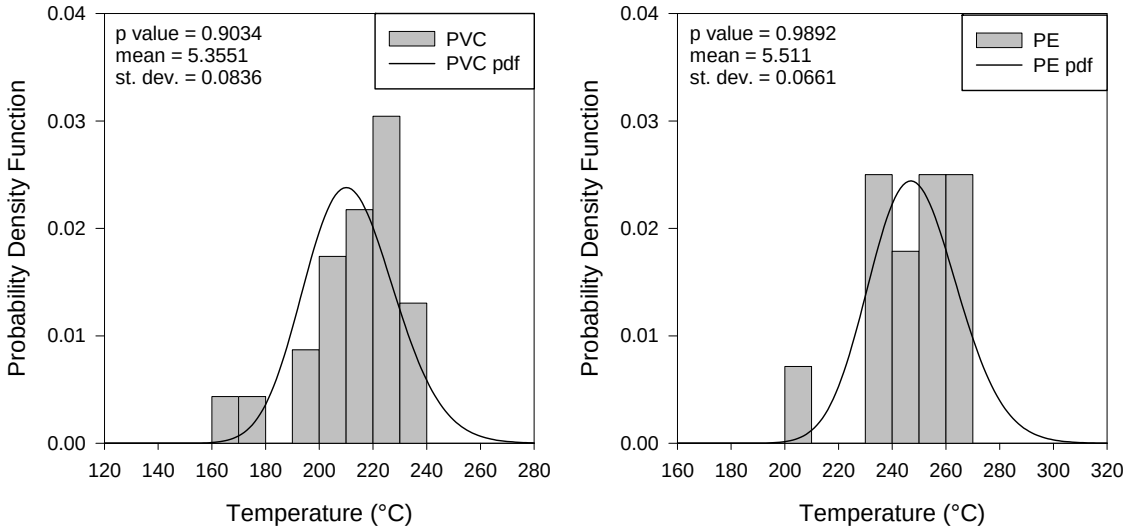

Figure 30. Overlay of PVC and PE log-normal distribution on SNL PVC and PE data histograms (with higher temperature data group removed)

Table 7. Numerical Results for Cable Thermal Fragility Distributions (log-normal) and distribution parameters

		Temperature (°C)		
Quantile, q	z-value	TS	PE	PVC
0.02	-2.054	362	216	178
0.05	-1.645	375	222	184
0.10	-1.282	387	227	190
0.15	-1.036	395	231	194
0.20	-0.842	402	234	197
0.25	-0.674	408	237	200
0.30	-0.524	414	239	203
0.35	-0.385	419	241	205
0.40	-0.253	423	243	207
0.45	-0.126	428	245	209
0.50	0.000	433	247	212
0.55	0.126	438	250	214
0.60	0.253	443	252	216
0.65	0.385	448	254	219
0.70	0.524	453	256	221
0.75	0.674	459	259	224
0.80	0.842	466	262	227
0.85	1.036	474	265	231
0.90	1.282	484	269	236
0.95	1.645	500	276	243
0.98	2.054	518	284	251
0.999	3.090	567	304	274
	Mean	6.0704	5.511	5.3551
	Standard Deviation	0.0872	0.0661	0.0836
	p value	0.8905	0.9892	0.9034

The evaluation of the NRC sponsored data sub-jacket temperatures at electrical functional failure confirmed that cables fail not at a single point but over a distribution of temperatures. In the TS class of cable insulation XLPE and EPR thermal performance was nearly identical with a mean failure temperature of 435 °C and 431 °C, respectively. However, XLPE cables experienced a minimum failure temperature of 335 °C while the minimum for the EPR cable was 364 °C, indicating that the XLPE fails at a lower temperature than EPR. This conclusion confirmed the NRC and Murphy's conclusion that XLPE insulated cables fail at lower temperatures than other thermoset insulation materials and should be used as a basis to select a generic thermoset threshold.

The three thermoplastic cable insulation materials indicated that PVC insulated cables failed at the lowest temperatures with a mean failure temperature of 220 °C. The NRC sponsored data from the PE and Tefzel insulation cables both show a mean failure temperature of 311 °C. The minimum failure temperature of these two cables indicates that PE is less robust to thermal insult than the Tefzel cable insulation. The data for the PE and PVC insulated cables show a larger standard deviation than that of the TS variety tested. The origional PE and PVC distribution fits passed the K-S statistical test, however these distribution fits are not as strong as the TS distribution fit. Following removal of the higher bi-modal data from the PVC and PE sets, the K-S tests showed a stronger agreement between the data and the developed distribution. Even with the distributions adequate fitting the experimental data, it was determined to be valuable to evaluate the tails of the distribution to ensure that they represent actual failure points. In other words, if a distribution's lower bound showed cables failing at 100 °C and the

minimum failure temperature from data was 150 °C, then that distribution was not accurately modeling the failure temperatures of the cable insulation.

For this evaluation, the 2nd quantile was used as it is typical for EPRI/NRC-RES fire PRA method to use the 98th percentile to quantify certain data sets, such as heat release rates [EPRI/NRC-RES 2005]. Here the 2nd quantile would correspond to the 98th percentile of the cable not experiencing damage. The distribution numerical results presented in Table 7 and the NRC sponsored test data will be used to provide the comparison.

For the TS distribution, the 2nd quantile corresponded to 362 °C. The minimum failure temperature identified in the data for thermoset insulated cables (excluding Kerite-FR) was 335 °C. Here the TS distribution 2nd quantile is approximately 8.1 % above the lowest data point. Therefore, the distribution was predicting failure temperatures that were realistic and representative of the NRC sponsored data set.

The PVC distribution 2nd quantile corresponded to 178 °C and the NRC sponsored data failure temperature for PVC was identified as 163 °C. Here the PVC distribution 2nd quantile was 9.2 % above the minimum observed failure temperature. Since the data shows that cable failure can occur below the 2nd quantile value for the PVC distribution the lower limit of the distribution was determined to be acceptable.

The PE distribution 2nd quantile was identified as 216 °C and the minimum failure temperature observed from the testing was 201 °C. The PE distribution 2nd quantile was approximately 7.5 % above the minimum observed failure temperature. Again, the testing has shown that cable failure can occur at temperatures lower than the 2nd quantile of the PE distribution and thus the PVC distribution lower limit was determined to be

acceptable. The thermal fragility curves developed here are used in section 5.3.2 to evaluate the current methods to calculate the cable damage probability. As discussed in the previous section 5.1, care should be taken when applying these thermal fragility curves. Since they are developed from a specific set of control cable insulation and jacket material configurations, these distributions are only applicable to cables of similar design. Use of these distributions with other cable configurations should be accompanied by an evaluation of the thermal failure temperature of the cable design for which the distribution is to be applied to. Failure to ensure alternative cable type failure temperatures fit the selected distribution may invalidate the results.

5.3 THIEF Model Predictions Based On Experimental Data

This section evaluates the FDT^s THIEF model prediction capabilities using the NRC FDT^s THIEF spreadsheet and the data from NRC sponsored tests. A determination of the FDT^s THIEF model bias and standard deviation based on the NRC data is also presented.

Data used in the evaluation of the FDT^s THIEF model included Penlight data from the CAROLFIRE and DESIREE-FIRE along with the CAROLFIRE intermediate-scale tests. The CAROLFIRE intermediate-scale tests were included to provide some comparison between the model prediction capabilities of real live fire environments to the radiant penlight results. The DESIREE-Fire intermediate-scale tests instrumented a limited number of special cable samples (Kerite-FR and Armored) for sub-jacket thermal response. Due to these cables' unique construction, the data from the intermediate-scale tests conducted in DESIREE-Fire were not used. Other data removed from this evaluation included tests where the thermally monitored cable was of a different

insulation material type than the electrically monitored cable. For example, the CAROLFIRE tests included cables in bundled pyramid configurations where a bundle of six cables (½ TS and ½ TP) monitored for electrical response and only one separate cable monitored for thermal response. For these cases, only the data from the electrically monitored cables that were identical to the thermally monitored cable were used. This was determined to be important because of the differences in the cable jacket thicknesses, diameters, and mass per unit lengths vary among cable products tested and would not allow for a direct comparison. In addition, cables that experienced ignition prior to electrical functional failure are noted in the evaluation. As will be shown, ignition prior to electrical functional failure has a significant effect on the ability of the THIEF model to accurately predict sub-jacket failure temperature.

The FDT^s THIEF model required several inputs, including a gas temperature profile, cable basic physical properties (diameter, mass per unit length, jacket thickness), raceway routing configuration, user specified failure temperature and a simulation time. The cable properties used for the evaluation conducted are presented in Table 8. The cable configuration properties were taken directly from test reports [McGrattan 2008]. Images of the cables are shown in Figure 31.

Table 8. Physical properties of cables evaluated in this Thesis [McGrattan 2008]

Cable Number	Cable Description (Insulation/Jacket No. Conductors)	Cable Chemical Classification	Jacket Thickness (mm)	Outer Diameter (mm)	Mass per Unit Length (kg/m)
1	PVC/PVC, 7/C	thermoplastic	1.1	12.4	0.324
2	EPR/CPE, 7/C	thermoset	1.52	15.1	0.383
3	XLPE/PVC, 7/C	Mixed	1.52	15.1	0.372
4	PVC/PVC, 2/C	thermoplastic	1.0	7.0	0.076
5	PVC/PVC, 3/C	thermoplastic	1.52	15.2	0.440
6	PVC/PVC, 12/C	thermoplastic	1.1	11.3	0.195
10	XLPE/CSPE, 7/C	thermoset	1.52	15.0	0.393
12	TEF/TEF, 7/C	thermoplastic	0.5	10.2	0.292
13	XLPE/CSPE, 12/C	thermoset	1.1	12.7	0.231
14	XLPE/CSPE, 3/C	thermoset	1.52	16.3	0.508
15	PE/PVC, 12/C	thermoplastic	1.14	15.0	0.522
16	XLPE/PVC Armored, 8/C	Mixed	1.27	24.4	0.981
K1	Kerite-FR, 10/C	thermoset	2.03	26.9	-
K3	Kerite-HTK, 3/C	thermoset	1.65	22.1	-
K5	Kerite-FR, 9/C	thermoset	1.65	21.6	-

Figure 31. End view of cables evaluated in this thesis [Nowlen and Wyant 2008]

The selection of the model's raceway configuration (tray or conduit) matched the actual experimental configuration (i.e., if the experiment tested a cable in 63 mm rigid steel conduit, the THIEF FDT^s model used a 63 mm rigid steel conduit). The simulation time was set to the length of the actual experiment. The user specified failure temperature was set to an arbitrary high temperature (1000 °C) to allow the simulation to run the duration specified by the simulation time. Specifying a generic cable failure temperature (205 °C for thermoplastic or 330 °C for thermoset) in the FDT^s THIEF spreadsheet would cause the model to stop calculating sub-jacket temperature when the predicted temperature exceeded the user specified failure temperature. This was not

desired because the model temperature prediction was compared to the actual experimental sub-jacket temperature which routinely exceeded these generic thresholds.

The shroud temperature was selected for the exposing gas temperature profile for the Penlight radiant tests. The shroud temperature was used instead of the air thermocouple measurements for two reasons. First the locations of the thermocouples measuring the external air temperature were not located at the middle of the exposure chamber, but approximately 0.25 m from the middle cross-section of the shroud. Due to the Penlight thermal exposure profile described in section 4.2.2.10, the air thermocouples would be recording a lower temperature than if they were located at the middle of the chamber where the most severe thermal exposure are located and the expected location for cable damage to occur. Secondly, the poor ability of the air to conduct radiant heat indicated that the shroud temperature was a better representation of the exposing thermal profile to the cable. The Penlight exposure profile was close to a step function, with a linear heat up from ambient to steady state conditions taking 1-2 minutes. The shroud exposure temperatures ranged from 300-525 °C for the thermoplastic cables and between 470-700 °C for the thermoset cables. For the intermediate-scale tests, the exposing gas temperature profile near the electrically monitored cable was used in the FDT^s THIEF simulations.

With an exposing temperature profile for each test and a corresponding sub-jacket temperature profile, the FDT^s THIEF model predictions were evaluated against the experimentally measured sub-jacket cable temperatures. Tables 9 through 13 present the results of the FDT^s THIEF model simulations. These tables present the FDT^s THIEF model sub-jacket temperature prediction at the time that the actual experimental circuit

electrical failure, the experimental sub-jacket temperature at time of electrical failure (typically two measurements), cable ignition status occurs prior to electrical functional failure, and the error between measured and predicted, calculated as;

$$\frac{[Predicted - Measured]}{Measured}\ x\ 100\%. \qquad \text{Equation 7}$$

Table 9. Comparison of THIEF model predictions versus CAROLFIRE penlight experimental results – thermoplastic data

Test #	Temperature (°C)			Error %		Cable ignition prior to Failure
	THIEF Predicted Failure	Experiment Measured Failure				
PT-4	229.6	195.5	200.6	17.4	14.5	No
PT-5	253.2	212.9	211.0	18.9	20.0	
PT-6	255.6	215.8	206.1	18.4	24.0	
PT-8	198.2	163.8	173.8	21.0	14.0	
PT-10	279.9	227.5	N/A*	23.0	N/A	
PT-14	289.5	237.9	237.4	21.7	21.9	
PT-15	274.4	266.2	246.2	3.1	11.5	
PT-16	278.1	244.0	236.0	14.0	17.8	
PT-21	245.0	229.0	196.0	7.0	25.0	
PT-22	404.8	384.4	382.3	5.3	5.9	
PT-29	269.7	239.2	232.3	12.8	16.1	
PT-30	235.6	256.0	243.0	-8.0	-3.0	
PT-35 E	412.2	384.7	325.3	7.1	26.7	
PT-37 B	521.9	440.2	419.2	18.6	24.5	
PT-37 C	523.2	440.0	447.3	18.9	17.0	
PT-46 E	397.5	307.3	320.5	29.4	24.0	
PT-49 C	521.8	471.9	452.3	10.6	15.4	
PT-50 A	433.8	309.2	355.5	40.3	22.0	
PT-63	251.5	208.4	205.5	20.7	22.4	
PT-65	275.3	237.7	N/A	15.8	N/A	
PT-68	507.4	411.9	415.3	23.2	22.2	
PT-35 B	453.5	510.7	474.4	-11.2	-4.4	Yes
PT-35 C	442.5	470.8	444.3	-6.0	-0.4	
PT-43 B	279.4	176.5	229.7	58.3	21.6	
PT-43 C	396.8	491.4	575.6	-19.3	-31.1	
PT-43 E	455.0	698.6	698.6	-34.9	-34.9	
PT-44A	468.3	227.5	556.2	105.8	-15.8	
PT-44E	499.2	295.3	597.6	69.0	-16.5	
PT-45 A	507.0	5375	N/A	-90.6	N/A	
PT-45E	475.1	556.3	N/A	-14.6	N/A	
PT-46B	405.6	245.6	532.1	65.1	-23.8	

* N/A indicates that a second temperature measurement was not available.

Table 10. Comparison of THIEF model predictions versus CAROLFIRE penlight experimental results – thermoset data

Test #	Temperature (°C)			Error %		Cable ignition prior to Failure
	THIEF Predicted Failure	Experimental Measured Failure				
PT-1	436.9	395.8	393.5	10.4	11.0	
PT-7	472.0	403.3	423.7	17.0	11.4	
PT-9	465.6	417.7	412.7	11.5	12.8	
PT-11	469.4	414.8	425.0	13.2	10.4	
PT-12	471.7	425.5	419.4	10.9	12.5	
PT-13	471.2	433.9	419.1	8.6	12.4	
PT-19	471.2	435.6	418.9	8.2	12.5	
PT-23	462.3	424.6	429.0	8.9	7.8	
PT-24	464.3	431.7	422.0	7.6	10.0	
PT-27	467.9	423.3	426.4	10.5	9.7	
PT-28	466.3	430.4	421.4	8.3	10.7	
PT-34 A	519.3	412.0	430.2	26.0	20.7	
PT-34 B	523.3	468.6	442.0	11.7	18.4	
PT-34 C	522.6	445.1	432.7	17.4	20.8	
PT-34 D	523.0	450.6	433.4	16.1	20.7	
PT-34 E	523.1	464.8	534.6	12.5	-2.2	
PT-34 F	523.1	501.1	454.4	4.4	15.1	
PT-36 A	517.1	463.6	455.7	11.5	13.5	
PT-36 B	512.2	439.3	459.8	16.6	11.4	No
PT-36 C	508.7	457.6	430.6	11.2	18.1	
PT-37 A	525.1	436.8	445.8	20.2	17.8	
PT-45 C	513.1	521.1	511.4	-1.5	0.3	
PT-47 A	515.8	438.0	457.3	17.8	12.8	
PT-47 B	518.8	422.9	451.5	22.7	14.9	
PT-47 C	495.4	366.5	423.7	35.2	16.9	
PT-48 A	508.5	393.0	426.5	29.4	19.2	
PT-48 B	523.3	484.0	465.5	8.1	12.4	
PT-48 C	522.6	469.2	462.0	11.4	13.1	
PT-49 A	525.5	481.8	464.2	9.1	13.2	
PT-49 B	525.6	481.2	461.5	9.2	13.9	
PT-50 B	511.0	407.0	445.6	25.6	14.7	
PT-50 C	524.4	454.0	469.7	15.5	11.6	
PT-61 A	514.1	422.4	438.3	21.7	17.3	
PT-61 B	522.5	453.6	466.2	15.2	12.1	
PT-61 C	519.9	437.2	455.6	18.9	14.1	
PT-68 D	515.8	399.4	394.5	29.1	30.7	
PT-68 F	514.1	398.7	403.5	28.9	27.4	
PT-19*	370.8	426.0	441.3	-13.0	-16.0	
PT-17	429.7	641.6	532.9	-33.0	-19.4	
PT-2	433.1	470.0	519.9	-7.9	-16.7	
PT-20	435.7	440.1	447.1	-1.0	-2.5	Yes
PT-3	418.9	452.9	529.6	-7.5	-20.9	
PT-35 A	517.9	657.2	652.2	-21.2	-20.6	
PT-35 D	517.6	631.7	603.1	-18.1	-14.2	

Test #	Temperature (°C)			Error %		Cable ignition prior to Failure
	THIEF Predicted Failure	Experimental Measured Failure				
PT-35 F	483.6	642.7	550.4	-24.8	-12.1	
PT-43 A	478.9	680.5	697.1	-29.6	-31.3	
PT-43 D	460.2	640.8	676.7	-28.2	-32.0	
PT-43 F	477.3	619.5	652.2	-23.0	-26.8	
PT-44 C	478.9	227.5	556.2	110.5	-13.9	
PT-44 D	498.3	295.3	597.6	68.7	-16.6	
PT-45 B	515.8	537.5	N/A	-4.0	N/A	
PT-46 D	504.5	552.5	572.4	-8.7	-11.9	
PT-46 F	432.7	382.8	613.3	13.0	-29.4	
PT-60 A	511.6	625.8	623.2	-18.2	-17.9	Yes
PT-60 B	461.7	498.7	447.8	-7.4	3.1	
PT-60 C	497.6	674.4	574.1	-26.2	-13.3	
PT-60 D	488.0	602.7	548.2	-19.0	-11.0	
PT-60 E	555.0	562.2	547.0	-1.3	1.5	
PT-60 F	511.6	625.8	632.2	-18.2	-19.1	
PT-62	371.8	520.4	460.5	-28.6	-19.3	
PT-64	363.3	588.9	N/A	-38.3	N/A	
PT-68 B	495.6	485.0	511.4	2.2	-3.1	
PT-68 C	471.3	399.4	394.5	18.0	19.5	

* DESIREE-FIRE test using ac MOV circuit

Table 11. Comparison of THIEF model predictions versus DESIREE-Fire penlight experimental results – thermoset data

Test #	Temperature (°C)			Error %		Cable ignition prior to Failure
	THIEF Predicted Failure	Experimental Measured Failure				
P-23-SOV1	344.0	383.9	390.3	-10.4	-11.9	No
P-23-SOV2	353.0	416.9	417.0	-15.3	-15.3	
P-24-SwGr-T	469.0	364.5	374.7	28.7	25.2	
P-25-MOV1	407.0	488.1	426.7	-16.6	-4.6	
P-25-MOV2	386.0	380.5	377.7	1.4	2.2	
P-35-SwGr-T	516.3	404.6	N/A	27.6	N/A	
P-35-SwGr-C	516.3	404.6	N/A	27.6	N/A	
P-37-MOV1	517.7	424.9	N/A	21.8	N/A	
P-37-MOV2	518.2	426.9	N/A	21.4	N/A	
P-42-SwGr-T	453.9	398.7	410.83	13.8	10.5	
P-24-SwGr-C	470.0	539.9	643.7	-12.9	-27.0	Yes
P-1-SOV1	401.2	510.7	522.8	-21.4	-23.3	
P-1-SOV2	387.3	499.8	530.4	-22.5	-27.0	
P-2-SOV1	392.7	436.9	498.0	-10.1	-21.1	
P-2-SOV2	406.6	475.1	477.1	-14.4	-14.8	
P-3-SwGr-T	418.0	487.9	499.0	-14.3	-16.2	
P-5-LgCoil	415.1	432.0	459.8	-3.9	-9.7	
P-5-Valve	408.2	432.0	459.8	-5.5	-11.2	
P-6-LgCoil	416.0	470.2	499.8	-11.5	-16.8	
P-6-Valve	412.9	451.0	465.2	-8.4	-11.2	
P-7-MOV1	392.0	457.0	467.9	-14.2	-16.2	
P-7-MOV1	381.3	588.17	600.9	-35.2	-36.5	
P-8-MOV1	379.0	467.65	579.3	-19.0	-34.6	
P-8-MOV1	367.9	398.0	401.7	-7.6	-8.4	
P-42-SwGr-C	457.3	386.9	387.8	18.2	17.9	

Table 12. Comparison of THIEF model predictions versus DESIREE-FIRE penlight experimental results – thermoplastic data

Test #	Temperature (°C)			Error %		Cable ignition prior to Failure
	THIEF Predicted Failure	Experimental Measured Failure				
P-9-SOV1	275	249.5	258.3	10.2	6.5	No
P-9-SOV2	271	246.1	250.4	10.1	8.2	
P-10-SwGr-T	279	253.5	264.6	10.1	5.4	
P-10-SwGr-C	281	254.3	281.0	10.5	0.0	
P-11-LgCoil	306	263.7	268.7	16.0	13.9	
P-11-Valve	307	265.3	269.7	15.7	13.8	
P-12-MOV1	275	236.2	238.5	16.4	15.3	
P-12-MOV2	308	255.0	256.0	20.8	20.3	
P-38-SOV1	428	459.3	N/A	-6.8	N/A	
P-38-SOV2	340	258.9	N/A	31.3	N/A	
P-40-LgCoil	445	427.8	N/A	4.0	N/A	
P-40-Valve	446	432.3	N/A	3.2	N/A	
P-31-SOV1	222	203.0	216.0	9.4	2.8	
P-31-SOV2	229	207.0	219.0	10.6	4.6	
P-32-SwGr-T	270	222.0	225.0	21.6	20.0	
P-32-SwGr-C	271	223.1	225.3	21.5	20.3	
P-33-MOV1	266	223.1	224.4	19.2	18.5	
P-33-MOV2	264	223.2	222.9	18.3	18.4	
P-28-SOV1	348	291.7	295.4	19.3	17.8	
P-28-SOV2	365	300.0	303.0	21.7	20.5	
P-29-SwGr-T	393	302.7	306.2	29.8	28.3	
P-29-SwGr-C	396	310.4	311.6	27.6	27.1	
P-30-MOV1	343	293.0	289.0	17.1	18.7	
P-30-MOV2	344	292.9	290.0	17.4	18.6	
P-39-SwGr-T	375	347.6	N/A	7.9	N/A	Yes
P-39-SwGr-C	477	504.1	N/A	-5.4	N/A	
P-41-MOV1	522	504.4	N/A	3.5	N/A	
P-41-MOV2	520	502.4	N/A	3.5	N/A	

Table 13. Comparison of THIEF model predictions versus CAROLFIRE intermediate-scale experimental results – both thermoset and thermoplastic

Insulation Type	Test #	Temperature (°C)			Error %		Cable ignition prior to Failure
		THIEF Predicted Failure	Experimental Measured Failure				
TP	IT-10-CK4	373	388.5	400.1	-4.0	-6.8	Unknown
	IT-11-CK3	151	224.0	N/A	-32.6	N/A	
	IT-12-CK3	179	67.2	71.0	166.4	152.1	
	IT-2-CK3	154	234.0	N/A	-34.2	N/A	
	IT-3-CK4	196	82.9	118.4	136.4	65.5	
	IT-7-CK1	165	190.4	N/A	-13.3	N/A	
	IT-9-CK4	217	290.5	N/A	-25.3	N/A	
	IT-11-CK2	191	89.1	115.8	114.4	64.9	
	IT-12-CK2	210	161.5	190.7	30.0	10.1	
TS	IT-1-CK1	378	291.1	N/A	29.9	N/A	
	IT-1-CK2	375	283.3	N/A	32.4	N/A	
	IT-1-CK3	345	221.6	N/A	55.7	N/A	
	IT-1-CK4	370	269.5	N/A	37.3	N/A	
	IT-6-CK3	740	828.0	824.3	-10.6	-10.2	
	IT-13-CK1	590	551.2	516.5	7.0	14.2	
	IT-14-CK1	562	536.9	428.3	4.7	31.2	
	IT-14-CK2	556	520.2	351.1	6.9	58.4	
	IT-10-CK1	250	219.8	232.4	13.7	7.6	
	IT-13-CK3	455	392.1	470.2	16.0	-3.2	
	IT-14-CK3	431	433.4	451.3	-0.6	-4.5	
	IT-14-CK4	404	390.9	416.9	3.4	-3.1	
	IT-9-CK1	396	335.9	422.2	17.9	-6.2	

Figure 32 shows the results of the THIEF FDT^s model predicted versus experimental measured temperature at the time of electrical cable functional failure for the CAROLFIRE small-scale radiant penlight tests. Figure 33 shows the results from the DESIREE-Fire Penlight test data and Figure 34 for the CAROLFIRE intermediate-scale testing. In all of these figures, a solid linear line with a slope of 1 has been inserted. Data points lying on this line represent a model prediction that is in agreement with the experimentally measured value. In some of the plots a long dashed line and two dotted lines have been inserted. The long dashed line represent the mean of the data and the dotted lines represent one standard deviation from the mean.

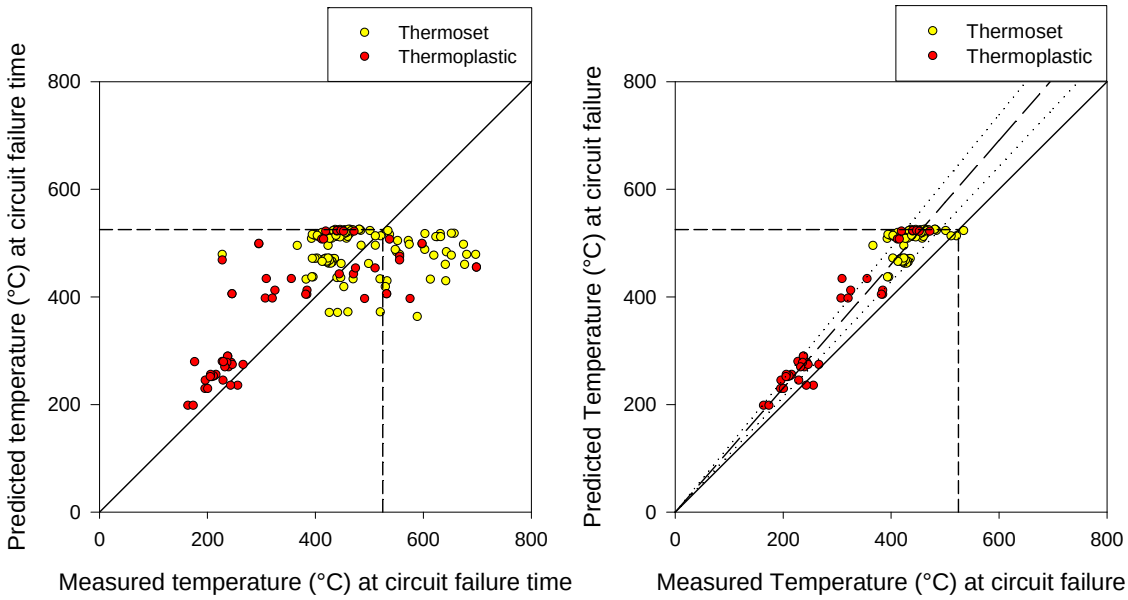

Figure 32. THIEF Temperature Prediction versus Measured Temperature at Time of 1st Electrical Failure for CAROLFIRE Penlight experiments showing effect of cable ignition. Plot on left contains all data points, plot on right shows only data points where cable electrical failure occurs prior to cable ignition (long dashed line is mean of data with doted lines one standard deviation).

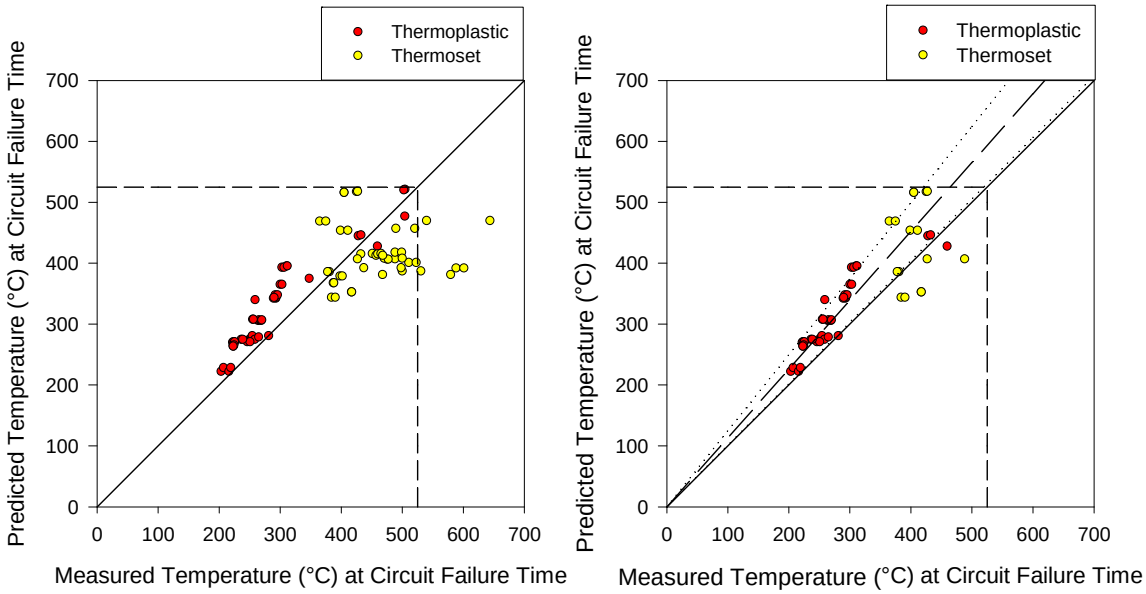

Figure 33. THIEF Temperature Prediction versus Measured Temperature at Time of 1st Electrical Failure for DESIREE-Fire Penlight experiments showing effect of cable ignition. Plot on left contains all data points, plot on right shows only data points where cable electrical failure occurs prior to cable ignition (long dashed line is mean of data with doted lines one standard deviation).

The left plot in Figures 32 and 33 contains all of the penlight small-scale test data for the respective test programs. As shown the predicted and measured points agree until approximately 400 °C. At this point and above, dispersion of the measured temperatures

occurs indicating that the model is under-predicting the sub-jacket temperature at electrical failure. This was likely due to cable ignition, the FDT^s THIEF's inability to predict cable ignition and subsequent cable burning, and the use of the Penlight shroud temperature as the model exposing gas temperature input profile. The maximum shroud temperatures used for the penlight tests was 525 °C. This corresponded to the maximum model input exposing temperature. As can be seen from the left plot in Figures 32 and 33, no data lies above 525 °C on the vertical (predicted temperature) axis. Since the model does not include cable combustion, the maximum predicted subjacket temperature cannot exceed the maximum input exposing temperature which was the Penlight shroud temperature. Therefore, when the cable ignited it was exposed to higher temperature than the shroud exposure and the corresponding cable subjacket temperature was higher than the temperature calculated by the FDT^s THIEF model. The plot on the right represents the same data shown to the left, but with data points removed that correspond to electrical failure occurring after the cable ignites. These results were nearly linear and indicate that when cable ignition was ignored, the model over-predicted the sub-jacket temperature by 15.1 % on average with a standard deviation of 7.2 %. As presented by McGrattan, the THIEF model does not include ignition and burning [McGrattan 2008]. For the Penlight DESIREE-FIRE data the model over-predicted the sub-jacket temperature by 13.0 % on average with a standard deviation of 11.9 %.

A similar approach can be taken for the CAROLFIRE intermediate-scale experiments. However, due to the experimental setup, cables in location A (refer to Figure 17) are immersed in flames from the onset of the test and cable ignition cannot be determined from the test data. So these data points have been removed entirely from the

evaluation. Figure 34 shows the results of this evaluation. On average, THIEF over-predicted the sub-jacket temperature by 22.0 %, with a standard deviation of 38.3 % for the CAROLFIRE intermediate-scale tests.

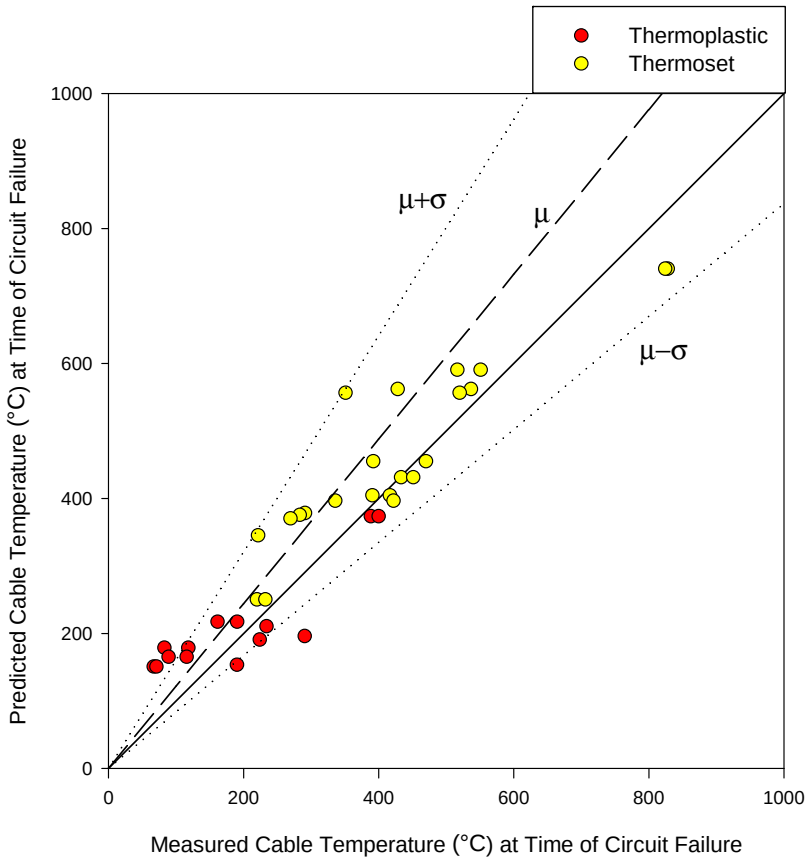

Figure 34. FDT^s THIEF Temperature prediction versus measured temperature at time of 1st failure for CAROLFIRE Intermediate-scale experiments with data parsed by insulation type.

This review of FDT^s THIEF temperature predictions based on experimental data has shown the model to over-predict the electrical cables sub-jacket temperatures based on a predefined cable failure time. The failure times used here were when the cable in each test experienced an electrical functional failure. The model's over-prediction of sub-jacket temperature corresponds to under-predicting the time to cable electrical damage because the FDT^s THIEF model uses a user defined failure temperature to predict time of damage. McGrattan has shown similar results when evaluating the THIEF model

predictive versus measured time to electrical cable sub-jacket temperature [McGrattan 2008]. This is slightly conservative, a desirable property for use in fire PRA applications. As a result of under-predicting the time to damage estimates, the fire PRA would over-predict the non-suppression probability to the fire scenario, which adds conservatism to the fire PRA.

The next section will quantify this models over-prediction based on the NRC sponsored experimental data. Once the model prediction capabilities are quantified, the model temperature prediction distributions will be combined with the cable thermal fragility distributions to develop joint probability of cable failure distributions that could find application in Fire PRA.

5.3.1 Determination of THIEF model bias and standard deviation

The NFPA performance-based standard for fire protection states that "only fire models that are acceptable to the authority having jurisdiction (i.e., NRC) shall be used in fire modeling calculations." In addition, acceptable fire models shall only be used within their limitations and shall be verified and validated (V&V) [NFPA 2001]. The NRC and EPRI performed a V&V study on five selected fire models, documented in NUREG-1824. The results of this study provided model statistics to understand the uncertainty of the model predictions. These statistics are developed here for the FDTs THIEF model using the available information for the NRC CAROLFIRE and DESIREE-FIRE test data.

The NRC and EPRI presented methods to derive a fire model's uncertainty statistics referred to as the *bias factor*, δ, that indicates the extent to which the model, on average, under- or over-predicted the measurement of a given quantity [EPRI/NRC-RES 2007, EPRI/NRC-RES 2011]. A bias factor greater than 1.0 indicated that model over-

predicted, while a bias factor less than 1.0 indicated under-prediction. The second statistic was the relative standard deviation of the model, $\tilde{\sigma}_M$, and of the experiment, $\tilde{\sigma}_E$, For a model prediction, M, these statistics and the assumption that the "true" value of the predicted quantity (temperature from THIEF) was a normally distributed random variable with a mean $\mu = M/\delta$, and a standard deviation $\sigma = \tilde{\sigma}_M(M/\delta)$ [EPRI/NRC-RES 2011].

NUREG-1934 presents the derivation of model uncertainty statistics as follows [EPRI/NRC-RES 2011].

$$\delta = \exp\left(\overline{\ln(M/E)} + \frac{\tilde{\sigma}_M^2 - \tilde{\sigma}_E^2}{2}\right) \quad \text{Equation 8}$$

$$\sqrt{\tilde{\sigma}_M^2 + \tilde{\sigma}_E^2} = \sqrt{\frac{1}{n-1}\sum_{i=1}^{n}\left[\ln(M_i/E_i) - \overline{\ln(M/E)}\right]^2} \quad \text{Equation 9}$$

$$\overline{\ln(M/E)} = \frac{1}{n}\sum_{i=1}^{n}\ln(M_i/E_i) \quad \text{Equation 10}$$

where M is the model prediction and E is the experimental measurement.

Using the experimental temperature measurements recorded at the time of circuit failure and the FDT^s THIEF model predictions (presented in section 5.3), the bias factor and model standard deviation were calculated using Equations 8 through 10. Data from CAROLFIRE and DESIREE-Fire Penlight tests, along with the CAROLFIRE intermediate-scale tests where electrical functional failures occurred prior to cable ignition were used. The results are:

$$\delta_{\text{THIEF}} = 1.15$$

$$\tilde{\sigma}_{THIEF} = 0.14$$

Therefore, the over-prediction of the FDT^s THIEF model is found to be 15 % on average with a 14 % standard deviation. For an experimental standard deviation, $\tilde{\sigma}_E$, the error associated with the Type K thermocouple measurement was used (0.75 %)

[OMEGA 2012]. Increasing the experimental standard deviation by one order of magnitude (7.5%) and re-calculating the model bias and standard deviation remained 1.15 for the bias factor and the standard deviation remained 0.14. Therefore the bias and standard deviation are insensitive to the value used for experimental uncertainty.

The FDT^s THEIF bias factor, δ, corresponded well to the mean error calculated for each data set in section 5.3 of 15.1 %, 22.0 %, and 13.0 % for the CAROLFIRE Penlight, intermediate-scale, and DESIREE-Fire Penlight respectively.

The THIEF model predicted cable damage by simply calculating the heat conducted through the cable jacket in one dimension, ignoring the complex geometry of the components enclosed within the cable jacket (modeled as lumped parameter) and using experimental cable sub-jacket failure temperatures to correlate cable failure. Although this approach was simplistic, the incorporation of the THIEF target model into fire models such as FDS, CFAST, and FDT^s has allowed for the time dependant thermal exposure conditions calculated by these fire models to be used to calculate the sub-jacket cable temperature. The complex cable routing configurations found in NPPs, the uncertainty of a cables location within a cable raceway, and the results of the THIEF model evaluation presented in this section, has shown that the THIEF model provides an adequate method of calculating cable damage that can be used in the field. However, the results of this model are dependent on the input parameters, and as such, the user must ensure that the cable properties (mass per unit length, cable diameter, jacket thickness), thermal exposure conditions, and sub-jacket cable failure temperature are known for the specific cable under evaluation and the associated fire scenario. Uncertainties associated with any of these model inputs should be accounted for in the evaluation.

The development of a two dimensional cable heat conduction model could provide improvements to the THIEF model, however there are numerous challenges to such a models development (proprietary cable material properties, accounting for numerous cable routing configurations, etc.) and any benefit from developing such a model for use in fire PRA applications may not outweigh the costs associated with its development. The area where greatest improvement to the THIEF model would be to develop a cable ignition model. As was shown in the previous section, one weakness of the THIEF model was a lack of modeling cable ignition and the subsequent thermal exposures associated with cable combustion. Rather than modifying the THIEF model to account for the ignition characteristics, it would be recommended to develop an cable ignition model. Then the prediction of the time to cable failure would be whatever model predicted cable failure first (electrical failure via THIEF or ignition). The data suggested that the tested cables failed shortly after ignition, therefore assuming cable damage at ignition seems reasonable.

5.3.2 Evaluation of the cable damage thermal fragility distributions using Monte Carlo Simulation

With the FDT^s THIEF prediction modeled as a normally distributed probability of the sub-jacket temperature and the cable thermal fragility probability distributions developed in section 5.2, these two distributions were combined to develop a joint cable damage probability based on the cable insulation material and the FDT^s THIEF model prediction. These results were then compared to the current method of calculating the probability of a sub-jacket cable temperature exceeding a single value threshold. Theoretically, a convolution of the two distributions could be computed, however the

analytical solution of this problem is complex and not always solvable. Therefore, it was chosen to use a Monte Carlo (MC) simulation instead.

MC simulation relies on random sampling of distributions to compute a mathematical result. For the scenarios conducted here, the MC simulation selects one random sample from the normally distributed "THIEF model predication" distribution and another independent random sample from the log-normal distributed cable thermal fragility distribution. These two samples constitute one trial. For each trial, if the FDT^s THIEF fire model prediction value exceeded the cable thermal fragility value, the result would be cable damage and assigned an value of 1. Conversely, if the fire model prediction value did not exceed the cable damage fragility sample, the cable would not be damage and this result was assigned a value of 0. Each simulation consisted of 1,000 trials and the result (1 or 0) of all 1,000 trials were averaged to develop the simulation probability of cable damage. Next, one thousand simulations were run for each FDT^s THIEF temperature prediction value and the mean of probabilities from these 1,000 simulations were recorded. The choice of using 1,000 simulations was based on the convergence of the results based on simulations run at 100, 1,000, and 3,300 repetitions. Next the FDT^s THIEF model prediction would be increased by 10 to 20 °C and the complete MC simulation would be repeated. This was continued until the fire model prediction distribution transverse the cable thermal fragility distribution. This was done for the three cable thermal fragility distributions developed in section 5.2, namely, thermoset insulated, PE insulated, and PVC insulated. These MC simulations were run using Microsoft Excel™ and a Visual Basic Macro documented in Appendix A. These

MC simulation results were then compared to the current method of calculating the cable damage probability, which is explained next.

Draft NUREG-1934 presented the current method for calculating the cable damage probability. This method used the THIEF fire model prediction distributions to identify what the probability of exceeding a specific single point failure threshold (205 °C for thermoplastic and 330 °C for thermoset insulated cables). The probability calculation are presented in Equation 11 based on a normal distribution, with an illustration shown in Figure 35.

$$P(x > x_c) = \frac{1}{2} erfc\left(\frac{x_c - \mu}{\sigma\sqrt{2}}\right) \qquad \text{Equation 11}$$

where,

$$erfc(x) = \frac{2}{\sqrt{\pi}} \int_x^{\infty} e^{-t^2} dt \qquad \text{Equation 12}$$

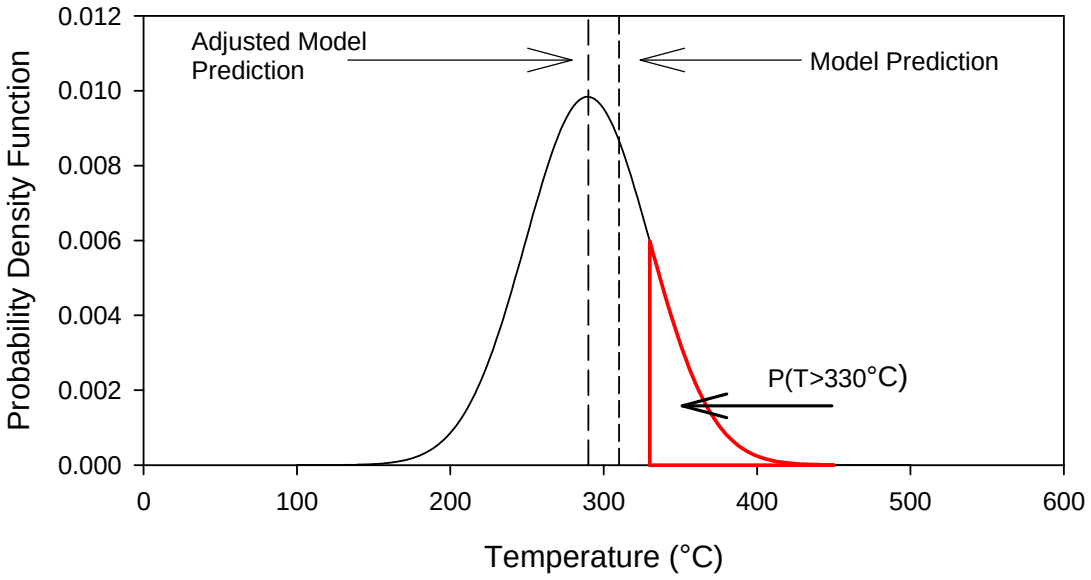

Figure 35. Normal distribution of true value of cable temperature showing probability of model prediction exceeding cable damage temperature threshold of 330°C

The results of the MC simulation (shown as blue circles) and the single threshold method used in NUREG-1934 (shown as red line) are presented in graphical and tabular forms. Figure 36 and Table 14 present the results for the thermoset case, Figure 37 and

Table 15 contain the PE insulated cable case results, and Figure 38 and Table 16 for the PVC insulated case.

It should be emphasized that these results were based on a limited variety of cable insulation materials (TS {XLPE, EPR} and PVC, PE). The applicability of these results to cables other than those used to develop these probabilities was uncertain. The same general method could be applied, however confirmation of the specific cable thermal failure point would need to be determined and compared to the results presented here. Lack of variability of experimental thermal exposure conditions also adds to the uncertainty of using these results generically.

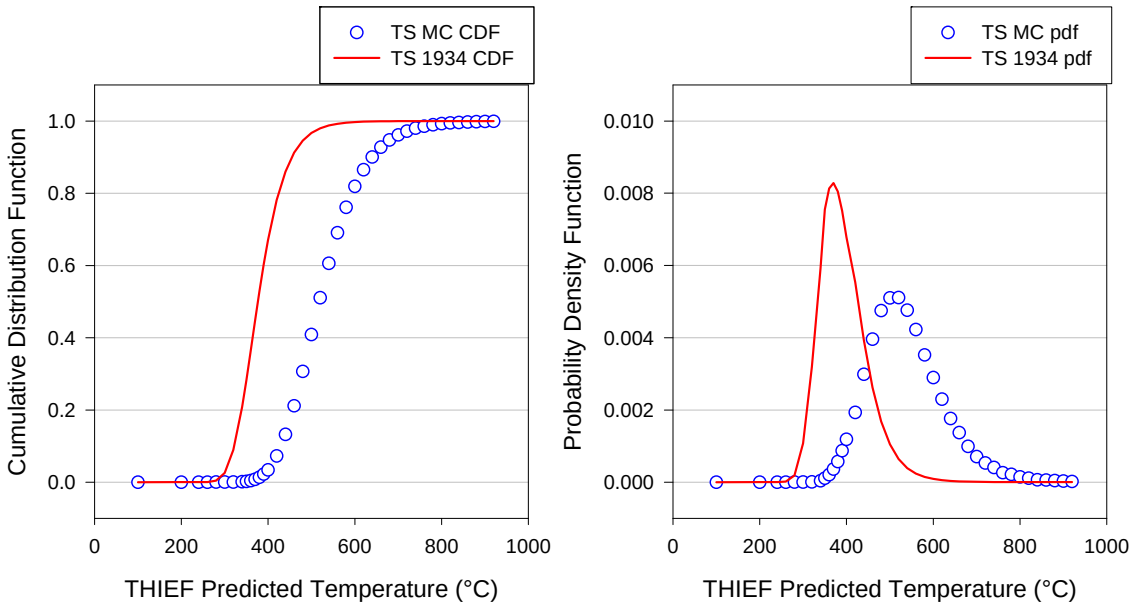

Figure 36. Probability of thermoset cable failure based on THIEF model prediction.

Table 14. Thermoset probabilities of cable damage based on THIEF prediction

THIEF Prediction Temperature (°C)	Single Threshold Probability P(T>330 °C)	Distribution Probability M.C. CDF	THIEF Prediction Temperature (°C)	Single Threshold Probability P(T>330 °C)	Distribution Probability M.C. CDF
200	1.24×10^{-12}	0	460	0.912	0.212
240	4.67×10^{-6}	0	480	0.946	0.306
260	2.63×10^{-4}	0	500	0.967	0.409
280	4.01×10^{-3}	2.00×10^{-6}	520	0.980	0.511
300	0.025	1.80×10^{-5}	540	0.988	0.606
320	0.089	1.44×10^{-4}	560	0.992	0.690

THIEF Prediction Temperature (°C)	Single Threshold Probability P(T>330 °C)	Distribution Probability M.C. CDF	THIEF Prediction Temperature (°C)	Single Threshold Probability P(T>330 °C)	Distribution Probability M.C. CDF
340	0.208	$9.38x10^{-4}$	600	0.997	0.819
350	0.283	$2.01x10^{-3}$	620	0.998	0.865
360	0.364	$4.01x10^{-3}$	640	0.999	0.900
370	0.447	$4.70x10^{-3}$	660	0.999	0.927
380	0.528	$1.34x10^{-2}$	680	0.999	0.947
390	0.603	$2.21x10^{-2}$	700	0.999	0.961
400	0.671	$3.40x10^{-2}$	720	0.999	0.972
420	0.781	$7.26x10^{-2}$	740	0.999	0.980
440	0.860	0.1324	760	0.9999	0.985

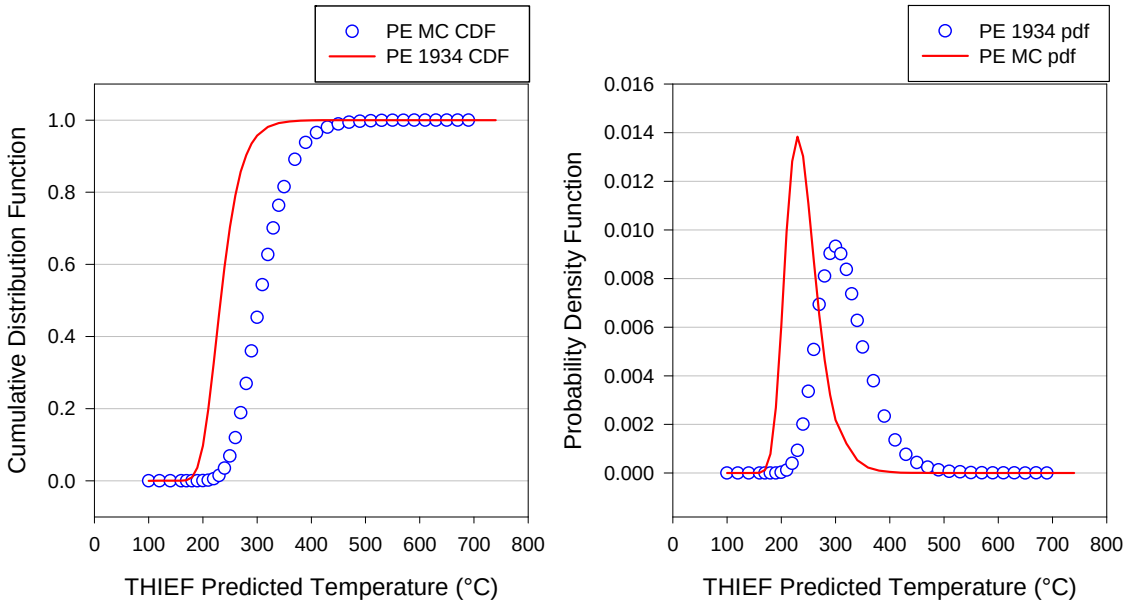

Figure 37. Probability of PE insulated cable failure based on THIEF model predication.

Table 15. PE insulated cable probabilities of cable damage based on THIEF prediction

THIEF Prediction Temperature (°C)	Single Threshold Probability P(T>205 °C)	Distribution Probability M.C. CDF	THIEF Prediction Temperature (°C)	Single Threshold Probability P(T>205 °C)	Distribution Probability M.C. CDF
140	$1.69x10^{-8}$	0	340	0.9917	0.7634
160	$1.03x10^{-4}$	0	350	0.9944	0.8152
170	$1.404x10^{-3}$	0	370	0.9975	0.8910
180	$9.26x10^{-3}$	0	390	0.9988	0.9378
190	$3.62x10^{-2}$	0	410	0.9994	0.9650
200	$9.69x10^{-2}$	0.0003	430	0.9997	0.9803
210	0.1962	0.0015	450	0.9998	0.9890
220	0.3244	0.0055	470	0.9999	0.9939
230	0.4627	0.0148	490	1.0	0.9965
240	0.5930	0.0349	510	1.0	0.9979
250	0.7039	0.0685	530	1.0	0.9989
260	0.7913	0.1193	550	1.0	0.9993
270	0.8564	0.1886	570	1.0	0.9996

THIEF Prediction Temperature (°C)	Single Threshold Probability P(T>205 °C)	Distribution Probability M.C. CDF	THIEF Prediction Temperature (°C)	Single Threshold Probability P(T>205 °C)	Distribution Probability M.C. CDF
280	0.9029	0.2696	590	1.0	0.9997
290	0.9351	0.3599	610	1.0	0.9998
300	0.9569	0.4531	630	1.0	0.9999
310	0.9715	0.5433	650	1.0	0.9999
320	0.9811	0.6270	670	1.0	1.0
330	0.9875	0.7007	690	1.0	1.0

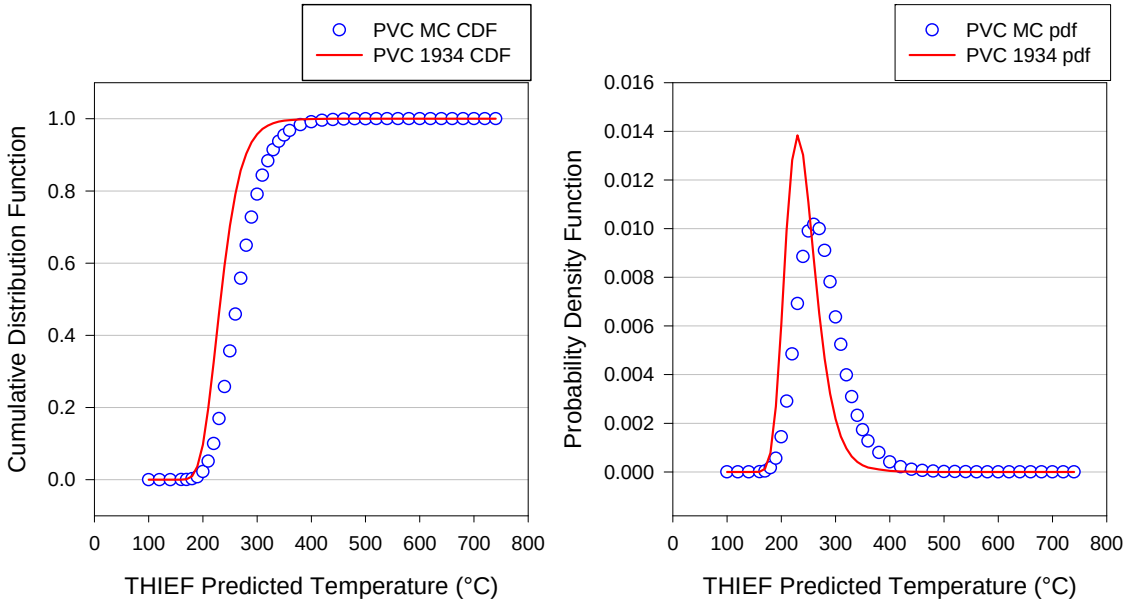

Figure 38. Probability of PVC insulated cable failure based on THIEF model predication

Table 16. PVC insulated cable probabilities of cable damage based on THIEF prediction

THIEF Prediction Temperature (°C)	Single Threshold Probability P(T>205 °C)	Distribution Probability M.C. CDF	THIEF Prediction Temperature (°C)	Single Threshold Probability P(T>205 °C)	Distribution Probability M.C. CDF
100	0	0	310	0.9715	0.8432
120	$3.88x10^{-16}$	0	320	0.9811	0.8830
140	$1.69x10^{-8}$	0	330	0.9875	0.9139
160	1.02x10-4	0.0001	340	0.9917	0.9371
170	1.40x10-3	0.0004	350	0.9944	0.9544
180	9.26x10-3	0.0021	360	0.9962	0.9671
190	$3.62x10^{-2}$	0.0077	380	0.9983	0.9830
200	$9.69x10^{-2}$	0.0221	400	0.9992	0.9912
210	0.1962	0.0512	420	0.9996	0.9954
220	0.3244	0.0997	440	0.9998	0.9975
230	0.4627	0.1689	460	0.9999	0.9987
240	0.5930	0.2574	480	0.9999	0.9993
250	0.7039	0.3564	500	1.0	0.9996
260	0.7913	0.4581	520	1.0	0.9998
270	0.8564	0.5580	540	1.0	0.9999
280	0.9029	0.6490	560	1.0	0.9999

THIEF Prediction Temperature (°C)	Single Threshold Probability P(T>205 °C)	Distribution Probability M.C. CDF	THIEF Prediction Temperature (°C)	Single Threshold Probability P(T>205 °C)	Distribution Probability M.C. CDF
290	0.9351	0.7271	580	1.0	1.0
300	0.9569	0.7908	600	1.0	1.0

The results indicated that the joint probability of cable damage using the cable fragility curves occur at higher temperatures than joint probability of cable damage using the single point failure threshold method. To evaluate the amount of difference between these two probabilities, a relative difference evaluation between the two distribution for each insulation types was conducted. To accomplish this evaluation, a MC simulation was conducted sampling from each joint distributions and a random variable was assigned the difference between the two sample temperatures (D = MC cable fragility distribution sample – single point distribution sample). Again, a MC simulation of one thousand simulations of one thousand trials were used. The results are presented in histogram form in Figure 39 for the TS and Figure 40 for PE and PVC.

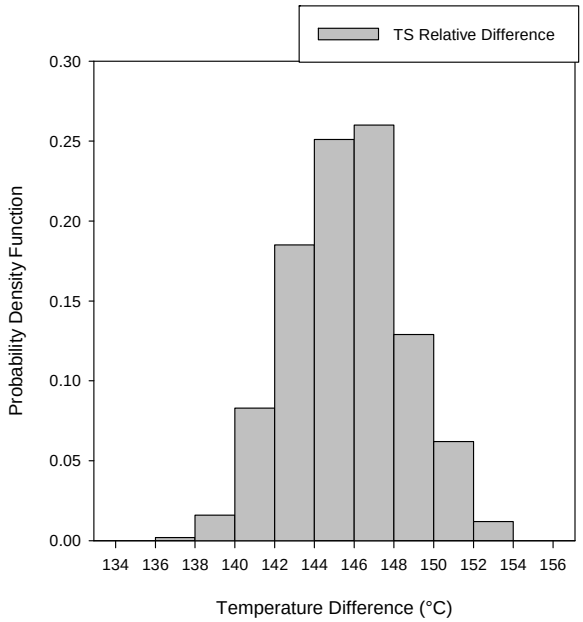

Figure 39. Histogram of relative difference simulation results for TS distributions

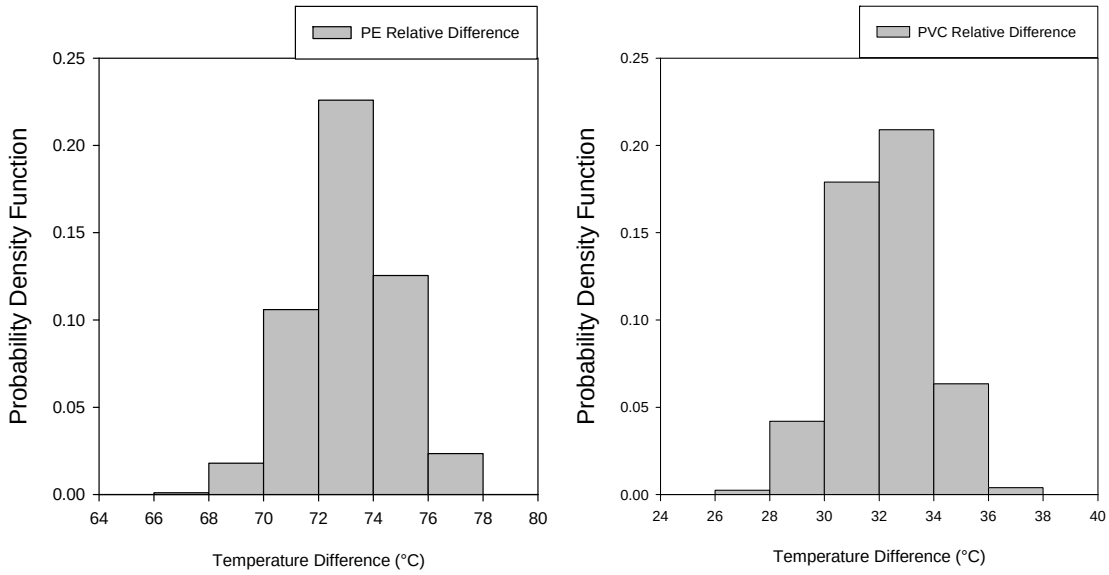

Figure 40. Histogram of relative difference simulation results for PE and PVC distributions

This relative difference evaluation indicated that the TS distributions differed by 145.5 °C, the PE distributions by 73.1 °C, and the PVC distributions by 32.2 °C. The smaller relative difference between the PVC distributions can be attributed to several of the PVC insulated cable test failures occurring prior to the generic 205 °C thermoplastic threshold. Therefore, this evaluation has identified that the current methods used to quantify the likelihood of cable damage to be larger than if thermal fragility distributions based on empirical data were used.

5.4 Evaluation of fire-induced cable failure circuit response characteristics

This section evaluates the NRC sponsored test data for characteristics that influence electrical cable failure modes (section 5.3.1) and evaluates the ungrounded dc test data for equipment spurious operation occurring as a result of multiple conductor shorts to ground (section 5.3.2).

5.4.1 Evaluation of cable and circuit configuration effect on failure mode likelihood estimates

The availability of the NRC test data allowed for an opportunity to compare these results with the previous EPRI/NEI results on the likelihood of a circuit experiencing fire-induced equipment spurious operation given cable damage. The database discussed in section 5 allowed for a systematic evaluation for the effects that circuit/cable configuration variables may have on influencing the likelihood of a circuit experiencing a spurious operation.

A graphical exploratory data analytical approach was taken to look at the effects various circuit configurations have on the likelihood of experiencing a fire-induced spurious operation. Circuit configurations such as fuse size, thermal exposure conditions, circuit type, cable insulation type, raceway type, conductor size, and circuit grounding were used as categories to evaluate their effect (if any) on the likelihood of a test experiencing at least one fire-induced spurious operation.

The evaluation looked at the test results in a binary fashion. If a circuit experienced one or more fire-induced spurious operations the likelihood for that circuit was set to "1." If a circuit did not experience any fire-induced spurious operations, the likelihood for that circuit was set to "0." The data was then sorted by various circuit configurations and the likelihood numbers (1 or 0) were summed for the specific configuration and divided by the total number of circuits in the specific configuration. Using insulation material type (TS, TP) as an example. There were 148 circuit tests using a thermoset insulated cable. Of these 148 circuits, 82 circuits experienced at least one fire-induced spurious operation. Therefore the likelihood would be 82/148 or 0.554 for a thermoset insulated cable to experience a spurious operation. The results from this

evaluation are shown in Figure 41, with the ac results shown in black and dc results in grey.

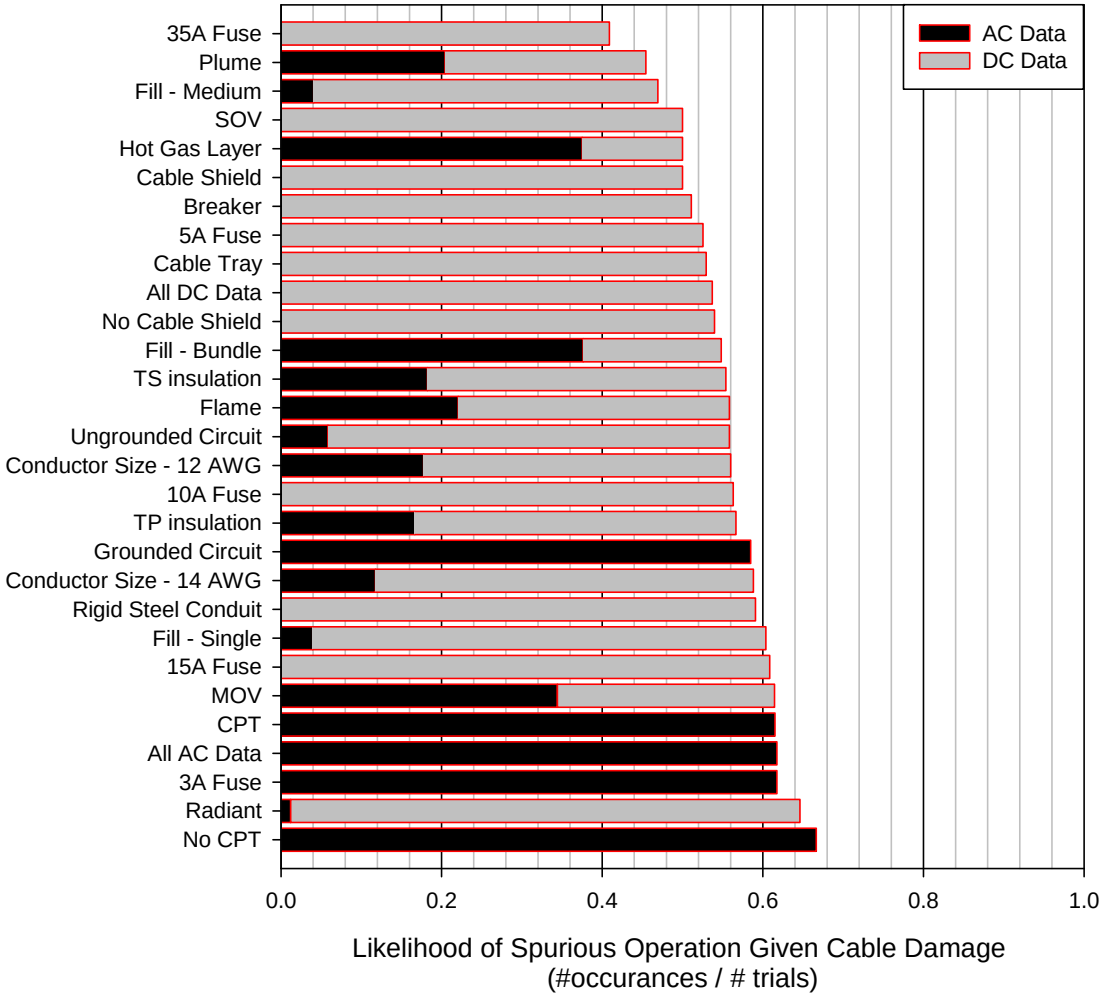

Figure 41. Fire-induced spurious operation likelihood bar chart by circuit configuration.

These results indicated that the probability of a circuit experiencing a hot short induced intra-cable spurious operation were between 0.41 and 0.67, given a cable damaged from fire. Comparing these results to the conditional probabilities found in the EPRI/NRC-RES fire PRA methodology shows similarities, with a few exceptions. First, the fire PRA methodology presents a best estimate probability of 0.30 when the circuit was powered from a CPT and 0.60 when no CPT was used. Figure 41 shows a probability of 0.62 when the CPT was used and 0.67 when no CPT was present.

Therefore, the new data indicated that the use of a CPT had little effect on reducing the probability of a circuit experiencing a spurious operation. A review of the EPRI/NEI testing showed that the basis for the CPT credit was based on only 5 of the 16 tests which used CPTs to power the circuit.

Secondly, the EPRI/NRC-RES method tables showed that the likelihood of an intra-cable spurious operation for a cable in a conduit to be ¼ of the likelihood for cables located in cable trays. The evaluation of the NRC sponsored test data showed that cables located in conduits have a 0.59 likelihood of experiencing a spurious operation when damaged by fire, which is slightly larger than that of the cable tray at 0.53. Therefore, the evaluation of the NRC sponsored test data showed that the probability credit for CPTs and cable trays in conduit does not appear to support the current methods identified the EPRI/NRC-RES fire PRA methodology.

5.5 Evaluation of ungrounded systems spurious operations caused by multiple shorts to ground.

The SNL test report did not identify any inter-cable spurious operation failures, nor was a review of the data conducted to specifically look for this failure mode [Nowlen, Brown, Olivier, Wyant 2012]. This section will evaluate the NRC sponsored DESIREE-Fire test data to show that a failure mode not before identified has occurred. This specific failure modes occurs when multiple conductors from different cables short to ground and cause spurious operations. For this to occur, both cables must be associated with the same ungrounded common power supply.

5.5.1 Description of the multiple short to ground failure mode

Inter-cable short circuit failures typically involve electrical conductors coming in physical contact with each other as a result of cable insulation degradation from fire damage. However, in their failure mode and likelihood analysis, LaChance-Nowlen-Wyant-Dandini identified the following,

> "Ungrounded circuits introduce a potential unique concern related to multiple shorts to ground. If, for example, one phase of the power supply circuit shorts to ground, this would 'float up' the ground potential to the voltage of the shorted conductor. A subsequent short to ground involving another conductor could then energize that second conductor. In effect, multiple shorts to ground can mimic a hot short [LaChance, Nowlen, Wyant, Dandini 2003]."

Therefore, when a common ungrounded power source, such as an ungrounded dc battery supply, is associated with cables that are degrading from severe thermal conditions any conductive electrical pathway can aid the inter-cable failure mode. A result of the lack of power supply isolation increases the number of potential cables, which if associated with the common power supply, could short to a common conductive plane and cause inter-cable hot shorts.

A very common and available electrical pathway in NPPs is electrical ground, which can include conductors intentionally grounded or electrical cable raceways, which are grounded per code requirements [NFPA 2007]. Fire experimentation shows that shorts to ground are a likely failure mode and most cables will eventually short to ground given time and sufficient thermal exposure [Wyant and Nowlen 2002]. Figure 42 provides one example of how the ground plane interactions can support inter-cable electrical shorting.

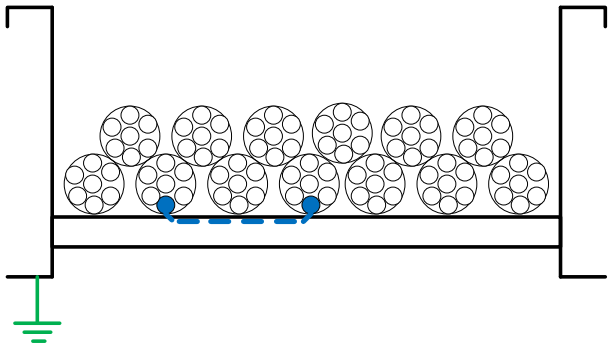

Figure 42. Illustration of fire-induced ground fault equivalent hot short between cables in same grounded cable tray

5.5.2 Approach used to identify Ground Fault Equivalent Spurious Operation

Each NRC sponsored DESIREE-Fire intermediate-scale test used seven circuits (eight energized cables) along with another energized circuit used to independently evaluate inter-cable testing configuration. This created 36 combinations of cable to cable interactions via the ground plane. This larger number of circuits complicated the evaluation of the inter-cable shorting events.

To identify inter-cable spurious operations, a simple yet beneficial approach was developed. For an individual circuit (MOV-1, SOV-2, large coil, etc.) the current within that circuit was summed such that currents supplied from the positive battery terminal were added and currents returning to the negative battery terminal were subtracted. Figure 43 and Equation 13 provide the graphical and mathematical representation of this approach.

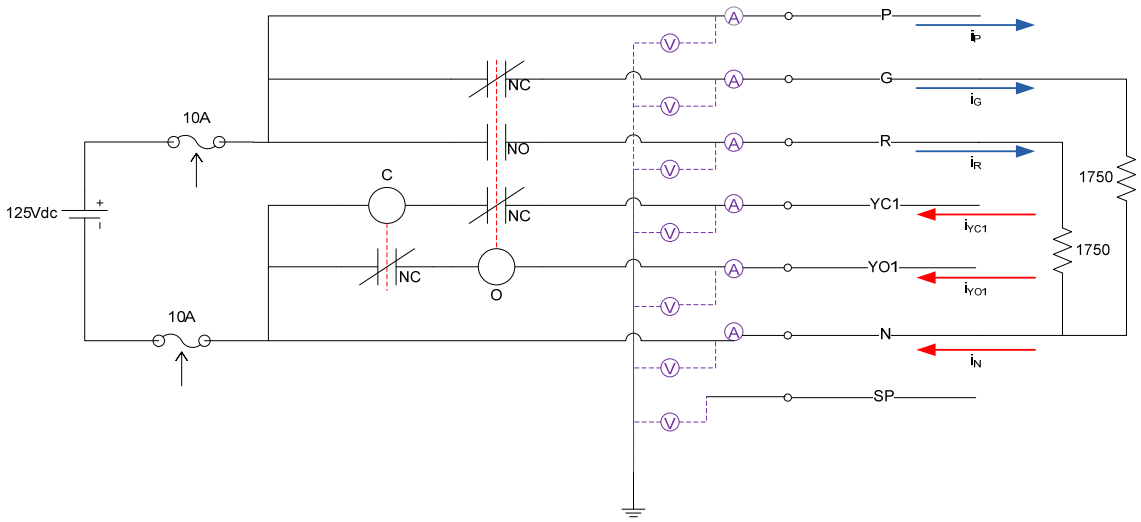

Figure 43. dc MOV schematic showing current summation used in identifying inter- cable shorting behavior

$$i_{sum\_dcMOV} = i_P + i_G + i_R - (i_{YC1} + i_{YO1} + i_N) \qquad \text{Equation 13}$$

Under normal conditions, the current within a circuit sums to zero (Kirchhoff's current law) [Del Toro 1972]. Under intra-cable only circuit failures, this law also holds such that the current within the circuit/cable remains in the cable and the sum is equal to zero. However, when inter-cable interactions occur, current from one circuit is leaving the electrical circuit and entering another; thus for the inter-cable case the individual circuit currents do not sum to zero and there is a net current. This net current is negative if the circuit if receiving current from some other circuit and positive if the circuit is supplying current to some other circuit.

This method provides an efficient tool to quickly identify circuits involved in inter-cable shorting. However there are a few drawbacks:

- First, this method only shows which circuits were involved and not what conductors. To determine the conductors involved in the short circuit, the data was reviewed for the perspective circuits and determine which conductors were involved.

- Next in the intermediate-scale testing, the inter-cable circuit configuration was included to attempt to observe proper polarity hot shorts, but this configuration was not instrumented for current measurement. Thus, in some cases the current source could not be identified. Therefore it can only be assumed that the source current was being supplied from the inter-cable circuit when no other source circuit was identified.
- Next, there were a few circuits (small SOV's in particular) which had a very low operating current (0.042 A). Although they were typically discernable in the evaluation, they were not as apparent as the other circuit inter-cable shorts.
- Next there may be cases where a circuit is losing and gaining current from other circuits simultaneously, these interactions could cancel one another and lead to difficulties in identifying the inter-cable short.
- Lastly, there were several cases where a single circuit shorted abruptly to the common ground plane and caused several circuit protective devices to clear simultaneously without direct indication of which circuit initiated the event. It is assumed that because of multiple fuse clears at the same time that there was a very abrupt current spike followed by fuse clear, which the data acquisition system (DAQ) was unable to capture.

Once the current summation was completed for each test, the summed current profiles were plotted to identify inter-cable shorting. Figure 44 shows a typical summation plot. This plot shows an instance during intermediate-scale test #3 where the 1-inch valve circuit operates spuriously via inter-cable short from the medium voltage switchgear control circuit through the ground plane.

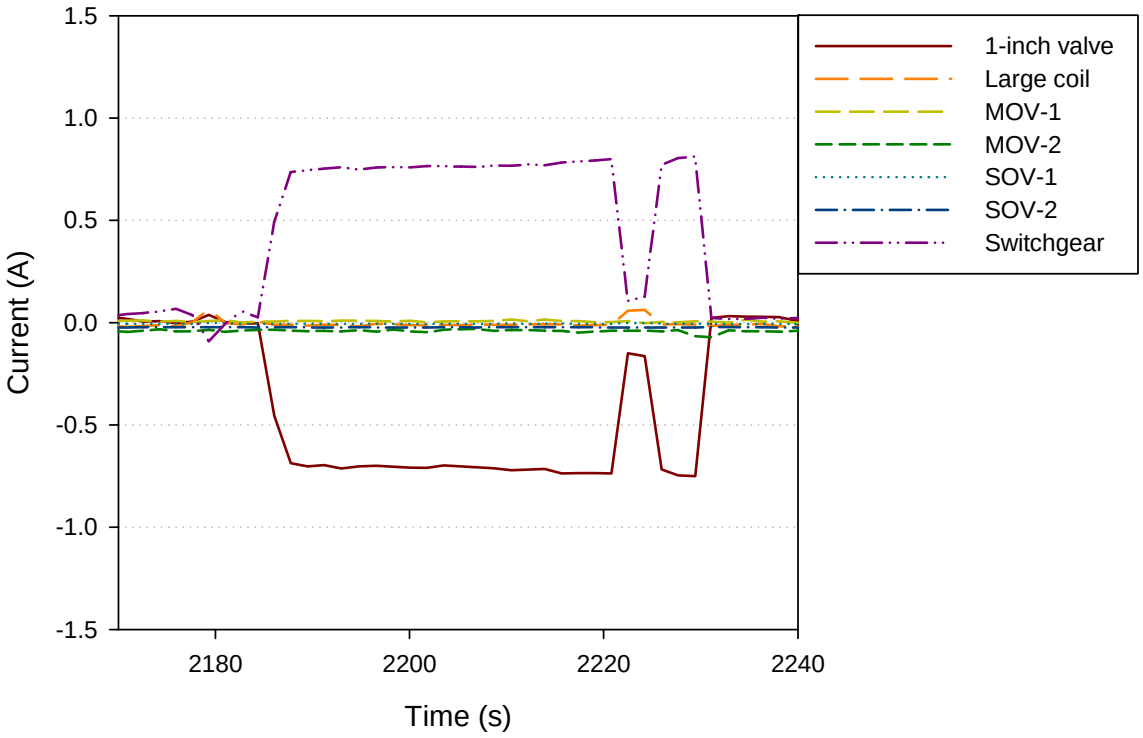

Figure 44. Current summation plot for Intermediate-Scale Test #3 showing spurious operation of 1-inch valve circuit being powered from switchgear circuit

Once the circuits involved were identified, the circuit conductor data was reviewed to identify the conductors within the circuits involved in the inter-cable short. This provides information on which conductor(s) acted as a source (provided the power) to energize the target conductors to cause spurious operation. The identification of the conductors involved in the spurious operation has proven that an inter-cable hot short occurred, but does not confirm that multiple shorts to ground were the failure mechanism that caused this short. To confirm this, one or two additional step(s) are required.

First, the physical location of the cable associated with the circuits involved was reviewed. If the target cable experiencing the spurious operation was located in a different cable raceway than the source cable supplying the power for the spurious operation, then it can be concluded that the only possibility for the inter-cable short was through the ground plane. An example of this is shown in Figure 45. In this figure, fire

damage has caused a conductor in a cable located in a cable tray to short to the cable tray rung, which is grounded per code requirements [NFPA 2007]. Another cable in a rigid steel conduit (different raceway) experiences a conductor short to the rigid steel conduit (also grounded). Assuming that the conductors which short to the raceways are associated with a common ungrounded power supply, the two conductors are now at the same electrical potential. A spurious operation would occur if one conductor were an energized source and the other was connected to a target to cause a spurious operation (motor starter contactor, solenoid operated valve, breaker trip coil, etc.). In this example, since the cables were located in different cable raceways, the only possibility of an inter-cable hot short is via ground plane interaction, indicating that this was an ground fault equivalent hot short.

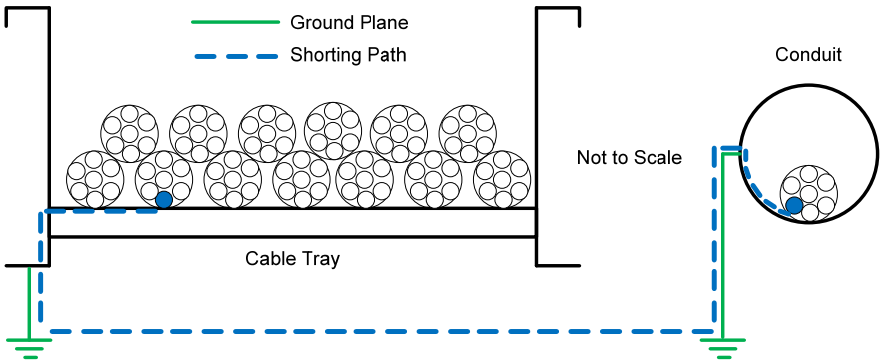

Figure 45. Illustration of ground fault equivalent hot short between different raceway. Cable tray and conduit do not necessarily have to be in the same location, but must be connected to the same ground potential and be damaged from the same fire.

If the source and target cables were located in the same cable raceway, the possibility exists for inter-cable spurious operation as a result of a cable-to-cable short that does not involve the ground plane (i.e., cable conductors of different cables physically touch due to fire damage). To identify if the ground plane was involved for these cases, the ground fault detection circuit voltage transducer signals were evaluated. A review of these

voltage profiles determined if the ground plane short to either battery potential occurred and aided in the ground fault equivalent spurious operation.

Figure 46 presents the ground fault detection circuit voltage signals for intermediate-scale test #3, along with the current summation profiles for the 1-inch valve and the large coil (as was shown in Figure 41). The voltage signals show the battery positive potential (shown as dashed black line "VTU_2") electrically floats to the ground potential during the spurious operation (shown as solid maroon line). The ground plane interaction with the battery voltage potential at the time of spurious operation, indicates that the ground plane was involved and the failure mode was not a cable-to-cable short independent of the ground plane.

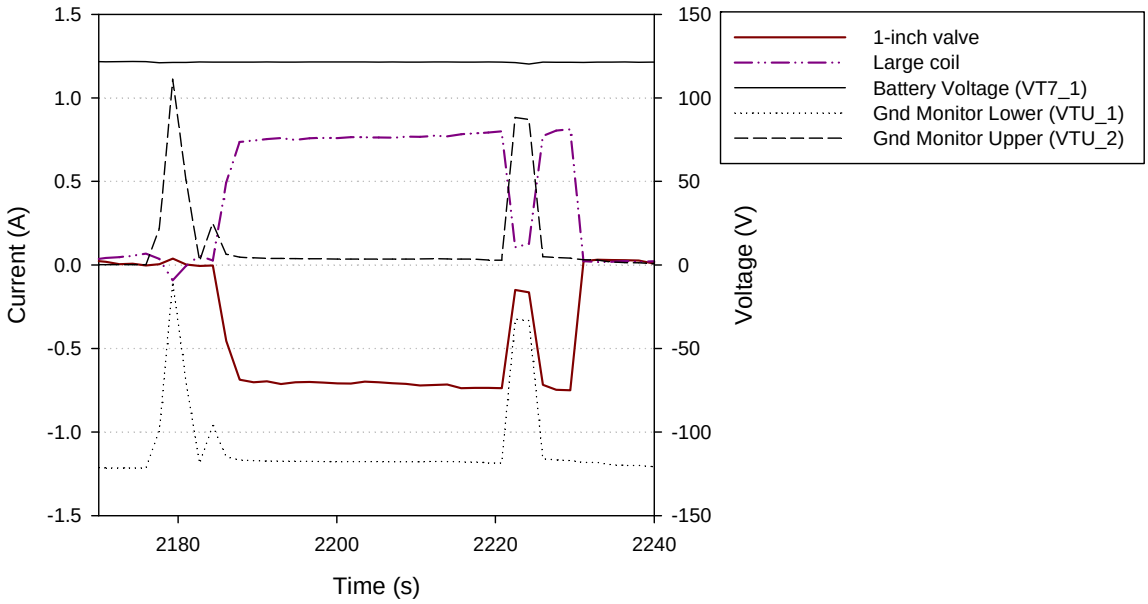

Figure 46. Ground fault detection circuit profile showing (battery positive/negative short to ground)

5.5.3 DESIREE-Fire Inter-cable Multiple Short to Ground Results

All of the intermediate-scale tests were evaluated using the procedure outlined previously to identify circuits involved in multiple short to ground spurious operations. The results of these evaluations are shown in Table 17, with the voltage and current plots

used to identify spurious operations that were a result of inter-cable (cable-to-cable) shorting through the ground plane presented in Appendix A.

Table 17. Intermediate-scale fire-induced common ground hot short results

Test #	Total # Circuits / Test	# Gnd equiv. SO	Duration (seconds)	Circuit Involved (Target/Source)	Cable Location(s)	Insulation Type
Prelim 1	6	0	-	-	-	-
Prelim 2	6	1	401	MOV-2 (T) SOV-2 (S)	E Cable Tray E Cable Tray	TP (PE) TP (PE)
IST-1	8	2	5	LgCoil (T) 1-inch (S)	B Cable Tray B Cable Tray	TS (XLPE) TS (XLPE)
			83	MOV-1 (T) 1-inch (S)	B Conduit B Cable Tray	TS (XLPE) TS (XLPE)
IST-2	6	0	-	-	-	
IST-3	8	2	33	SOV-2 (T) SwGr-t (S)	B Cable Tray B Conduit	TS (XLPE) TS (XLPE)
			36	1-inch (T) SwGr-t (S)	D Cable Tray B Conduit	TS (XLPE) TS (XLPE)
IST-4	8	0	-	-	-	
IST-5	8	1	12	SOV-1 (T) SwGr-t (S)	B Conduit D Cable Tray	TP (PE) TP (PE)
IST-6	8	0	-	-	-	
IST-7	8	0	-	-	-	
IST-8	8	1	97	MOV-1 (T) LgCoil (S)	A Cable Tray A Cable Tray	TP (PE) TP (PE)
IST-9	8	3	24	MOV-2 (T) LgCoil (S)	D Cable Tray B Cable Tray	TP (PE) TS (XLPE)
			28	SOV-2 (T) LgCoil (S)	D Cable Tray B Cable Tray	TS (XLPE) TS (XLPE)
			16	MOV-1 (T) SwGr-t (S)	B Cable Tray D Cable Tray	TP (PE) TS (XLPE)
IST-10	8	3	37	MOV-2 (T) Unknown (S)	B Cable Tray -	TS (K-FR) -
			15	MOV-1 (T) Unknown (S)	C Cable Tray -	TS (K-FR) -
			52	MOV-1 (T) Unknown (S)	C Cable Tray -	TS (K-FR) -
IST-11	6	1	59	SOV-2 (T) LgCoil (S)	D Cable Tray B Cable Tray	TS (EPR) TS (EPR)
IST-12	6	3	107	MOV-2 (T) Unknown (S)	B Cable Tray -	TS (EPR) -
			51	LgCoil (T) Unknown (S)	D Cable Tray -	TS (EPR) -
			5	SOV-1 (T) LgCoil (S)	D Cable Tray D Cable Tray	TS (EPR) TS (EPR)
Cont. A	2	0	-	-	-	
Cont. B	2	0	-	-	-	

A review of the DESIREE-Fire testing results specifically evaluating spurious operations caused by more than one cable shorting to ground has been shown to occur. The information in Table 17 indicates several parameters that influence the likelihood of experiencing these faults. First is the timing issue. The cables involved need to be damaged within the same time frame and have at least one fuse operable to participate in this type of short. This timing issue results in the likelihood of cables of the same design (number of conductors, insulation materials, etc.) and located in the same raceway to be more likely to experience these types of failure. In all but two cases, the same insulation materials were involved in the multiple shorts to ground. The two cases where a thermoset and thermoplastic experienced multiple shorts to ground occurred due to the thermal exposure differences caused by the experimental setup. This shows the importance fire exposure and raceway loading has in determining concurrent shorts to ground. The duration of these multiple short to ground spurious operations in the test program ranged from 5 to 401 seconds, with a mean duration of 62 seconds.

6 Conclusion

This thesis has presented a thorough review of the most recent cable functionality testing under severe fire conditions. The following conclusions can be made based on this review.

1. The thermal failure temperature data sets for the ac CAROLFIRE and dc DESIREE-Fire tests can be merged by insulation material. Based on evaluation of data points where electrical failure occurred prior to cable ignition, statistical evaluation has shown that the thermal failure temperatures were not influenced by circuit power source (ac or dc).
2. Thermoset insulated cables that were tested (with the exception of Kerite-FR) performed at or above the generic failure threshold (330 °C). The performance of thermoplastic insulated cables varied. PVC was the worst performer with a minimum failure temperature of 163.8 °C or approximately 41.2 °C below the generic threshold (205 °C). One of 48 PE insulated cable samples failed at 202 °C, just below the generic 205 °C thermoplastic generic threshold. All of the Tefzel insulated conductors failed above the generic threshold, with the lowest failure point occurring at 289 °C.
3. Development of insulation material specific cable fragility distributions could aid in adding realism to the fire PRA. However, the massive variety and proprietary formulations of electrical cable insulation results in the applicability of generic distributions being questionable with respect to the uncertainty that should be assigned. Use of the fragility distributions developed here should be used with caution.

4. The FDT^s THIEF model prediction capabilities have been shown to be a valuable tool for evaluating cable damage, provided that cable ignition does not occur. Cable ignition will cause the cable to fail sooner than that predicted by FDT^s THIEF model. Therefore actual fire conditions may cuase a cable to fail prior to the model prediction, resulting in a non-conservative fire PRA estimate.
5. The likelihood of a fire-induced damaged cable experiencing a spurious operation was evaluated. The evaluation did not support the current likelihood prediction tables presented in the EPRI/NRC-RES fire PRA methodology for the use of control power transformers nor did it support the reduction in likelihood for cables located in rigid steel conduit raceway. The evaluation conducted here suggests that the conditional probability of a circuit experiencing a spurious operation given cable damage is 0.60 when control power transformers are used and 0.67 with no control power transformer. Likewise, the NRC sponsored test data has shown that the cables in rigid steel conduit have a higher likelihood of experiencing a spurious operation at 0.59 versus current guidance of 0.15 for thermoplastic and 0.075 for thermoset insulated cables.
6. The DESIREE-FIRE data has provided the first source of data that has been used in this thesis to show that fire-induced cable damage can result in multiple cables shorting to ground in a configuration that will support short circuits through the cable raceway to cause equipment to spuriously operate.

For this to occur, the affected cables must be powered from a common power supply and be ungrounded.

As a final note, one limitation to the conclusions presented here were based on severe fire conditions damaging the electrical cables. The applicability of the result to other cable failure mechanisms (water intrusion, aging, etc.) was not warranted.

7 Future Research

This thesis has identified several areas where additional research will help to advance the current state-of-the-art methods, they are;

1. A performance based standard should be developed which exposes electrical cables to severe thermal exposures and identifies the sub-jacket temperature and time of failure using electrical failure criteria representative of functional failure for equipment found in a typical NPP. This would allow for a consistent method to evaluate cable damage and possibly the development of a data base which could be used to further advance the fire PRA methods by understanding the variability of cable insulation materials to thermal damage.
2. The THIEF model should be complemented with a cable ignition submodel. A submodel should take into consideration the various geometric cable configurations found in NPPs. This submodel should allow for identification of cable ignition and fire growth, which would allow for a more realistic gas temperature profile for the model to predict cable damage. Alternatively, a independent model could be developed to complement the THIEF model. This model could estimate when cable ignition occurs and assume cable damage at the time of ignition. This approach is considered appropriate given that the data suggests cable failure will occur shortly after cable ignition.
3. Future testing should increase the variability of the cable configurations. Most of the testing to date has made only small variations from the base case. The use of tray bends and vertical orientations are areas where limited data exists. Also

variations in the thermal exposure (especially heat flux) would allow for verification of some of the results presented in this thesis.

4. The fire-induced electrical cable damage data evaluated in this thesis were new, unused electrical cables. Electrical cables used in NPPs age from natural conditions and from harsh or elevated thermal conditions and these aging mechanisms may cause electrical cables to fail at temperatures different than those temperature presented in this thesis. Thus, to understand the effects aging has of fire-induced electrical cable failure characteristics, research should be completed to understand the aging effects to adequately quantify the fire risks associated with aged cable conditions representative of what is found in NPPs. In addition, NPP conditions may occur where electrical cables are repeatedly exposed to elevated thermal conditions for long durations. No research has been conducted to evaluate the mechanical failure mechanisms that these exposure conditions may induce.
5. A model to correlate constant heat flux experimental exposures to actual fire scenario conditions (growth, steady state, decay) would allow for refinements in the overall NPP fire risk assessment.

APPENDIX A : SUPPORTING INFORMATION

A.1 SCHEMATICS OF DC CIRCUITS AND CURRENT SUMMATION EQUATIONS

Motor Operated Valve Circuit

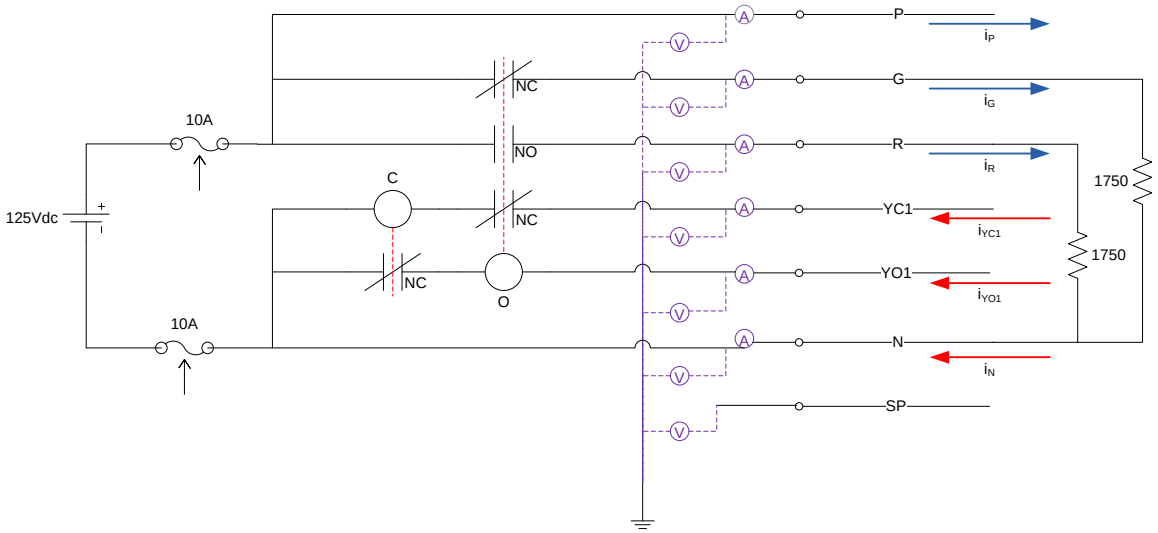

Figure A-1. Illustration of dc motor operated valve circuit showing current convention for current summation

$$i_{sum\_dcMOV} = i_P + i_G + i_R - (i_{YC1} + i_{YO1} + i_N) \qquad \text{Equation A-1}$$

Small Solenoid Operated Valve Circuit

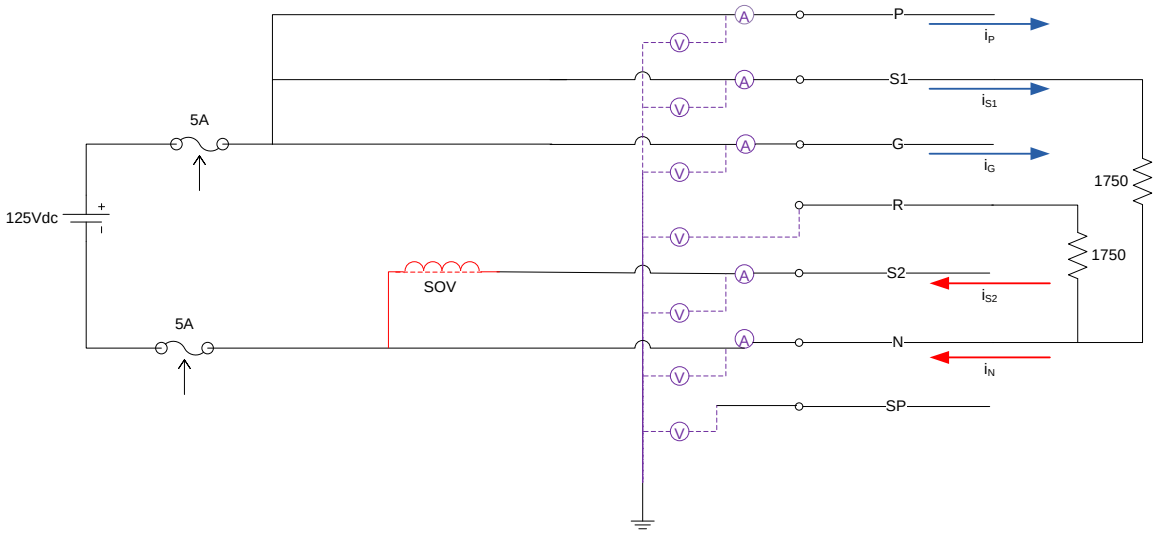

Figure A-2. Illustration of small dc solenoid operated valve circuit showing current convention for current summation

$$i_{sum\_dcSOV} = i_P + i_{S1} + i_G - (i_{S2} + i_N) \qquad \text{Equation A-2}$$

1-Inch Valve Solenoid Operated Valve Circuit

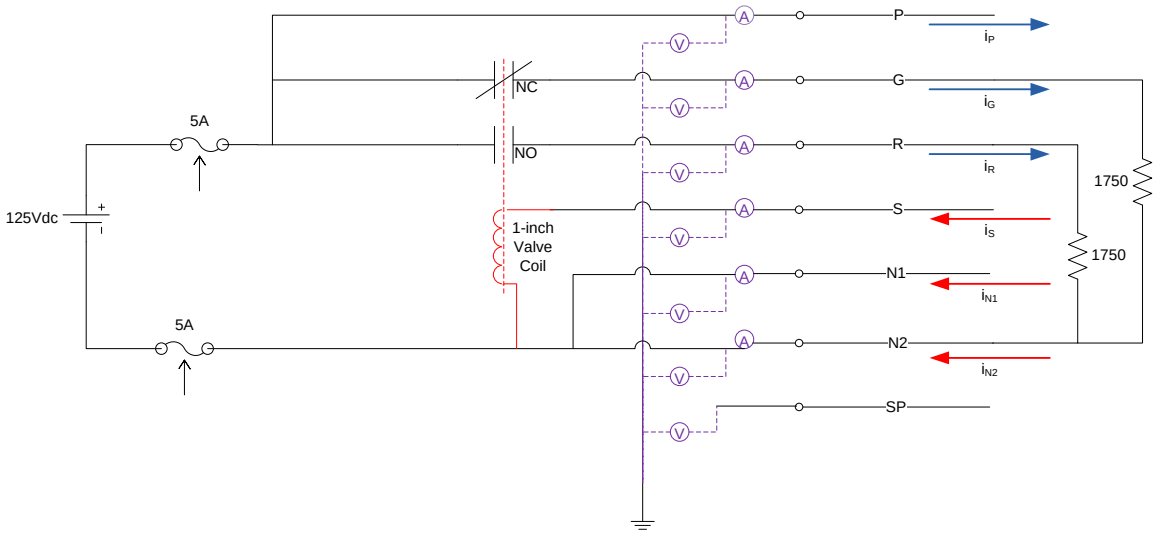

Figure A-3. Illustration of dc 1-inch valve solenoid operated valve circuit showing current convention for current summation

$$i_{sum\_dc1\text{-}INCH} = i_P + i_G + i_R - (i_S + i_{N1} + i_{N2}) \qquad \text{Equation A-3}$$

Large Coil Circuit

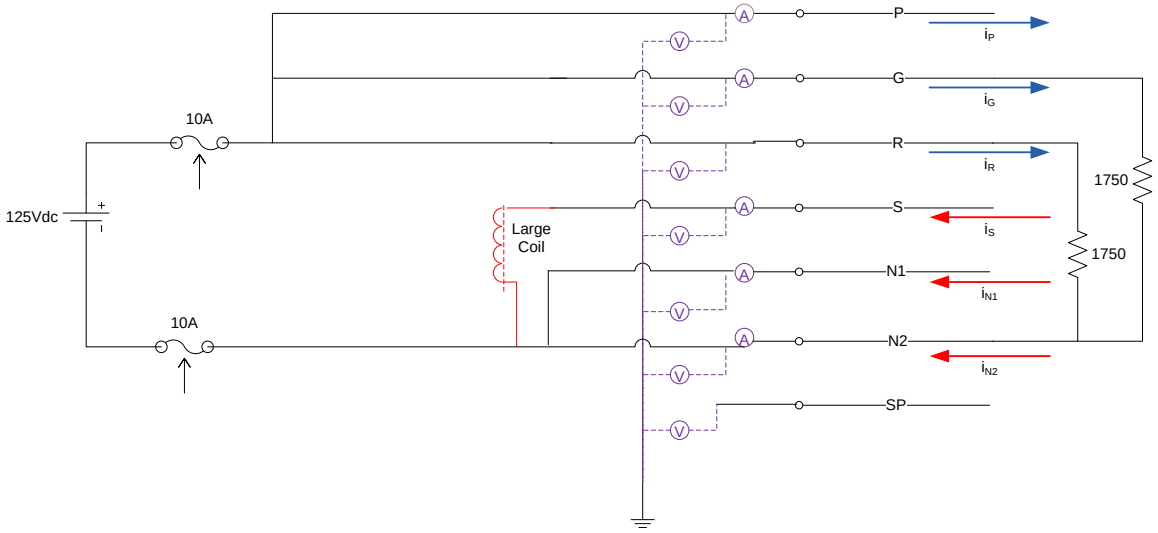

Figure A-4. Illustration of dc large coil circuit showing current convention for current summation

$$i_{sum\_dcLGCOIL} = i_P + i_G + i_R - (i_S + i_{N1} + i_{N2}) \qquad \text{Equation A-4}$$

Medium Voltage Switchgear Circuit

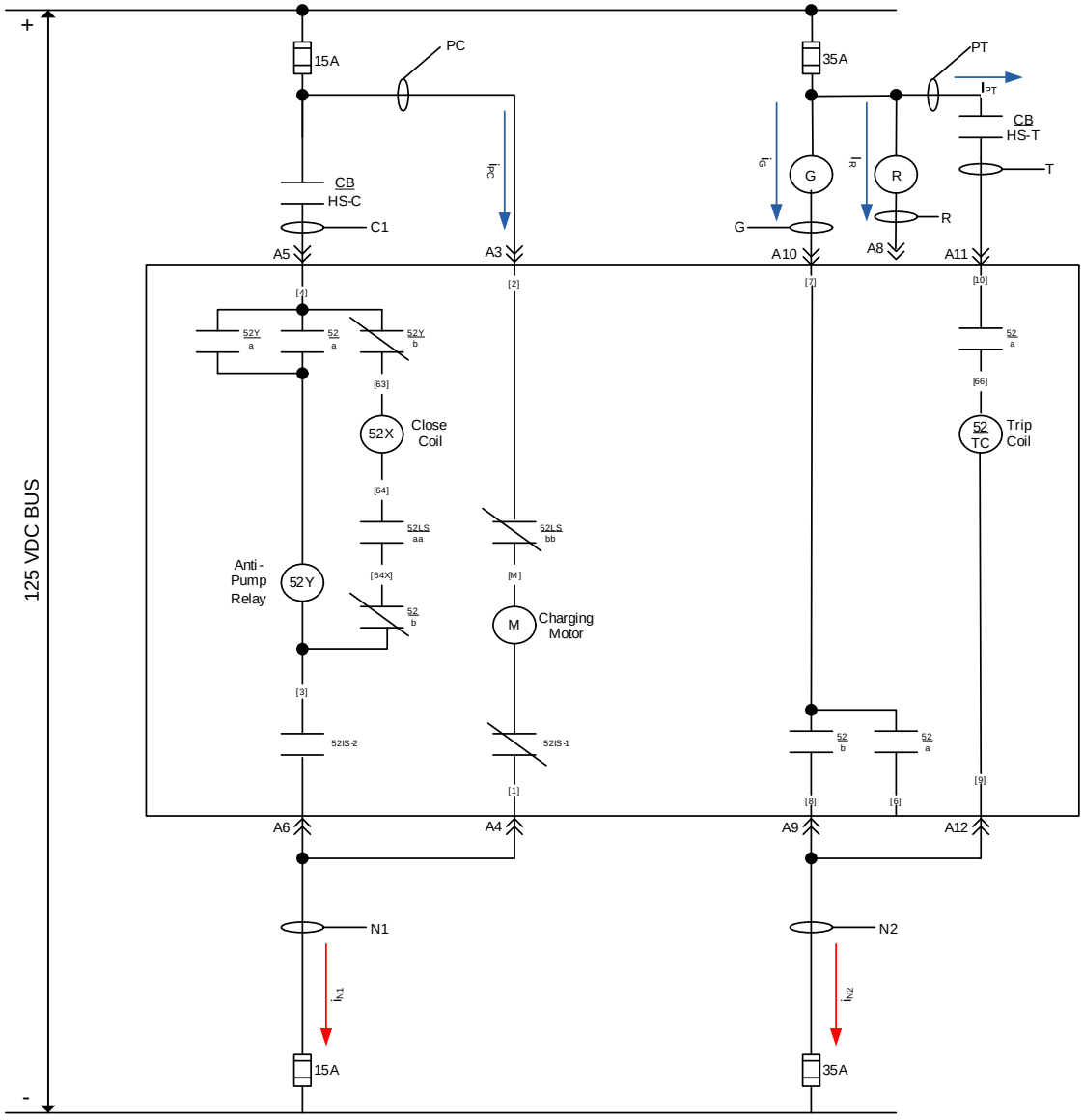

Figure A-5. Illustration of medium voltage switchgear dc control circuit showing current convention for current summation

$$i_{sum\_dcMOV} = i_{PC} + i_{PT} + i_G + i_R - (i_{N1} + i_{N2}) \qquad \text{Equation A-5}$$

A.2 DESIREE-FFIRE Intermediate-Scale Multiple Short to Ground Circuit Failure – Detailed Test Information

Preliminary Test #2

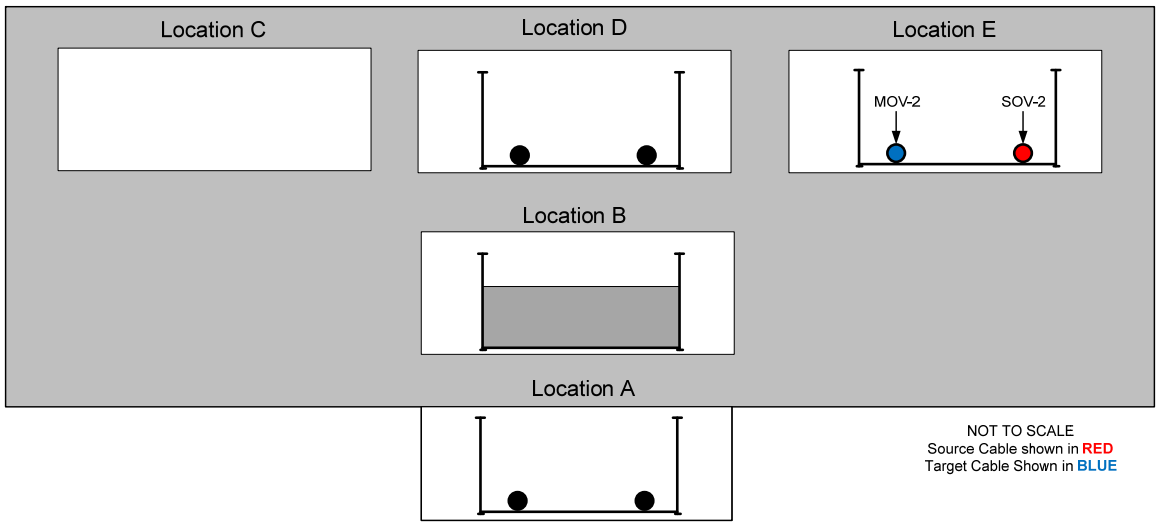

Figure A-6. Cable – circuit location in hood of intermediate-scale preliminary test #2

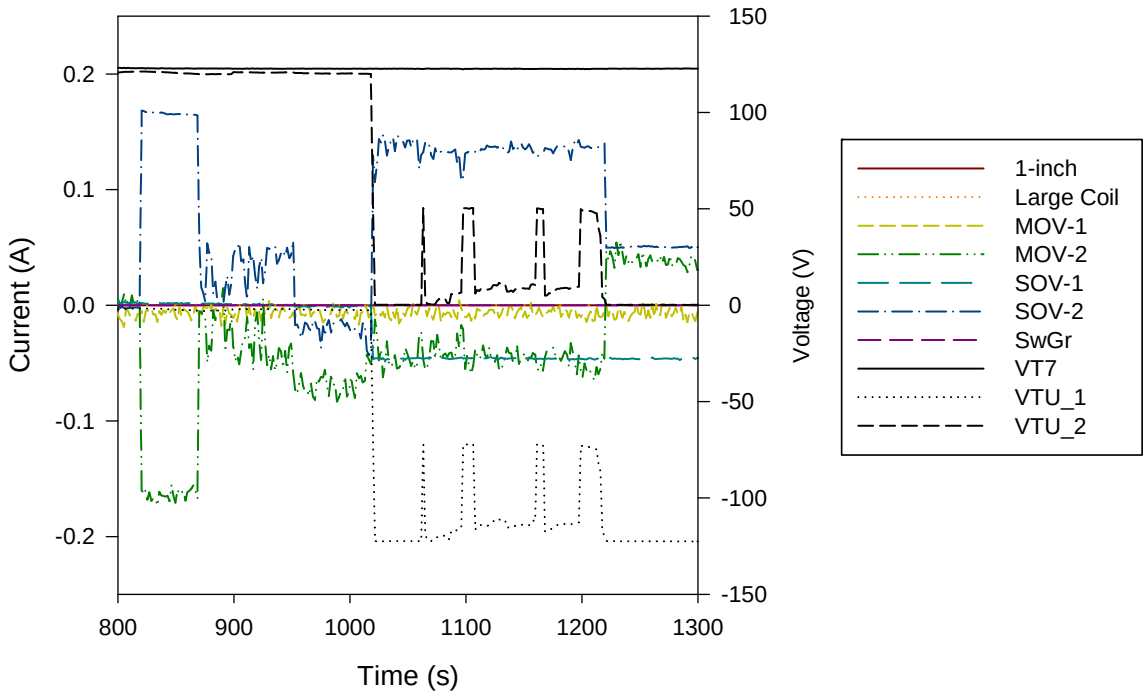

Figure A-7. Current summation plot for intermediate-scale preliminary test #2 with ground monitoring circuit voltage signals.

Test #1

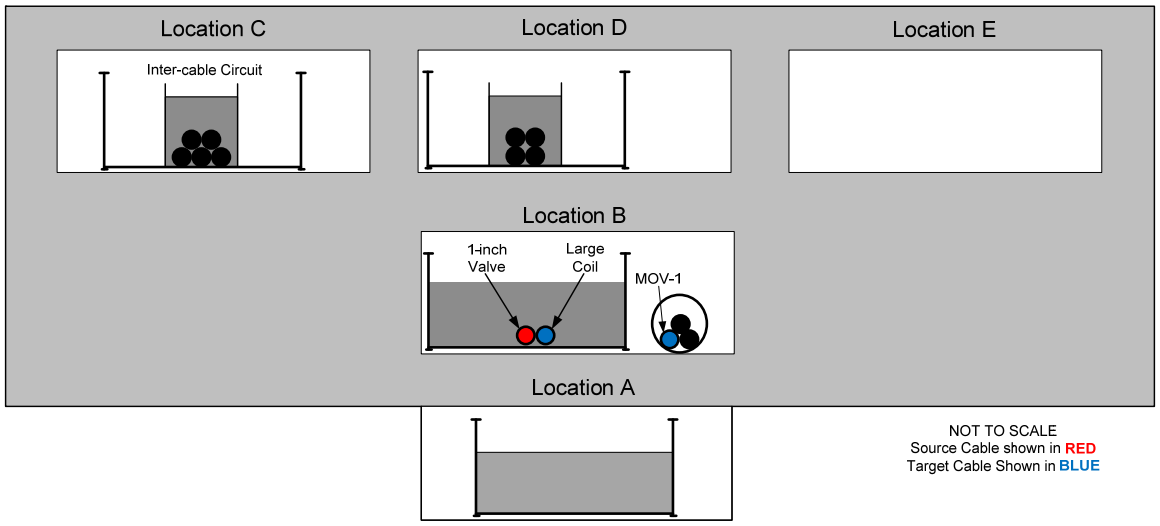

Figure A-8. Cable – circuit location in hood of intermediate-scale test #1

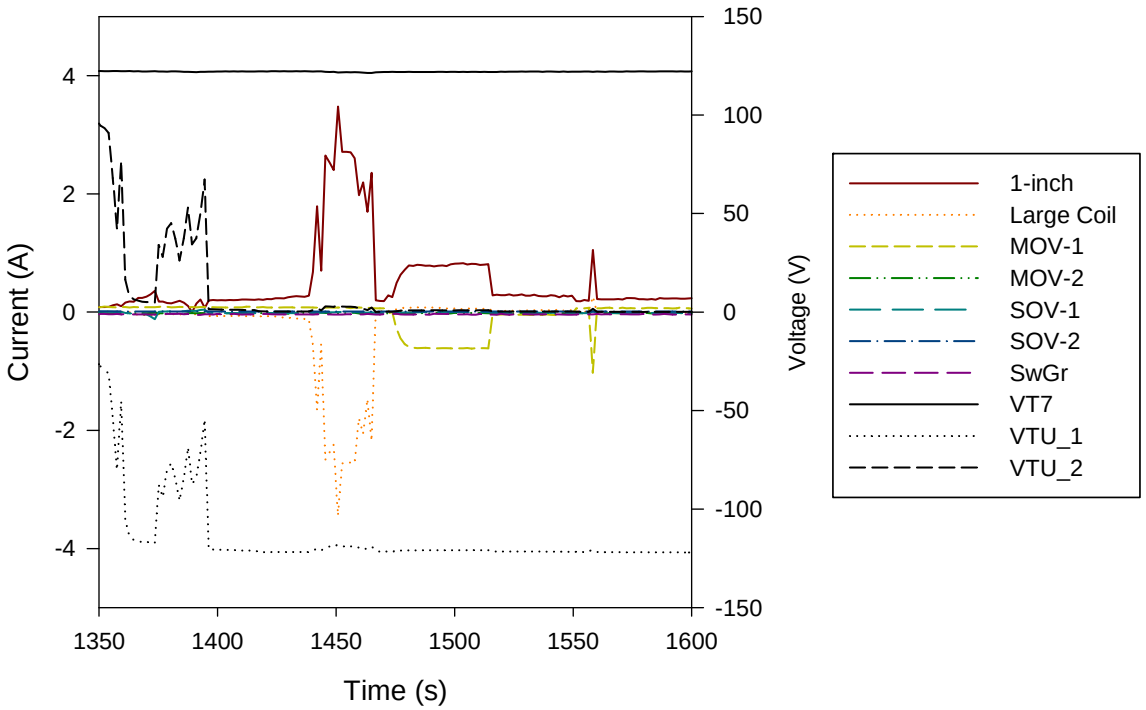

Figure A-9. Current summation plot for intermediate-scale test #1 with ground monitoring circuit voltage signals.

Test #3

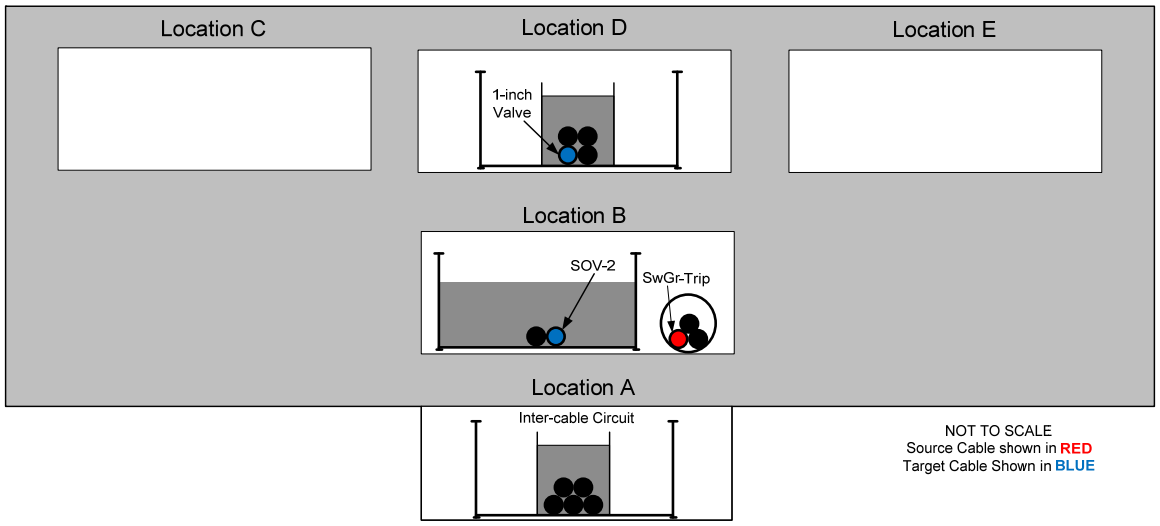

Figure A-10. Cable – circuit location in hood of intermediate-scale test #3

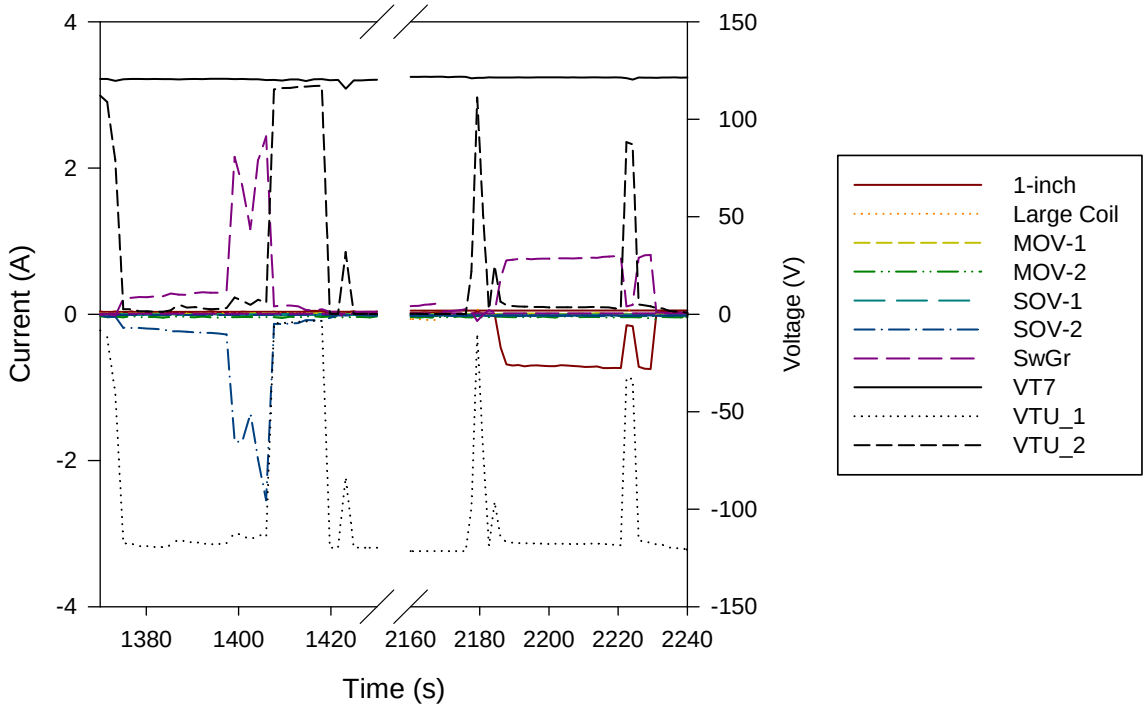

Figure A-11. Current summation plot for intermediate-scale test #3 with ground monitoring circuit voltage signals.

Test #5

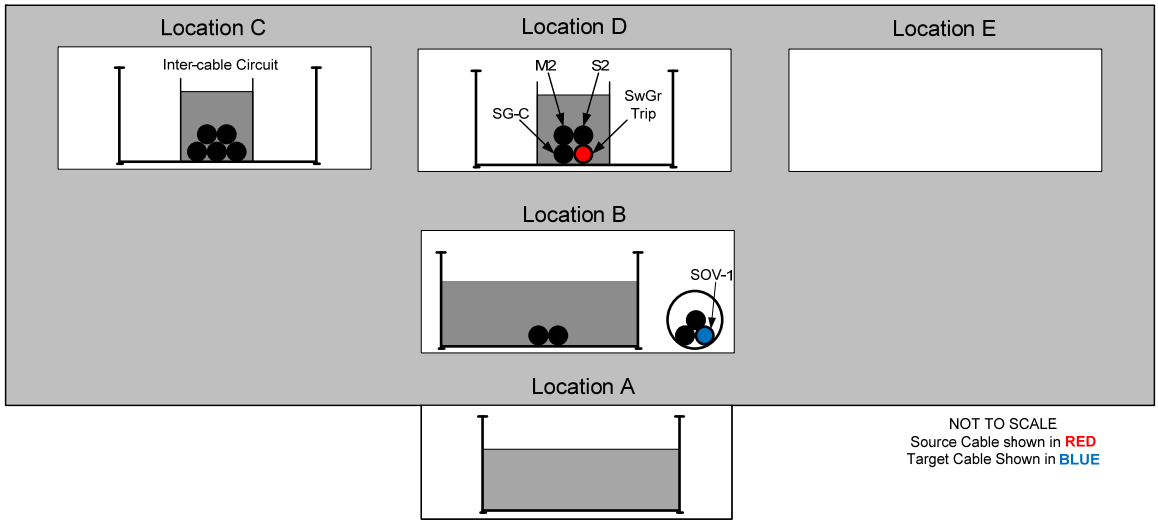

Figure A-12. Cable – circuit location in hood of intermediate-scale test #5

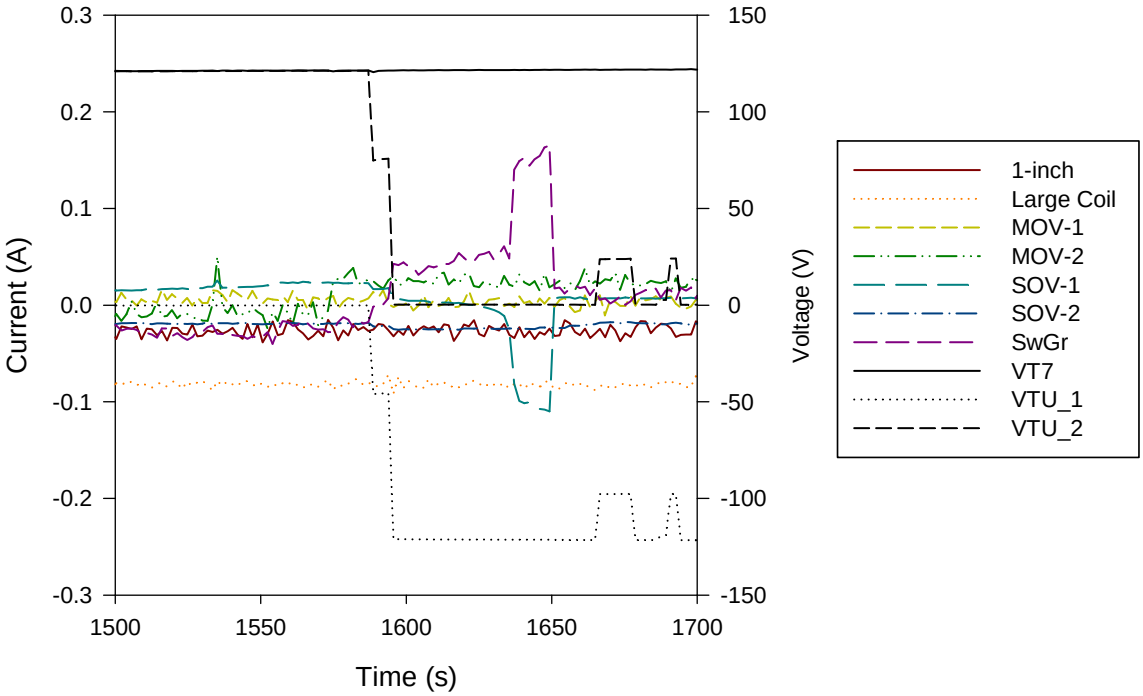

Figure A-13. Current summation plot for intermediate-scale test #5 with ground monitoring circuit voltage signals.

Test #8

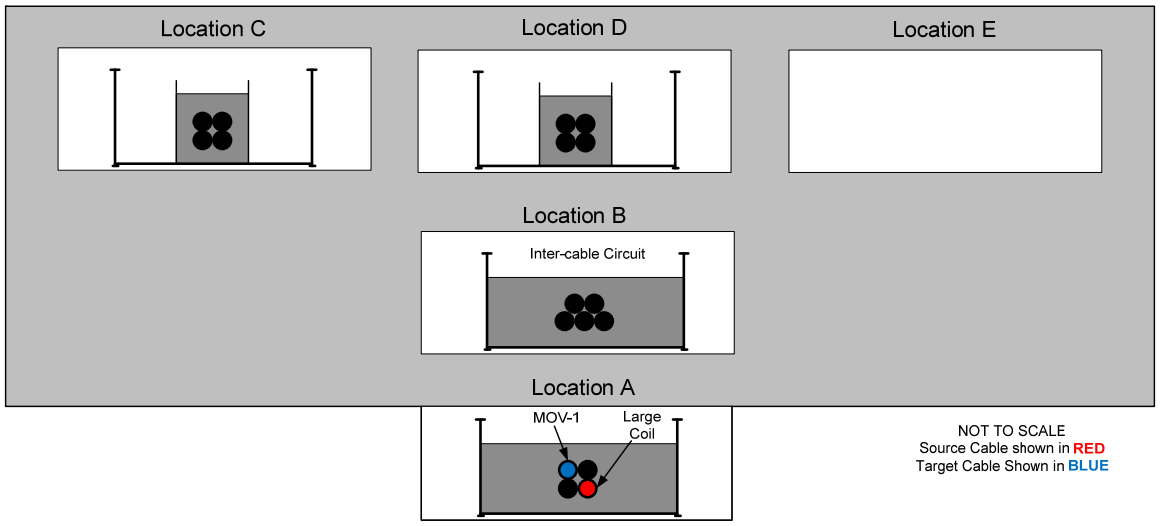

Figure A-14. Cable – circuit location in hood of intermediate-scale test #8

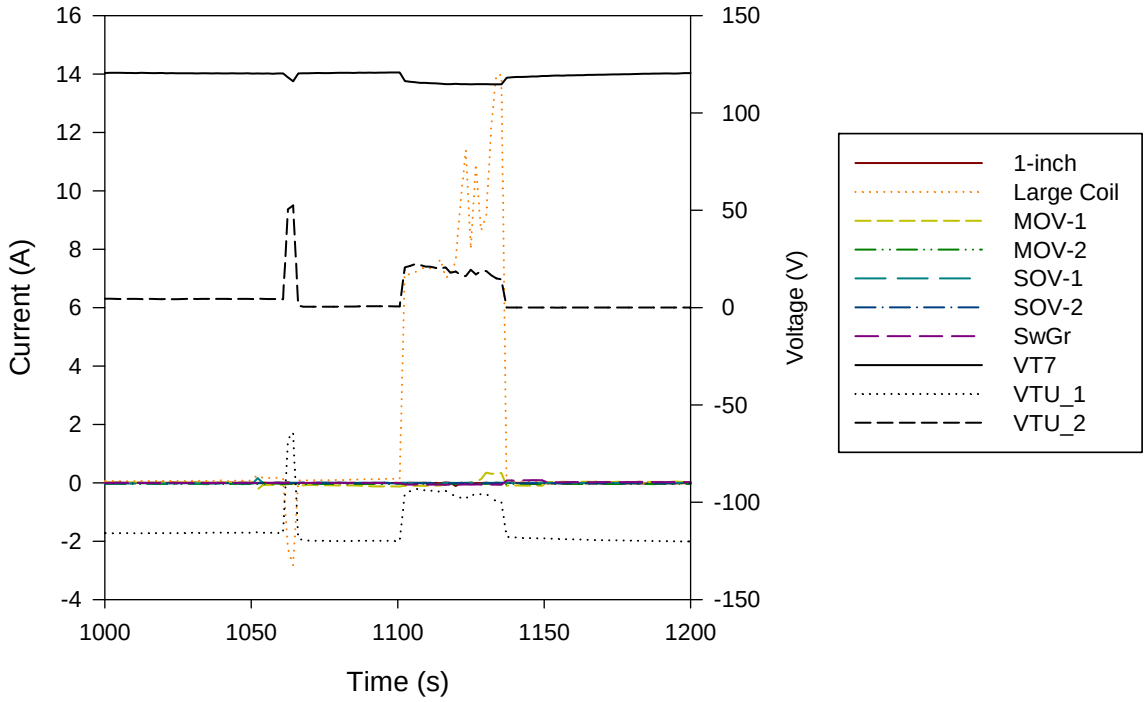

Figure A-15. Current summation plot for intermediate-scale test #8 with ground monitoring circuit voltage signals.

Test #9

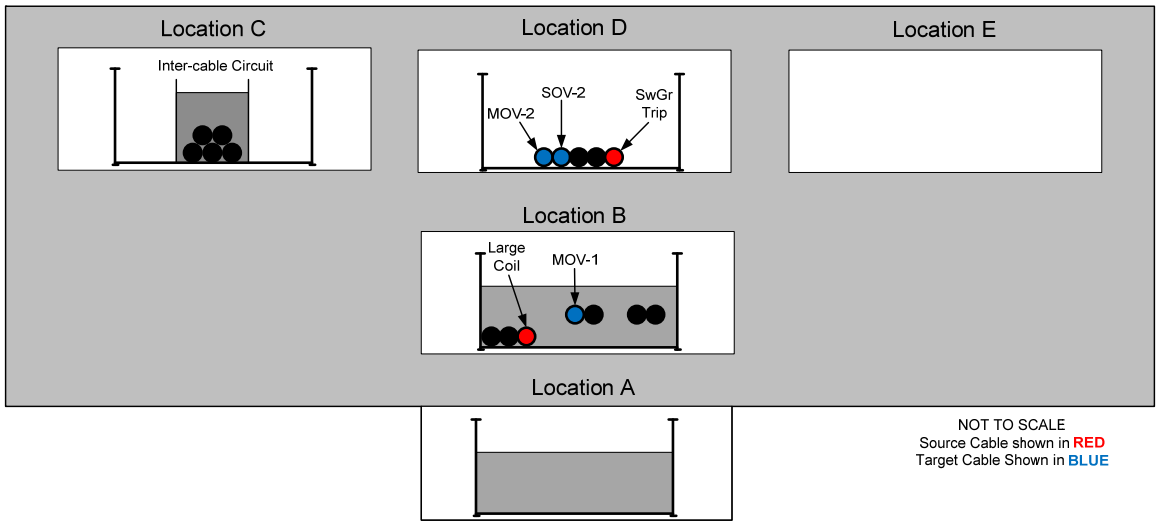

Figure A-16. Cable – circuit location in hood of intermediate-scale test #9

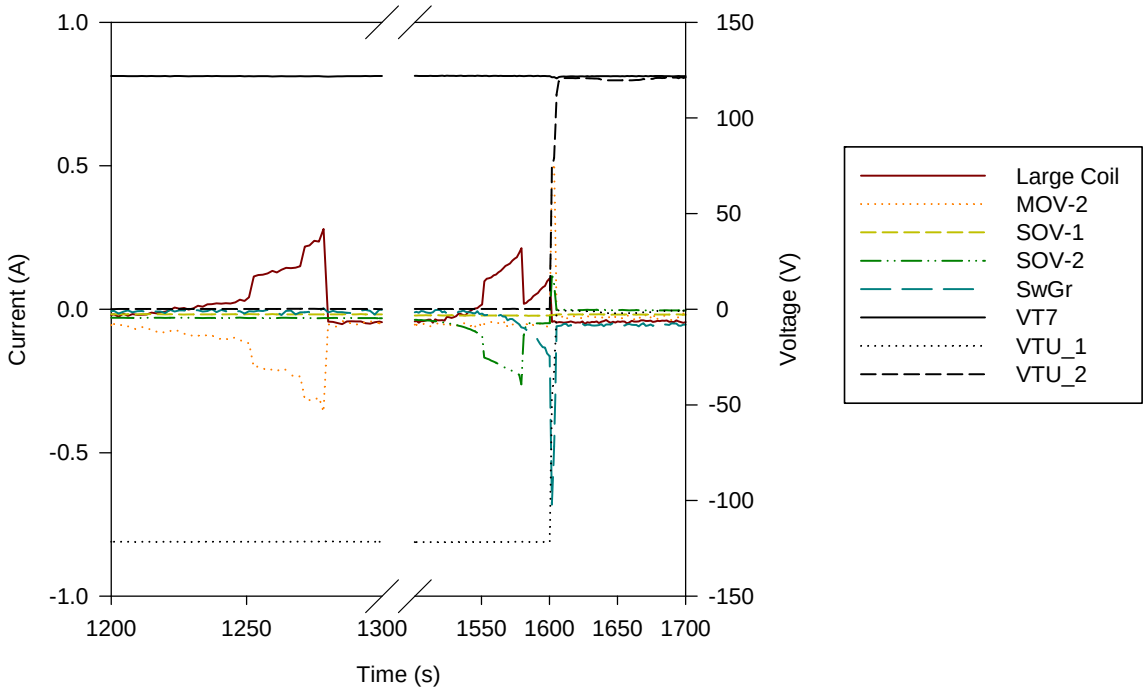

Figure A-17. Current summation plot for intermediate-scale test #9 with ground monitoring circuit voltage signals.

Test #10

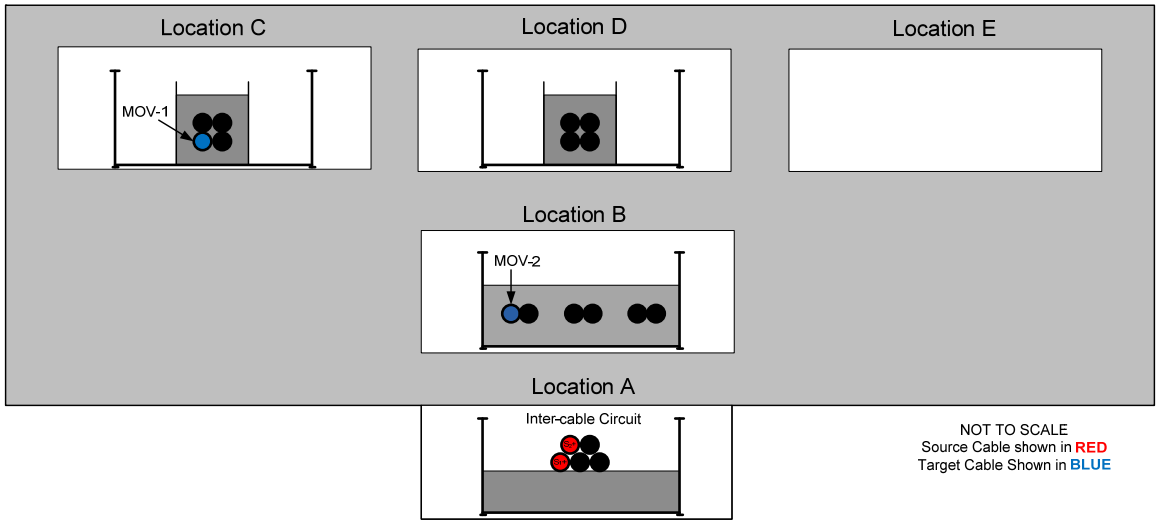

Figure A-18. Cable – circuit location in hood of intermediate-scale test #10

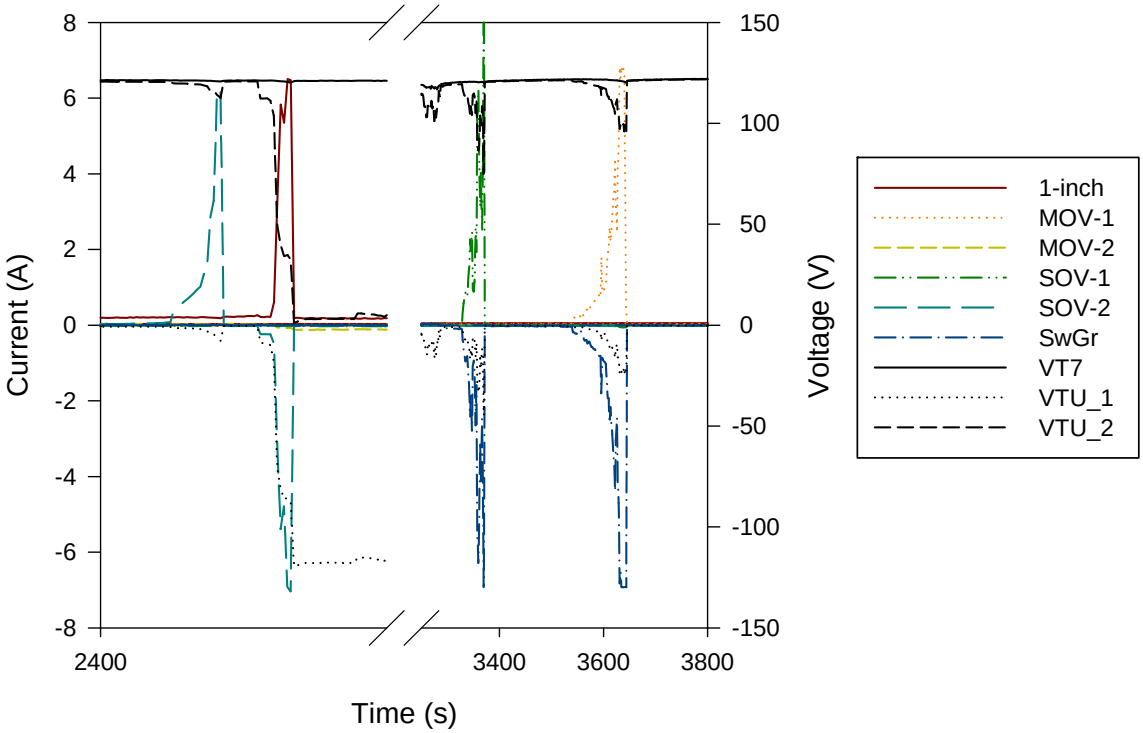

Figure A-19. Current summation plot for intermediate-scale test #10 with ground monitoring circuit voltage signals.

Test #11

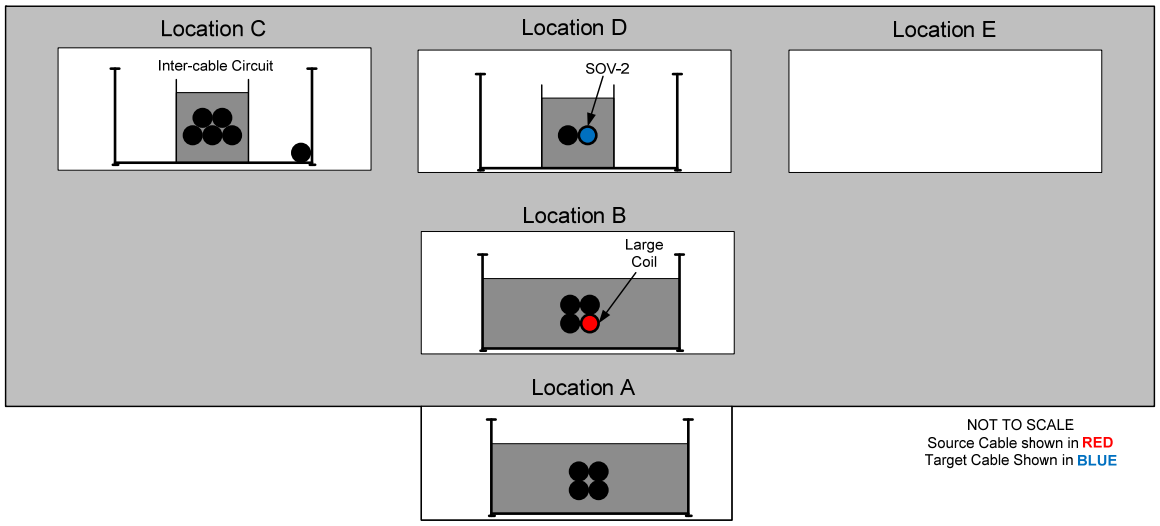

Figure A-20. Cable – circuit location in hood of intermediate-scale test #11

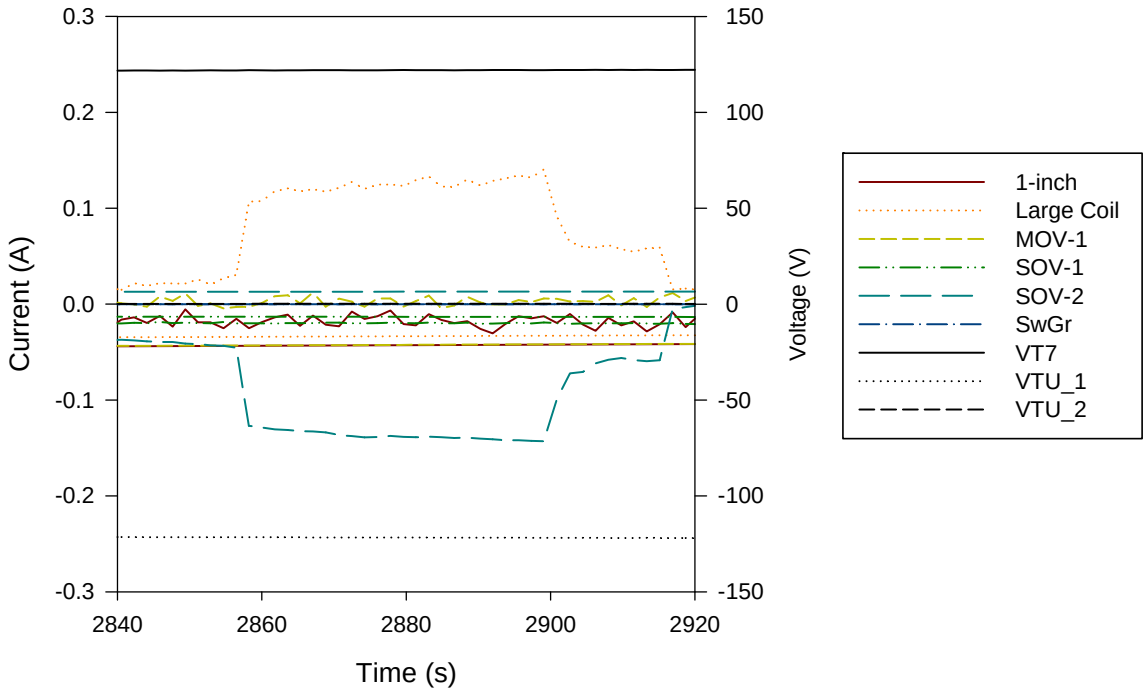

Figure A-21. Current summation plot for intermediate-scale test #11 with ground monitoring circuit voltage signals.

Test #12

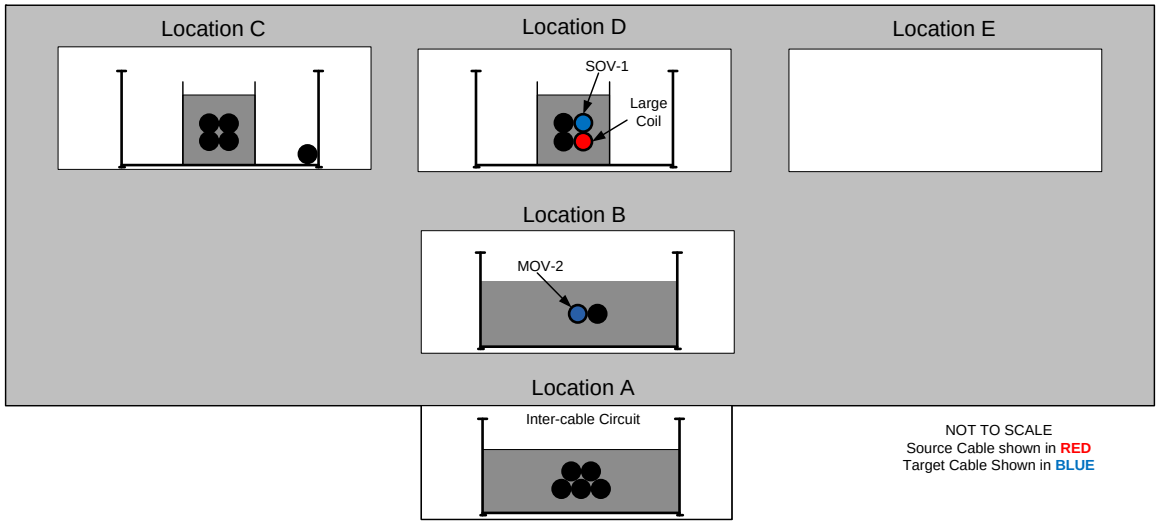

Figure A-22. Cable – circuit location in hood of intermediate-scale test #12

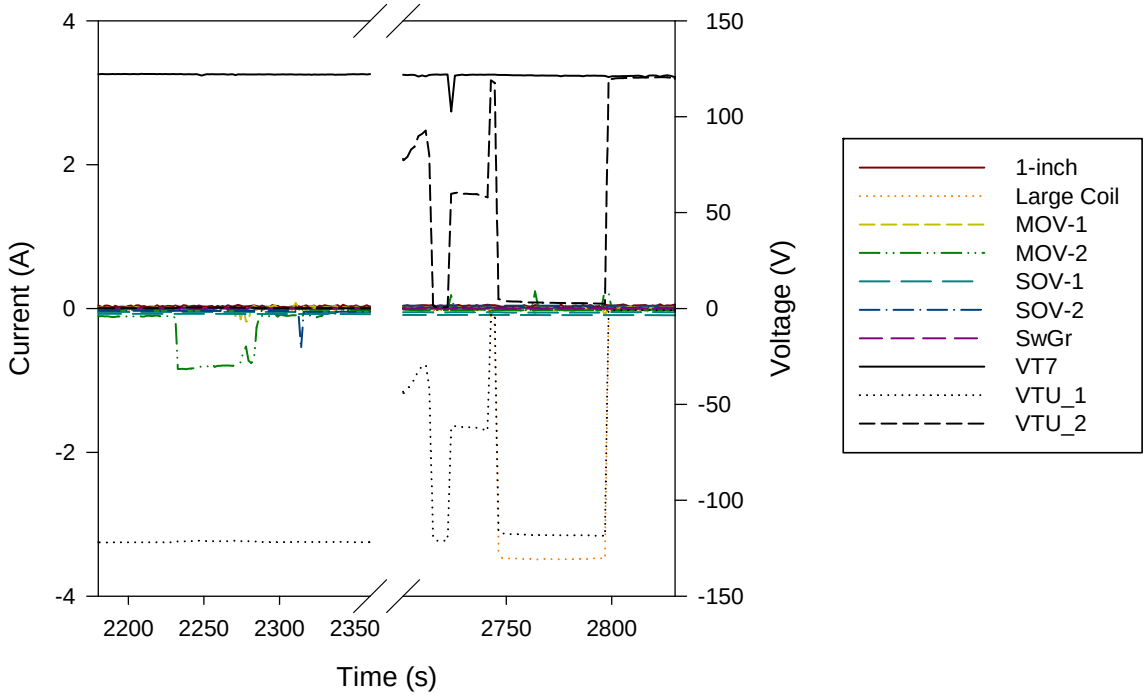

Figure A-23. Current summation plot 1 of 2 for intermediate-scale test #12 with ground monitoring circuit voltage signals.

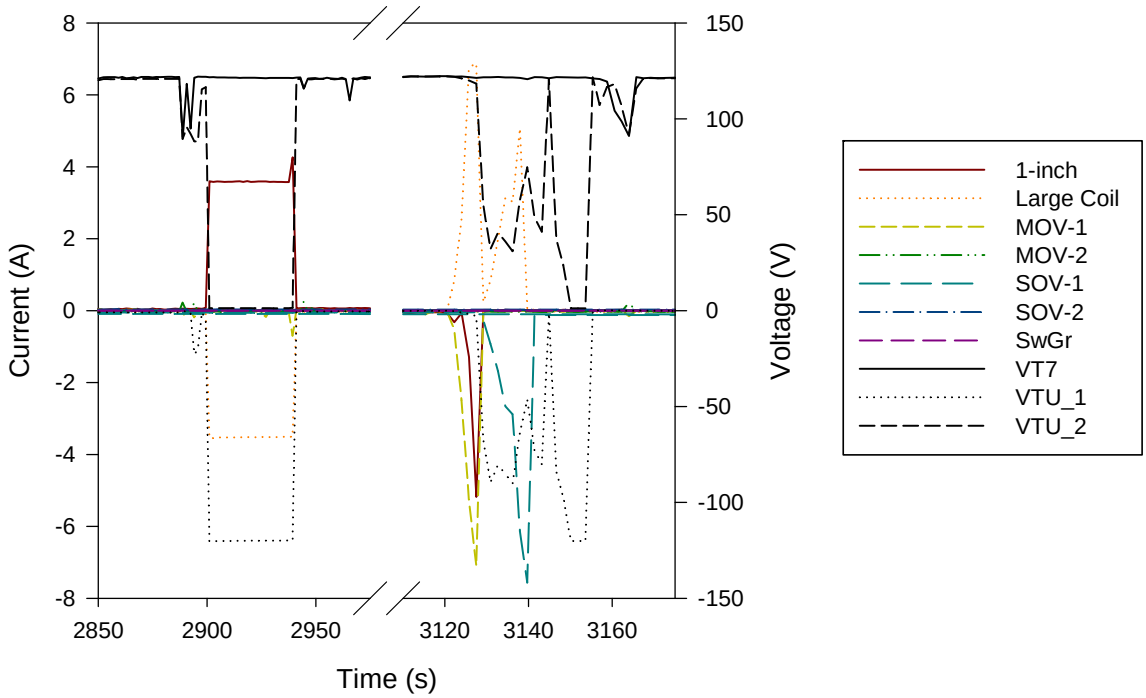

Figure A-24. Current summation plot 2 of 2 for intermediate-scale test #12 with ground monitoring circuit voltage signals.

A.3 Microsoft Excel Marco Visual Basic Language for MC Simulation

```
Sub Trial1()
'
' Trial1 Macro
'g
' do loop that copies the simulation run percentage into a new cell and repeats with new
' simulation until done.  Sum is number of simulations, number of trials is set in
' spreedsheet

    Sum = 0
    y = Sum + 2
    Do While Sum < 1000

 ' G1 is where mean trial probability is calculated for each simulation
    Range("G1").Select
    Selection.Copy
' Selects proper cell in column of simulation results
    ActiveCell.Offset(y, 8).Select
    Selection.PasteSpecial Paste:=xlPasteValues, Operation:=xlNone, SkipBlanks _
        :=False, Transpose:=False
    Sum = Sum + 1
    y = y + 1
    Loop

End Sub
```

References

Anderson, P., Van Hees, P. (2005). *Performance of Cables Subjected to Elevated Temperatures*, Fire Safety Science – Proceedings of the Eighth International Symposium, International Association of Fire Safety Science.

Anixter. (1996). *Anixter Wire & Cable Handbook*, Wire & Cable Group, 3rd Edition.

American Society for Testing and Materials. (2005, February). ASTM E 1355: *Standard Guide for Evaluating the Predictive Capability of Deterministic Fire Models.*

Babrauskas, V. (2003). *Ignition Handbook*, Fire Science Publishers, Issaquah, WA.

Budnitz, R.J. (2002). *Spurious Actuation of Electrical Circuits Due to Cable Fires: Results of an Expert Elicitation*, Electric Power Research Institute, EPRI TR 1006961, Palo Alto, CA.

Callan, L.J. (1998 June) *White Paper on Risk-Informed and Performance-Based Regulation*, SECY-98-144, U.S. Nuclear Regulatory Commission, June 1998.

Cooper, L.Y., Steckler, K.D. (1996, August). *Methodology for Development and Implementing Alternative Temperature-Time Curves for Testing the Fire Resistance of Barriers for Nuclear Power Plant Applications*, National Institute of Standards and Technology, NUREG-1547, NISTIR 5842.

Del Toro, V. (1972). *Electrical Engineering Fundamentals.* Prentice-Hall Inc. Englewood Cliffs, NJ.

Draka. (2012). *Lifeline® Fire Protection Cable Systems.* North Dighton, MA. www.drakausa.com

EPRI/NRC-RES. (2005, September). *EPRI/NRC-RES Fire PRA Methodology for Nuclear Power Facilities, Second Draft Report for Comment,* Electric Power Research Institute TR 1011989, Nuclear Regulatory Commission NUREG/CR-6850.

EPRI/NRC-RES. (2007, May). *Verification and Validation of Selected Fire Models for Nuclear Power Plant Applications, Volume 2, Experimental Uncertainty.* Electric Power Research Institute 1011999, Nuclear Regulatory Commission NUREG-1824.

EPRI/NRC-RES. (2011, July). *Nuclear Power Plant Fire Modeling Application Guide*, Electric Power Research Institute TR 1023259, U.S. Nuclear Regulatory Commission NUREG-1934.

Gonzalez, F., Dreisbach, J. (2008, October). *Response to NFPA 805 Frequently Asked Question 06-0022 regarding acceptable electrical cable construction tests*, U.S. Nuclear Regulatory Commission FAQ 06-0022.

Hirschler, M.M., Morgan, A.B. (2008). *Thermal Decomposition of Polymers (Chapter 1-7), SFPE Handbook of Fire Protection Engineering*, Quincy, Massachusetts.

Institute of Electrical and Electronics Engineers. (2004, June). IEEE 383: *IEEE Standard for Qualifying Class 1E Electric Cables and Field Splices for Nuclear Power Generating Stations.* 2003 Edition. IEEE Power Engineering Society, New York, NY.

Institute of Electrical and Electronics Engineers. (2006, September). IEEE 1202: *IEEE Standard for Flame-Propagation Testing of Wire and Cable*. 2006 Edition. IEEE Power Energy Society, New York, NY.

Institute of Electrical and Electronics Engineers. (2011). IEEE P1717: *Draft IEEE Standard for Testing Circuit Integrity Cables Using the Hydrocarbon Pool Fire Test Protocol*, IEEE Power Energy Society, New York, NY.

Iqbal, N., Salley, M.H. (2004, December). *Fire Dynamic Tools (FDTs): Quantitative Fire Hazard Analysis Methods for the U.S. Nuclear Regulatory Commission Fire Protection Inspection Program*, U.S. Nuclear Regulatory Commission, NUREG-1805.

Jacobus, M.J., Fuehrer, G.F. (1990, April). *Submergence and High Temperature Steam Testing of Class 1E Electrical Cables*, Sandia National Laboratories, NUREG/CR-5655, SAND90-2629.

Kazarians, M., Apostolakis, G. (1981, September). *Fire Risk Analysis for Nuclear Power Plants*, University of California, NUREG/CR-2258, UCLA-ENG-8102.

Klamerus, L.J. (1977, October) *A Preliminary Report on Fire Protection Research Program (July 6, 1977 Test)*, Sandia National Laboratories, SAND77-1424, Albuquerque, NM.

Klamerus, L.J. (1978a, August). *Fire Protection Research Quarterly Progress Report October-December 1977*, Sandia National Laboratories, NUREG/CR-0366, SAND78-0477.

Klamerus, L.J. (1978b, September). *A Preliminary Report on Fire Protection Research Program Fire Barriers and Fire Retardant Coatings Tests*, Sandia National Laboratories, NUREG/CR-0381, SAND78-0477 R-2.

Klein, A.R. (2012, February). *Close-out of National Fire Protection Association Standard 805 Frequently Asked Question 08-0053, Kerite-FR Cable Failure Thresholds.* Nuclear Regulatory Commission, ADAMS Accession No. ML120060267.

LaChance, J.L., Nowlen, S.P., Wyant, F.J., Dandini, V.J. (2003, September). *Circuit Analysis - Failure Mode and Likelihood Analysis*, Sandia National Laboratories, NUREG/CR-6834, SAND2002-1942P.

Lambright, J.A., Nowlen, S.P., Nicolette, V.F., Bohn, M.P. (1989 January). *Fire Risk Scoping Study: Investigation of Nuclear Power Plant Fire Risk, Including Previously Unaddressed Issues*, Sandia National Laboratories, NUREG/CR-5088, SAND88-0177.

Lee, J.L. (1981, March). *A study of Damageability of Electrical Cables in Simulated Fire Environments*, Factory Mutual Research Corporation, EPRI NP-1767.

Lukens, L.L. (1982, October). *Nuclear Power Plant Electrical Cable Damageability Experiments*, Sandia National Laboratories, NUREG/CR-2927, SAND82-0236.

MathWorks. (2012). *Statistical Toolbox, Two-sample Kolmogorov-Smirnov test.* The MathWorks, Inc., R2011b, Natick, Massachusetts.

McGrattan, K. (2008). *Cable Response to Live Fire (CAROLFIRE) Volume 3: Thermally-Induced Electrical Failure (THIEF) Model*, National Institute of Standards and Technology, NUREG/CR-6931 Volume 3, NISTIR 7472.

Murphy, J.E. (2004, January). *Determination of Failure Criteria for Electrical Cables Exposed to Fire for Use in Nuclear Power Plant Risk Analysis*, Masters of Science Thesis, Worcester Polytechnic Institute.

National Fire Protection Association. (2001, February). NFPA 805: Performance-Based Standard for Fire Protection for Light Water Reactor Electric Generating Plants, 2001 Edition, Quincy, MA.

National Fire Protection Association. (2007, August). NFPA 70: *National Electrical Code*®, 2008 Edition, Quincy, MA.

Nowlen, S.P. (1989, December). *A Summary of Nuclear Power Plant Fire Safety Research at Sandia National Laboratories 1975-1987*, Sandia National Laboratories, NUREG/CR-5384, SAND89-1259.

Nowlen, S.P. (1991, May). *An Investigation of Effects of Thermal Aging on the Fire Damageability of Electric Cables.* Sandia National Laboratories, NUREG/CR-5546, SAND90-0696.

Nowlen, S.P., Jacobus, M.J. (1992 September). *The Estimation of Electrical Cable Fire-Induced Damage Limits*, Sandia National Laboratories, SAND92-1404C, Albuquerque, New Mexico.

Nowlen, S.P. (2000, August), *Ampacity Derating and Cable Functionality for Raceway Fire Barriers*, Sandia National Laboratories, NUREG/CR-6681, SAND2000-1825, August, 2000.

Nowlen, S.P., Kazarians, M., Wyant, F. (2001, September) *Risk Methods Insights Gained from Fire Incidents*, Sandia National Laboratories, NUREG/CR-6738, SAND2001-1676P.

Nowlen, S.P., Wyant, F.J. (2008, April) *Cable Response to Live Fire (CAROLFIRE) Volume 1: Test Descriptions and Analysis of Circuit Response Data*, Sandia National Laboratories, NUREG/CR-6931, SAND2007-600, Volume 1.

Nowlen, S.P., Brown, J.W. (2011 December). *Kerite Analysis in Thermal Environment of FIRE (KATE-Fire): Test Results*, NUREG/CR-7102, SAND2011-6548P.

Nowlen, S.P., Brown, J.W., Olivier, T.J., Wyant, F.J. (2012, April). *Direct Current Electrical Shorting in Response to Exposure Fire (DESIREE-Fire): Test Results*, Sandia National Laboratories, NUREG/CR-7100, SAND2012-0323P.

Nuclear Regulatory Commission. (1987, June). *Standard Review Plan for Review of Safety Analysis Reports for Nuclear Power Plants: Light Water Reactor Edition.* NUREG-0800,

Nuclear Regulatory Commission. (1999, June). Information Notice 99-17, *Problems associated with post-fire safe-shutdown circuit analysis*.

Nuclear Regulatory Commission. (2000, February). Enforcement Guidance Memorandum 98-002, *Disposition of Violations of 10 CFR Part 50, Appendix R, Sections III.G and III.L, Regarding Circuit Failures*" ADAMS Accession No. ML003710123.

Nuclear Regulatory Commission. (2002, April). *Perspectives Gained From the Individual Plant Examination of External Events (IPEEE) Program, Volume 1*, NUREG-1742.

Nuclear Regulatory Commission. (2004, March). Regulatory Issue Summary 2004-03, *Risk-Informed Approach for Post-Fire Safe-Shutdown Associated Circuits Inspections*.

Nuclear Regulatory Commission. (2005, February). *Technical Basis for Fire Protection Significant Determination Process At Power Operations.* Inspection Manual Chapter 0308, Attachment 3, Appendix F.

Nuclear Regulatory Commission, (2009, April). *Fire Protection for Nuclear Power Plants*, Regulatory Guide 1.189.

Nuclear Regulatory Commission, Section 50.48 of 10 CFR, *Fire Protection*, and Appendix R, *Fire Protection Program for Nuclear Power Facilities Operating Prior to January 1, 1979, to 10 CFR Part 50*.

Nuclear Regulatory Commission. (1976). *Guidelines for Fire Protection for Nuclear Power Plants*, Branch Technical Position (BTP) APCSB 9.5-1, Appendix A.

OMEGA. (2012). *OMEGA Engineering Technical Reference.* www.omega.com/prodinfo/thermocouples.html

Przybyla, L., Christian, W.J. (1978, June). *Development and Verification of Fire Tests for Cable Systems and System Components*, Underwriters Laboratories, NUREG/CR-0152, UL-USNC-7502-3.

Rockbestos-Surprenant. (2003). *Rockbestos-Surprenant Product Catalog*. East Granby, CT. www.r-scc.com/PDF/Firezone-S7.pdf

Salley, M.H., (2000). *An Examination of the Methods and Data Used to Determine Functionality of Electrical Cables when Exposed to Elevated Temperatures as a Result of a Fire in a Nuclear Power Plant*, Masters of Science Thesis, University of Maryland.

Salley, M.H. (2004, January). *Knowledge Base for Post-Fire Safe-Shutdown Analysis*, Draft Report for Comment, U.S. Nuclear Regulatory Commission, NUREG-1778.

Subudhi, M. (1996 April) *Literature Review of Environmental Qualification of Safety-Related Electrical Cables*, Brookhaven National Laboratories, NUREG/CR-6384, BNL-NUREG-52480, Volume 1.

Taylor, G., Salley, M. (2010, May). *Electric Raceway Fire Barrier Systems in U.S. Nuclear Power Plants.* U.S. Nuclear Regulatory Commission, NUREG-1924.

Underwriters Laboratories. (2001, May). UL 2196: *Tests for Fire Resistive Cables*, Northbrook, IL.

Wheelis, W.T. (1986, September). *Transient Fire Environment Cable Damageability Test Results Phase 1*, Sandia National Laboratories, NUREG/CR-4638, SAND86-0839.

Wyant, F.J., Nowlen, S.P. (2002, June). *Cable Insulaiton Resistance Measurements Made During Cable Fire Tests*, Sandia National Laboratories, NUREG/CR-6776, SAND2002-0447P.